

Fluorescent pyranoindole congeners: synthesis and photophysical properties of
pyrano[3,2-f], [2,3-g], [2,3-f], and [2,3-e]indoles

Ainur D. Sharapov, Ramil F. Fatykhov, Igor A. Khalymbadzha, Maria I. Valieva, Igor L. Nikonov,
Olga S. Taniya, Dmitry S. Kopchuk, Grigory V. Zyryanov, Alexander S. Novikov and
Oleg N. Chupakhin

Supporting Information

Table of Contents

| | |
|--|----------|
| Experimental Section | 5 |
| General Information:..... | 5 |
| Synthesis and characterization of pyranoindole compounds..... | 5 |
| Table S1. Yields, NMR data, elemental analysis and melting points for compounds 2 , 3 , 6-10 , 12 and 14 .. | 6 |
| Figure S1. ^1H NMR spectrum of 2 | 13 |
| Figure S2. ^{13}C NMR spectrum of 2 | 13 |
| Figure S3. ^1H NMR spectrum of 3 | 14 |
| Figure S4. ^{13}C NMR spectrum of 3 | 14 |
| Figure S5. ^1H NMR spectrum of 6a | 15 |
| Figure S6. ^{13}C NMR spectrum of 6a | 15 |
| Figure S7. ^1H NMR spectrum of 6b | 16 |
| Figure S8. ^{13}C NMR spectrum of 6b | 16 |
| Figure S9. ^1H NMR spectrum of 7a | 17 |
| Figure S10. ^{13}C NMR spectrum of 7a | 17 |
| Figure S11. ^1H NMR spectrum of 8a | 18 |
| Figure S12. ^{13}C NMR spectrum of 8a | 18 |
| Figure S13. ^1H NMR spectrum of 7b | 19 |
| Figure S14. ^{13}C NMR spectrum of 7b | 19 |
| Figure S15. ^1H NMR spectrum of 8b | 20 |
| Figure S16. ^{13}C NMR spectrum of 8b | 20 |
| Figure S17. ^1H NMR spectrum of 7c | 21 |
| Figure S18. ^{13}C NMR spectrum of 7c | 21 |
| Figure S19. ^1H NMR spectrum of 8c | 22 |
| Figure S20. ^{13}C NMR spectrum of 8c | 22 |
| Figure S21. ^1H NMR spectrum of 7d | 23 |
| Figure S22. ^{13}C NMR spectrum of 7d | 23 |
| Figure S23. ^1H NMR spectrum of 8d | 24 |
| Figure S24. ^{13}C NMR spectrum of 8d | 24 |
| Figure S25. ^1H NMR spectrum of 7e | 25 |
| Figure S26. ^{13}C NMR spectrum of 7e | 25 |

| | |
|--|----|
| Figure S27. ^1H NMR spectrum of 8e | 26 |
| Figure S28. ^{13}C NMR spectrum of 8e | 26 |
| Figure S29. ^1H NMR spectrum of 7f | 27 |
| Figure S30. ^{13}C NMR spectrum of 7f | 27 |
| Figure S31. ^1H NMR spectrum of 8f | 28 |
| Figure S32. ^{13}C NMR spectrum of 8f | 28 |
| Figure S33. ^1H NMR spectrum of 7g | 29 |
| Figure S34. ^{13}C NMR spectrum of 7g | 29 |
| Figure S35. ^1H NMR spectrum of 8g | 30 |
| Figure S36. ^{13}C NMR spectrum of 8g | 30 |
| Figure S37. ^1H NMR spectrum of 7h | 31 |
| Figure S38. ^{13}C NMR spectrum of 7h | 31 |
| Figure S39. ^1H NMR spectrum of 7i | 32 |
| Figure S40. ^{13}C NMR spectrum of 7i | 32 |
| Figure S41. ^1H NMR spectrum of 9a | 33 |
| Figure S42. ^{13}C NMR spectrum of 9a | 33 |
| Figure S43. ^1H NMR spectrum of 9b | 34 |
| Figure S44. ^{13}C NMR spectrum of 9b | 34 |
| Figure S45. ^1H NMR spectrum of 9c | 35 |
| Figure S46. ^{13}C NMR spectrum of 9c | 35 |
| Figure S47. ^1H NMR spectrum of 9d | 36 |
| Figure S48. ^{13}C NMR spectrum of 9d | 36 |
| Figure S49. ^1H NMR spectrum of 10 | 37 |
| Figure S50. ^{13}C NMR spectrum of 10 | 38 |
| Figure S51. ^1H NMR spectrum of 2,3-diphenyl-6-methoxyindole 13 | 38 |
| Figure S52. ^1H NMR spectrum of 2,3-diphenyl-6-methoxyindole 13 | 38 |
| Photophysical data | 39 |
| Materials and Methods | 39 |
| Equipment, measurements and characterization methods..... | 39 |
| Photoluminescence Absolute quantum yield (PLQY) measurement | 39 |
| Solvatochromic behavior of pyranoindole compounds | 39 |
| Table S2. Orientation polarizability for solvents (Δf), absorption and fluorescence emission maxima (λ_{abs} , λ_{em} , nm) and Stokes shift (nm, cm^{-1}) of 2 in different solvents. | 39 |
| Table S3. Orientation polarizability for solvents (Δf), absorption and fluorescence emission maxima (λ_{abs} , λ_{em} , nm) and Stokes shift (nm, cm^{-1}) of 6b in different solvents. | 39 |
| Table S4. Orientation polarizability for solvents (Δf), absorption and fluorescence emission maxima (λ_{abs} , λ_{em} , nm) and Stokes shift (nm, cm^{-1}) of 7a in different solvents. | 39 |

| | |
|--|----|
| Table S5. Orientation polarizability for solvents (Δf), absorption and fluorescence emission maxima (λ_{abs} , λ_{em} , nm) and Stokes shift (nm, cm^{-1}) of 7c in different solvents. | 40 |
| Table S6. Orientation polarizability for solvents (Δf), absorption and fluorescence emission maxima (λ_{abs} , λ_{em} , nm) and Stokes shift (nm, cm^{-1}) of 7e in different solvents. | 40 |
| Figure S53. Normalized fluorescence spectra of 7e in different solvents ($C = 10^{-5} \text{ M}^{-1}$). | 40 |
| Table S7. Orientation polarizability for solvents (Δf), absorption and fluorescence emission maxima (λ_{abs} , λ_{em} , nm) and Stokes shift (nm, cm^{-1}) of 8a in different solvents. | 40 |
| Table S8. Orientation polarizability for solvents (Δf), absorption and fluorescence emission maxima (λ_{abs} , λ_{em} , nm) and Stokes shift (nm, cm^{-1}) of 8c in different solvents. | 41 |
| Table S9. Orientation polarizability for solvents (Δf), absorption and fluorescence emission maxima (λ_{abs} , λ_{em} , nm) and Stokes shift (nm, cm^{-1}) of 8d in different solvents. | 41 |
| Figure S54. Fluorescence photograph of pyranoindole 7e (1 mM, excitation with 365 nm Hg lamp) in different solvents (left to right: <i>n</i> -heptane, toluene, tetrahydrofuran, dichloromethane, DMSO, acetonitrile, methanol). | 41 |
| Table S10. Orientation polarizability for solvents (Δf), absorption and fluorescence emission maxima (λ_{abs} , λ_{em} , nm) and Stokes shift (nm, cm^{-1}) of 8e in different solvents. | 41 |
| Figure S55. Normalized fluorescence spectra of 8e in different solvents ($C = 10^{-5} \text{ M}^{-1}$). | 42 |
| Table S11. Orientation polarizability for solvents (Δf), absorption and fluorescence emission maxima (λ_{abs} , λ_{em} , nm) and Stokes shift (nm, cm^{-1}) of 8f in different solvents. | 42 |
| Table S12. Orientation polarizability for solvents (Δf), absorption and fluorescence emission maxima (λ_{abs} , λ_{em} , nm) and Stokes shift (nm, cm^{-1}) of 8g in different solvents. | 42 |
| Table S13. Orientation polarizability for solvents (Δf), absorption and fluorescence emission maxima (λ_{abs} , λ_{em} , nm) and Stokes shift (nm, cm^{-1}) of 9a in different solvents. | 42 |
| Table S14. Orientation polarizability for solvents (Δf), absorption and fluorescence emission maxima (λ_{abs} , λ_{em} , nm) and Stokes shift (nm, cm^{-1}) of 9b in different solvents. | 43 |
| Table S15. Orientation polarizability for solvents (Δf), absorption and fluorescence emission maxima (λ_{abs} , λ_{em} , nm) and Stokes shift (nm, cm^{-1}) of 10 in different solvents. | 43 |
| Table S16. Orientation polarizability for solvents (Δf), absorption and fluorescence emission maxima (λ_{abs} , λ_{em} , nm) and Stokes shift (nm, cm^{-1}) of 12 in different solvents. | 43 |
| Table S17. Lippert-Mataga plot for compounds 2 , 6 , 7 , 8 , 9 , 10 , and 12 | 43 |
| Table S18. The photophysical properties of compounds in different solvents. | 44 |
| Table S19. Fluorescence lifetime of probe 8c , 8g , 9a ($C = 2 \times 10^{-6} \text{ M}$) in MeOH. | 45 |
| Table S20. Energies of HOMO and LUMO, and energy gap for compounds 7 and 8 | 45 |
| Figure S56. Calculated UV-Vis spectra for optimized equilibrium model structure 7c (CAM-B3LYP/6-31+G* level of theory). | 46 |
| Figure S57. Calculated UV-Vis spectra for optimized equilibrium model structure 8c (CAM-B3LYP/6-31+G* level of theory). | 46 |
| Figure S58. Molecular orbital and energy levels of 7a-8a , 7c-8c , 7d-8d , 7e-8e , 7g-8g pyranoindole fluorophores, calculated at the CAM-B3LYP/6-31+G* level of theory. | 47 |
| Figure S59. Visualization of HOMOs and LUMOs responsible for observed UV-Vis spectra in optimized equilibrium model structure 7c (CAM-B3LYP/6-31+G* level of theory). | 48 |

| | |
|---|----|
| Figure S60. Visualization of HOMOs and LUMOs responsible for observed UV-Vis spectra in optimized equilibrium model structure 8c (CAM-B3LYP/6-31+G* level of theory)..... | 48 |
| Table S21. Optimized structures in S ₀ in gas phase and visualization of molecular electrostatic potential distribution..... | 49 |
| Table S22. Calculated indexes related to hole-electron distribution in model structures..... | 51 |

Experimental Section

General Information:

All reagents were purchased from commercial sources and used without further purification. Silica gel 60 (Kieselgel 60, 230-400 mesh) was used for the column chromatography. NMR spectra were recorded on a Bruker Avance-400 spectrometer, 298 K, digital resolution \pm 0.01 ppm, using TMS as internal standard and (Bruker Avance-600 spectrometer, 298 K, digital resolution \pm 0.01 ppm, using residue signals of solution as internal standard). UV–Vis spectra were recorded on Lambda 45 spectrophotometer (Perkin Elmer). Luminescence spectra were recorded on a Horiba-Fluoromax-4 spectrofluorimeter equipped with integrated sphere.

Synthesis and characterization of pyranoindole compounds

Synthesis of ethyl 9-methyl-5-oxo-1,2,3,4,5,10-hexahydroisochromeno[3,4-f]indole-8-carboxylate 2

A mixture of ethyl 5-hydroxy-2-methyl-1*H*-indole-3-carboxylate **1** (5 mmol, 1095 mg, 1.0 equiv), ethyl 2-oxocyclohexane-1-carboxylate (5.5 mmol, 936 mg, 1.1 equiv), and MsOH (0.5 mmol, 48 mg, 0.1 equiv) was stirred at ambient temperature for 4 hours. The reaction mixture was crystallized from DMF to obtain pure **2** (992 mg, 61% yield).

*Synthesis of 9-methyl-2,3,4,10-tetrahydroisochromeno[3,4-f]indol-5(1*H*)-one 3*

3-Carbethoxyindole **2** (1 mmol, 325 mg) was added to a solution of 0.2 mL H₂SO₄ in 1.5 mL AcOH. The reaction mixture was stirred under heating for 36 hours, poured into water and the precipitate was filtered off. The resulting precipitate was purified by flash chromatography (chloroform/silica gel) affording pyranoindole **3** (124 mg, 49% yield).

Synthesis of pyrano pyrano[2,3-e]indoles 6

A mixture of 2,3-diphenyl-1*H*-indol-4-ol **4** (856 mg, 3.0 mmol, 1.0 equiv), 2-ketoester (3.3 mmol, 1.1 equiv), and MsOH (0.3 mmol, 29 mg, 0.1 equiv) were stirred at 70°C for 5 hours. After completion of the reaction, the resulting mixture was recrystallized from DMF providing **6**.

Synthesis of pyrano[3,2-f] and [2,3-g]indoles 7 and 8

A mixture of 2,3-diphenyl-1*H*-indol-6-ol **5** (856 mg, 3.0 mmol, 1.0 equiv), 2-ketoester (3.3 mmol, 1.1 equiv), and MsOH (0.3 mmol, 29 mg, 0.1 equiv) were stirred at ambient temperature (for compounds) or at 50°C (for compounds **7,8a** and **7,8b**) for 5 hours. After completion of the reaction, the crude mixture was separated to obtain isomeric indoles **7** and **8** using silica gel chromatography (chloroform-hexane (1:1) as eluent).

*Alkylation of pyrano[3,2-f]indol-2(8*H*)-ones 7*

To a solution of pyrano[3,2-f]indol-2(8*H*)-one **7** (1 mmol) and ethyl iodide (1.2 mmol, 187 mg) or benzyl bromide (1.2 mmol, 171 mg) in DMF a suspension of sodium hydride (1.2 mmol, 60%, 48 mg) was added. The reaction mixture is stirred for 8 hours, then water was added and the pH of

the resulting mixture is adjusted to 6 by adding acetic acid. The resulting precipitate was filtered off, washed with hexane, and recrystallized from ethanol to obtain pure **9**.

Aromatization of 2,3-diphenyl-8,9,10,11-tetrahydroisochromeno[3,4-g]indol-7(1H)-one

A solution of 2,3-diphenyl-8,9,10,11-tetrahydroisochromeno[3,4-g]indol-7(1H)-one **8g** (1 mmol, 392 mg) and DDQ (3 mmol, 681 mg) was heated under reflux for 6 hours. The reaction mixture was diluted with methylene chloride and the resulting solution was passed through a layer of aluminum oxide. The eluate was evaporated and the resulting solid was recrystallized from ethyl alcohol yielding 162 mg, 42% 2,3-diphenylisochromeno[3,4-g]indol-7(1H)-one **10**.

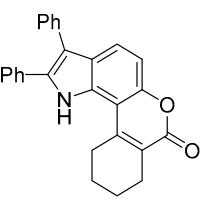
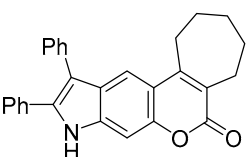
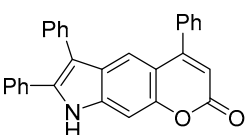
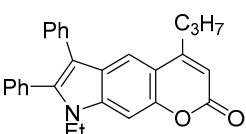
Table S1. Yields, NMR data, elemental analysis and melting points for compounds **2**, **3**, **6-10**, **12** and **14**.

| Cmpd | Structure | Characterization |
|-----------|-----------|--|
| 2 | | Off-white solid, m.p. > 300 °C. ¹ H NMR (400 MHz, DMSO-d ₆) δ 12.00 (s, 1H), 7.62 (s, 1H), 7.43 (s, 1H), 4.28 (q, <i>J</i> = 7.1 Hz, 2H), 2.75 (br s, 2H); 2.66 (s, 3H), 2.38 (br s, 2H), 1.68–1.78 (m, 4H), 1.37 (t, 3H). ¹³ C{ ¹ H} NMR (101 MHz, DMSO-d ₆) δ 164.6, 161.0, 148.6, 147.3, 146.9, 131.8, 128.5, 120.2, 114.8, 105.8, 104.9, 102.7, 59.0, 24.6, 23.7, 21.2, 20.9, 14.4, 13.9. Anal. Calcd for C ₁₉ H ₁₉ NO ₄ : C, 70.14; H, 5.89; N, 4.31. Found: C, 69.97; H, 5.02; N, 4.19. |
| 3 | | Light yellow solid with m.p. = 279–281 °C. ¹ H NMR (400 MHz, DMSO-d ₆) δ 11.19 (s, 1H), 7.51 (s, 1H), 7.33 (s, 1H), 6.21 (s, 1H), 2.84–2.87 (m, 2H), 2.43 (m, 5H), 1.72–1.84 (m, 4H). ¹³ C{ ¹ H} NMR (101 MHz, DMSO-d ₆) δ 161.4, 147.9, 145.7, 140.8, 133.4, 130.5, 119.2, 113.6, 104.1, 104.0, 99.3, 24.8, 23.8, 21.4, 21.1, 13.6. Anal. Calcd for C ₁₆ H ₁₅ NO ₂ : C, 75.87; H, 5.97; N, 5.53. Found: 75.79; H, 6.08; N, 5.35. |
| 6a | | Yield 1406 mg, 68%. Beige solid with m.p. = 254–255 °C. ¹ H NMR (400 MHz, DMSO-d ₆) δ 12.18 (s, 1H), 7.53–7.59 (m, 5H), 7.28–7.43 (m, 11H), 7.15 (d, <i>J</i> = 8.7 Hz, 1H), 6.15 (s, 1H). ¹³ C{ ¹ H} NMR (151 MHz, DMSO-d ₆) δ 159.7, 156.9, 149.4, 138.7, 136.2, 135.7, 134.8, 131.6, 131.1 (2C), 129.4, 128.8 (2C), 128.50 (2C), 128.47 (2C), 128.3 (2C), 127.9 (2C), 127.8, 126.7, 120.0, 115.5, 114.1, 110.4, 110.2, 109.0. Anal. Calcd for C ₂₉ H ₁₉ NO ₂ : C, 84.24; H, 4.63; N, 3.39. Found: C, 84.07; H, 5.74; N, 3.19. |

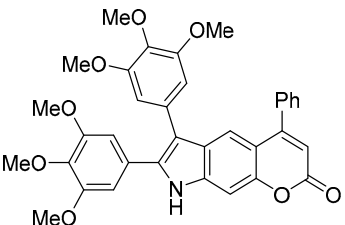
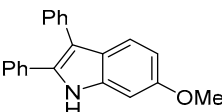
| Cmpd | Structure | Characterization |
|-----------|-----------|--|
| 6b | | Yield 1195 mg, 63%. Light gray solid with m.p. = 252 °C. ¹ H NMR (600 MHz, DMSO-d ₆) δ 12.13 (s, 1H), 7.54 (d, <i>J</i> = 8.7 Hz, 1H), 7.43 (d, <i>J</i> = 8.7 Hz, 1H), 7.27–7.38 (m, 10H), 6.10 (s, 1H), 2.78–2.81 (m, 2H), 1.68–1.71 (m, 2H), 0.98–1.00 (m, 3H). ¹³ C{ ¹ H} NMR (151 MHz, DMSO-d ₆) δ 160.0, 158.0, 149.0, 138.5, 135.4, 134.8, 131.7, 131.1 (2C), 128.4 (2C), 128.3 (2C), 127.8 (2C), 127.7, 126.6, 118.1, 115.4, 114.0, 110.6, 109.4, 108.8, 33.8, 21.6, 13.7. Anal. Calcd for C ₂₆ H ₂₁ NO ₂ : C, 82.30; H, 5.58; N, 3.69. Found: C, 82.37; H, 5.66; N, 3.86. |
| 7a | | Yield 931 mg, 53%. Yellow solid with m.p. = 270°C. ¹ H NMR (400 MHz, DMSO-d ₆) δ 11.93 (s, 1H), 7.76 (s, 1H), 7.33–7.48 (m, 11H), 6.23 (s, 1H), 2.44 (s, 3H). ¹³ C{ ¹ H} NMR (101 MHz, DMSO-d ₆) δ 160.4, 154.0, 149.7, 137.9, 136.2, 134.3, 131.7, 129.8 (2C), 128.9 (2C), 128.6 (2C), 128.1 (2C), 128.0, 126.6, 125.7, 114.9, 113.8, 113.7, 111.1, 97.6, 18.5. Anal. Calcd for C ₂₄ H ₁₇ NO ₂ : C, 82.03; H, 4.88; N, 3.99. Found: C, 81.92; H, 4.98; N, 3.84. |
| 8a | | Yield 614 mg, 32%. Yellow solid with m.p. >300°C. ¹ H NMR (400 MHz, DMSO-d ₆) δ 10.82 (s, 1H), 7.68 (d, <i>J</i> = 8.6 Hz, 1H), 7.31–7.49 (m, 10H), 7.15 (d, <i>J</i> = 8.6 Hz, 1H), 6.35 (s, 1H), 2.93 (s, 3H). ¹³ C{ ¹ H} NMR (101 MHz, DMSO-d ₆) δ 159.9, 153.1, 151.1, 136.0, 133.9, 131.8, 130.9, 129.8 (2C), 129.2 (2C), 128.7 (2C), 128.3 (2C), 127.8, 126.6, 125.7, 123.0, 114.8, 112.7, 110.2, 106.6, 22.1. Anal. Calcd for C ₂₄ H ₁₇ NO ₂ : C, 82.03; H, 4.88; N, 3.99. Found: C, 82.08; H, 4.75; N, 4.07. |
| 7b | | Yield 767 mg, 42%. Beige solid with m.p. > 300 °C. ¹ H NMR (400 MHz, DMSO-d ₆) δ 11.74 (s, 1H), 7.74 (s, 1H), 7.30–7.48 (m, 11H), 2.39 (s, 3H), 2.11 (s, 3H). ¹³ C{ ¹ H} NMR (101 MHz, DMSO-d ₆) δ 161.3, 148.2, 147.0, 137.0, 135.8, 134.4, 131.7, 129.6 (2C), 128.6 (2C), 128.3 (2C), 127.9 (2C), 127.7, 126.3, 125.6, 117.3, 114.3, 114.1, 113.6, 97.1, 14.8, 12.9. Anal. Calcd for C ₂₅ H ₁₉ NO ₂ : C, 82.17; H, 5.24; N, 3.83. Found: C, 82.00; H, 5.37; N, 3.88. |
| 8b | | Yield 730 mg, 40%. Beige solid with m.p. > 300 °C. ¹ H NMR (400 MHz, DMSO-d ₆) δ 10.84 (s, 1H), 7.62 (d, <i>J</i> = 8.6 Hz, 1H), 7.31–7.48 (m, 10H), 7.12 (d, <i>J</i> = 8.6 Hz, 1H), 2.88 (s, 3H), 2.17 (s, 3H). ¹³ C{ ¹ H} NMR (101 MHz, DMSO-d ₆) δ 160.9, 149.1, 146.7, 135.7, 134.1, 131.9, 130.7, 129.9, 129.2, 128.7, 128.3 (2C), 127.7 (2C), 126.5 (2C), 125.9 (2C), 121.7, 119.1, 114.7, 110.0, 107.4, 18.7, 13.0. Anal. Calcd for C ₂₅ H ₁₉ NO ₂ : C, 82.17; H, 5.24; N, 3.83. Found: C, 82.29; H, 5.34; N, 3.70. |

| Cmpd | Structure | Characterization |
|------|-----------|--|
| 7c | | Yield 1176 mg, 62%. Yellow needles with m.p. > 300 °C. ¹ H NMR (400 MHz, DMSO-d ₆) δ 11.82 (s, 1H), 7.77 (s, 1H), 7.32–7.48 (m, 11H), 6.15 (s, 1H), 2.76–2.79 (m, 2H), 1.64–1.74 (m, 2H), 0.95–0.99 (m, 3H). ¹³ C{ ¹ H} NMR (101 MHz, DMSO-d ₆) δ 160.3, 156.9, 149.8, 137.7, 136.2, 134.2, 131.6, 129.6 (2C), 128.6 (2C), 128.3 (2C), 127.9 (2C), 127.8, 126.4, 125.6, 114.2, 113.6, 112.9, 109.9, 97.7, 32.8, 20.8, 13.4. Anal. Calcd for C ₂₆ H ₂₁ NO ₂ : C, 82.30; H, 5.58; N, 3.69. Found: C, 82.22; H, 5.69; N, 3.46. |
| 8c | | Yield 284 mg, 15%. Beige solid with m.p. > 300 °C. ¹ H NMR (600 MHz, DMSO-d ₆) δ 10.87 (s, 1H), 7.70 (d, J = 8.6 Hz, 1H), 7.31–7.44 (m, 10H), 7.18 (d, J = 8.6 Hz, 1H), 6.31 (s, 1H), 3.32–3.35 (m, 2H), 1.80–1.82 (m, 2H), 1.09–1.12 (m, 3H). ¹³ C{ ¹ H} NMR (151 MHz, DMSO-d ₆) δ 160.5, 156.9, 151.9, 136.6, 134.4, 132.3, 130.4 (2C), 130.1, 129.6 (2C), 129.2 (2C), 128.9 (2C), 128.3, 127.1, 126.5, 123.5, 115.3, 112.1, 111.0, 106.7, 35.8, 20.6, 13.9. Anal. Calcd for C ₂₆ H ₂₁ NO ₂ : C, 82.30; H, 5.58; N, 3.69. Found: C, 82.36; H, 5.60; N, 3.74. |
| 7d | | Yield 1324 mg, 60%. Yellow solid with m.p. > 275 °C. ¹ H NMR (400 MHz, DMSO-d ₆) δ 11.79 (s, 1H), 7.80 (s, 1H), 7.17–7.48 (m, 16H), 3.99 (s, 2H), 2.46 (s, 3H). ¹³ C{ ¹ H} NMR (101 MHz, DMSO-d ₆) δ 161.3, 148.6, 148.5, 139.4, 137.3, 136.0, 134.3, 131.6, 129.6 (2C), 128.6 (2C), 128.3 (2C), 128.2 (2C), 127.9 (2C), 127.8 (2C), 127.7, 126.4, 125.7, 125.7, 120.6, 114.7, 114.2, 113.7, 97.1, 32.2, 15.2. Anal. Calcd for C ₃₁ H ₂₃ NO ₂ : C, 84.33; H, 5.25; N, 3.17. Found: C, 84.16; H, 5.23; N, 3.36. |
| 8d | | Yield 441 mg, 20%. Yellow solid with m.p. = 275 °C. ¹ H NMR (400 MHz, DMSO-d ₆) δ 10.84 (s, 1H), 7.66 (d, J = 8.6, 1H), 7.18–7.48 (m, 15H), 7.16 (d, J = 8.6 Hz, 1H), 4.07 (s, 2H), 2.95 (s, 3H). ¹³ C{ ¹ H} NMR (101 MHz, DMSO-d ₆) δ 161.0, 149.5, 148.5, 139.4, 135.8, 134.0, 131.8, 130.8, 129.9 (2C), 129.1 (2C), 128.70 (2C), 128.66, 128.4 (2C), 128.3 (2C), 128.0 (2C), 127.7, 126.5, 126.0, 126.0, 122.3, 122.2, 114.8, 110.1, 107.5, 31.9, 19.0. Anal. Calcd for C ₃₁ H ₂₃ NO ₂ : C, 84.33; H, 5.25; N, 3.17. Found: C, 84.23; H, 5.18; N, 3.22. |
| 7e | | Yield 1292 mg, 67%. Yellow solid with m.p. > 220 °C dec. ¹ H NMR (400 MHz, DMSO-d ₆) δ 11.98 (s, 1H), 7.77, (s, 1H) 7.33–7.46 (m, 11H), 2.56 (s, 3H). ¹³ C{ ¹ H} NMR (101 MHz, DMSO-d ₆) δ 156.6, 149.4, 147.6, 137.7, 136.6, 134.2, 131.5, 129.8 (2C), 128.9 (2C), 128.6 (2C), 128.2 (2C), 128.1, 126.7, 126.0, 115.8, 115.3, 113.7, 113.4, 97.6, 16.3. Anal. Calcd for C ₂₄ H ₁₆ CINO ₂ : C, 74.71; H, 4.18; N, 3.63. Found: C, 74.89; H, 4.05; N, 3.39. |

| Cmpd | Structure | Characterization |
|------|-----------|---|
| 8e | | Yield 289 mg, 15%. Yellow solid with m.p. > 230 °C. ¹ H NMR (400 MHz, DMSO-d ₆) δ 11.01 (s, 1H), 7.72 (d, <i>J</i> = 8.7 Hz, 1H), 7.47–7.49 (m, 2H), 7.31–7.43 (m, 8H), 7.19 (d, <i>J</i> = 8.7 Hz, 1H), 3.08 (s, 3H). ¹³ C{ ¹ H} NMR (101 MHz, DMSO-d ₆) δ 156.2, 148.7, 148.4, 136.3, 133.8, 131.6, 130.4, 129.9 (2C), 129.3 (2C), 128.7 (2C), 128.3 (2C), 127.9, 126.6, 126.2, 123.2, 117.5, 114.9, 110.0, 106.7, 19.7. Anal. Calcd for C ₂₄ H ₁₆ CINO ₂ : C, 74.71; H, 4.18; N, 3.63. Found: C, 74.89; H, 4.04; N, 3.34. |
| 7f | | Yield 1076 mg, 57%. Yellow solid with m.p. > 300 °C. ¹ H NMR (600 MHz, DMSO-d ₆) δ 11.83 (s, 1H), 7.55 (br s, 1H), 7.32–7.47 (m, 11H), 3.07–3.11 (m, 2H), 2.75–2.78 (m, 2H), 2.07–2.12 (m, 2H). ¹³ C{ ¹ H} NMR (151 MHz, DMSO-d ₆) δ 159.4, 157.0, 150.2, 137.4, 136.0, 134.4, 131.7, 129.6 (2C), 128.6 (2C), 128.4 (2C), 127.9 (2C), 127.8, 126.4, 125.6, 123.0, 114.5, 113.5, 112.5, 97.4, 31.7, 30.1, 21.8. Anal. Calcd for C ₂₆ H ₁₉ NO ₂ : C, 82.74; H, 5.07; N, 3.71. Found: C, 82.80; H, 5.03; N, 3.81. |
| 8f | | Yield 528 mg, 28%. Beige solid with m.p. > 300°C. ¹ H NMR (600 MHz, DMSO-d ₆) δ 10.90 (s, 1H), 7.64 (d, <i>J</i> = 8.7 Hz, 1H), 7.30–7.41 (m, 2H), 7.45–7.47 (m, 8H), 7.16 (d, <i>J</i> = 8.7 Hz, 1H), 3.61–3.63 (m, 2H), 2.77–2.80 (m, 2H), 2.16–2.21 (m, 2H). ¹³ C{ ¹ H} NMR (151 MHz, DMSO-d ₆) δ 159.1, 154.4, 151.2, 136.0, 134.1, 131.8, 130.5, 129.8 (2C), 129.3 (2C), 128.7 (2C), 128.3 (2C), 127.8, 126.5, 125.2, 125.0, 121.9, 114.8, 109.9, 105.0, 34.2, 29.6, 22.1. Anal. Calcd for C ₂₆ H ₁₉ NO ₂ : C, 82.74; H, 5.07; N, 3.71. Found: C, 82.69; H, 4.97; N, 3.89. |
| 7g | | Yield 665 mg, 34%. White solid with m.p. > 290 °C. ¹ H NMR (600 MHz, DMSO-d ₆) δ 11.86 (s, 1H), 7.69 (s, 1H), 7.32–7.48 (m, 11H), 2.80 (br s, 2H), 2.44 (br s, 2H), 1.68–1.78 (m, 4H). ¹³ C{ ¹ H} NMR (151 MHz, DMSO-d ₆) δ 161.0, 148.2, 147.8, 136.9, 135.8, 134.5, 131.8, 129.7 (2C), 128.6 (2C), 128.4 (2C), 127.9 (2C), 127.7, 126.3, 125.5, 119.0, 113.8, 113.5, 112.9, 97.2, 24.6, 23.6, 21.2, 20.9. Anal. Calcd for C ₂₇ H ₂₁ NO ₂ : C, 82.84; H, 5.41; N, 3.58. Found: C, 82.93; H, 5.43; N, 3.39. |

| Cmpd | Structure | Characterization |
|------|---|---|
| 8g |  | Yield 626 mg, 32%. Cream solid with m.p. > 300 °C. ¹ H NMR (400 MHz, DMSO-d ₆) δ 10.75 (s, 1H), 7.62 (d, <i>J</i> = 8.6 Hz, 1H), 7.45–7.47 (m, 2H), 7.29–7.42 (m, 8H), 7.12 (d, <i>J</i> = 8.6 Hz, 1H), 3.40 (br s, 2H), 2.48 (br s, 2H), 1.75–1.87 (m, 4H). ¹³ C{ ¹ H} NMR (101 MHz, DMSO-d ₆) δ 160.5, 149.2, 148.0, 135.7, 134.1, 131.9, 130.3, 129.9 (2C), 129.3 (2C), 128.7 (2C), 128.2 (2C), 127.7, 126.5, 125.7, 121.6, 120.5, 114.6, 110.1, 106.9, 28.2, 24.1, 21.3, 20.9. Anal. Calcd for C ₂₇ H ₂₁ NO ₂ : C, 82.84; H, 5.41; N, 3.58. Found: C, 82.93; H, 5.32; N, 3.33. |
| 7h |  | Yield 1379 mg, 68%. Off-white solid, m.p. > 300 °C. ¹ H NMR (600 MHz, DMF-d ₇) δ 11.98 (s, 1H), 8.07 (s, 1H), 7.61–7.63 (m, 2H), 7.39–7.56 (m, 8H), 3.10–3.12 (m, 2H), 2.93–2.95 (m, 2H), 1.91–1.93 (m, 2H), 1.70–1.71 (m, 2H), 1.60–1.62 (m, 2H). ¹³ C{ ¹ H} NMR (151 MHz, DMF-d ₇) δ 156.0, 150.8, 139.0, 137.5, 136.1, 133.4, 131.3 (2C), 130.0 (2C), 129.7 (2C), 129.4 (2C), 129.0, 127.8, 127.4, 125.5, 115.5, 115.4 (2C), 115.1, 98.9, 32.8, 28.9, 27.5, 26.9, 26.3. Anal. Calcd for C ₂₈ H ₂₃ NO ₂ : C, 82.94; H, 5.72; N, 3.45. Found: C, 82.85; H, 5.80; N, 3.31. |
| 7i |  | Yellow solid, m.p. > 300 °C. Yield 1199 mg, 58%. ¹ H NMR (400 MHz, DMSO-d ₆) δ 12.01 (s, 1H), 7.26–7.59 (m, 17H), 6.23 (s, 1H). ¹³ C{ ¹ H} NMR (101 MHz, DMSO-d ₆) δ 160.3, 156.3, 150.3, 137.9, 136.3, 135.6, 134.1, 131.5, 129.6 (3C), 128.7 (4C), 128.6 (2C), 128.5 (2C), 128.1 (3C), 126.7, 125.8, 117.1, 113.8, 112.6, 111.2, 98.1. Anal. Calcd for C ₂₉ H ₁₉ NO ₂ : C, 84.24; H, 4.63; N, 3.39. Found: C, 84.01; H, 4.85; N, 3.23. |
| 9a |  | Yield 354 mg, 87%. Cream solid with m.p. > 200-201 °C. ¹ H NMR (600 MHz, DMSO-d ₆) δ 7.92 (s, 1H), 7.67 (s, 1H), 7.46–7.47 (m, 3H), 7.38–7.40 (m, 2H), 7.29–7.32 (m, 2H), 7.26–7.28 (m, 2H), 7.19–7.21 (m, 1H), 6.19 (s, 1H), 4.12–4.16 (m, 2H), 2.80–2.82 (m, 2H), 1.67–1.73 (m, 2H), 1.13–1.16 (m, 3H), 0.96–0.98 (m, 3H). ¹³ C{ ¹ H} NMR (151 MHz, DMSO-d ₆) δ 160.5, 157.0, 149.8, 139.1, 137.3, 133.8, 130.9, 130.7 (2C), 129.2 (2C), 128.6, 128.5 (2C), 128.4 (2C), 126.0, 123.9, 114.9, 114.7, 113.1, 110.2, 97.3, 38.5, 32.9, 21.0, 14.7, 13.6. Anal. Calcd for C ₂₈ H ₂₅ NO ₂ : C, 82.53; H, 6.18; N, 3.44. Found: C, 83.85; H, 6.40; N, 3.24. |

| Cmpd | Structure | Characterization |
|-----------|-----------|---|
| 9b | | Yield 294 mg, 70%. Beige solid with m.p. > 205–207 °C. ¹ H NMR (400 MHz, DMSO-d ₆) δ 7.86 (s, 1H), 7.65 (s, 1H), 7.12–7.49 (m, 10H), 4.11–4.16 (m, 2H), 2.86 (br s, 2H), 2.45 (br s, 2H), 1.72–1.79 (m, 4H), 1.12–1.15 (s, 3H). ¹³ C{ ¹ H} NMR (101 MHz, DMSO-d ₆) δ 161.1, 148.2, 148.0, 138.8, 136.6, 134.0, 131.0, 130.8 (2C), 129.3 (2C), 128.7, 128.6 (2C), 128.4 (2C), 125.9, 123.8, 119.3, 114.8, 114.1, 113.4, 96.8, 38.5, 24.7, 23.7, 21.3, 21.0, 14.8. Anal. Calcd for C ₂₉ H ₂₅ NO ₂ : C, 83.03; H, 6.01; N, 3.34. Found: C, 82.98; H, 6.10; N, 3.56. |
| 9c | | Yield 397 mg, 90%. Yellow crystals with m.p. > 210 °C. ¹ H NMR (600 MHz, DMSO-d ₆) δ 7.81 (s, 1H), 7.70 (s, 1H), 7.60–7.62 (m, 2H), 7.55–7.56 (m, 3H), 7.46–7.47 (m, 3H), 7.39–7.40 (m, 2H), 7.19–7.22 (m, 2H), 7.11–7.15 (m, 3H), 6.26 (s, 1H), 4.18 (q, J = 7.1 Hz, 2H), 1.16 (t, J = 7.1 Hz, 3H). ¹³ C{ ¹ H} NMR (151 MHz, DMSO-d ₆) δ 160.4, 156.2, 150.3, 139.2, 137.4, 135.5, 133.6, 130.8, 130.7 (2C), 129.6, 129.1 (2C), 128.8, 128.7 (2C), 128.6 (2C), 128.5 (2C), 128.3 (2C), 126.1, 124.0, 117.4, 115.0, 112.7, 111.3, 97.6, 38.6, 14.8. Anal. Calcd for C ₃₁ H ₂₃ NO ₂ : C, 84.33; H, 5.25; N, 3.17. Found: C, 84.18; H, 5.36; N, 3.02. |
| 9d | | Yield 448 mg, 89%. Yellow solid with m.p. > 260 °C. ¹ H NMR (600 MHz, DMSO-d ₆) δ 7.21–7.72 (m, 15H), 6.93 (br s, 2H), 6.25 (br s, 1H), 5.44 (br s, 2H). ¹³ C{ ¹ H} NMR (151 MHz, DMSO-d ₆) δ 160.7, 156.6, 150.8, 140.1, 138.7, 137.8, 136.0, 133.9, 131.3 (2C), 130.9, 130.1, 129.7 (2C), 129.3, 129.2 (2C), 129.1 (6C), 128.9 (2C), 127.8, 126.8 (2C), 126.7, 124.5, 118.0, 115.9, 113.5, 112.0, 98.7, 47.4. Anal. Calcd for C ₃₆ H ₂₅ NO ₂ : C, 85.86; H, 5.00; N, 2.78. Found: C, 85.90; H, 4.85; N, 2.92. |
| 10 | | Yield 162 mg, 42%. Beige solid with m.p.= 250 °C. ¹ H NMR (400 MHz, DMSO-d ₆) δ 11.62 (s, 1H), 8.90 (m, 1H), 8.37 (m 1H), 8.05 (m, 1H), 7.73 (m, 1H), 7.67 (d, J = 8.7 Hz, 1H), 7.53–7.54 (m, 2H), 7.30–7.43 (m, 8H), 7.22 (d, J = 8.7 Hz, 1H). ¹³ C{ ¹ H} NMR (101 MHz, DMSO-d ₆) δ 160.5, 148.2, 136.6, 135.2, 134.1, 133.5, 131.9, 130.7, 129.9 (2C), 129.8, 129.5 (2C), 128.7 (2C), 128.4, 128.2 (2C), 127.8, 126.5 (2C), 125.8, 121.4, 120.2, 115.0, 110.7, 104.1. Anal. Calcd for C ₂₇ H ₁₇ NO ₂ : C, 83.70; H, 4.42; N, 3.62. Found: C, 83.82; H, 4.35; N, 3.52. |

| Cmpd | Structure | Characterization |
|------|---|---|
| 12 |  | <p>Yield 1211 mg, 68%. Beige solid with m.p.= 210–212 °C.</p> <p>¹H NMR (400 MHz, DMSO-d₆) δ 11.96 (s, 1H), 7.61–7.63 (m, 3H), 7.53–7.54 (m, 3H), 7.48 (s, 1H), 6.84 (s, 2H), 6.62 (s, 2H), 6.23 (s, 1H), 3.68 (s, 3H), 3.66 (s, 6H), 3.64 (s, 3H), 3.60 (s, 6H). ¹³C{¹H} NMR (101 MHz, DMSO-d₆) δ 160.4, 156.4, 153.0 (2C), 152.7 (2C), 150.3, 137.6, 137.5, 136.3, 136.1, 135.8, 129.5, 128.7 (2C), 128.5 (2C), 126.6, 125.6, 117.3, 113.6, 112.6, 111.2, 107.0 (2C), 105.8 (2C), 97.9, 60.14 (3C), 60.07 (3C), 55.8 (6C), 55.7 (6C). Anal. Calcd for C₃₅H₃₁NO₈: C, 70.82; H, 5.26; N, 2.36. Found: C, 70.72; H, 5.16; N, 2.51.</p> |
| 13 |  | <p>¹H NMR (400 MHz, DMSO) δ 11.37 (s, 1H), 7.24–7.44 (m, 11H), 6.94 (d, J = 2.3 Hz, 1H), 6.71 (dd, J = 8.7 Hz, J = 2.3 Hz, 1H), 3.80 (s, 3H). ¹³C{¹H} NMR (101 MHz, DMSO) δ 156.1, 136.9, 135.4, 132.7 (2C), 129.6 (2C), 128.6 (2C), 128.4 (2C), 127.8 (2C), 127.1, 126.0, 122.4, 119.3, 113.3, 109.9, 94.4, 55.2.</p> |

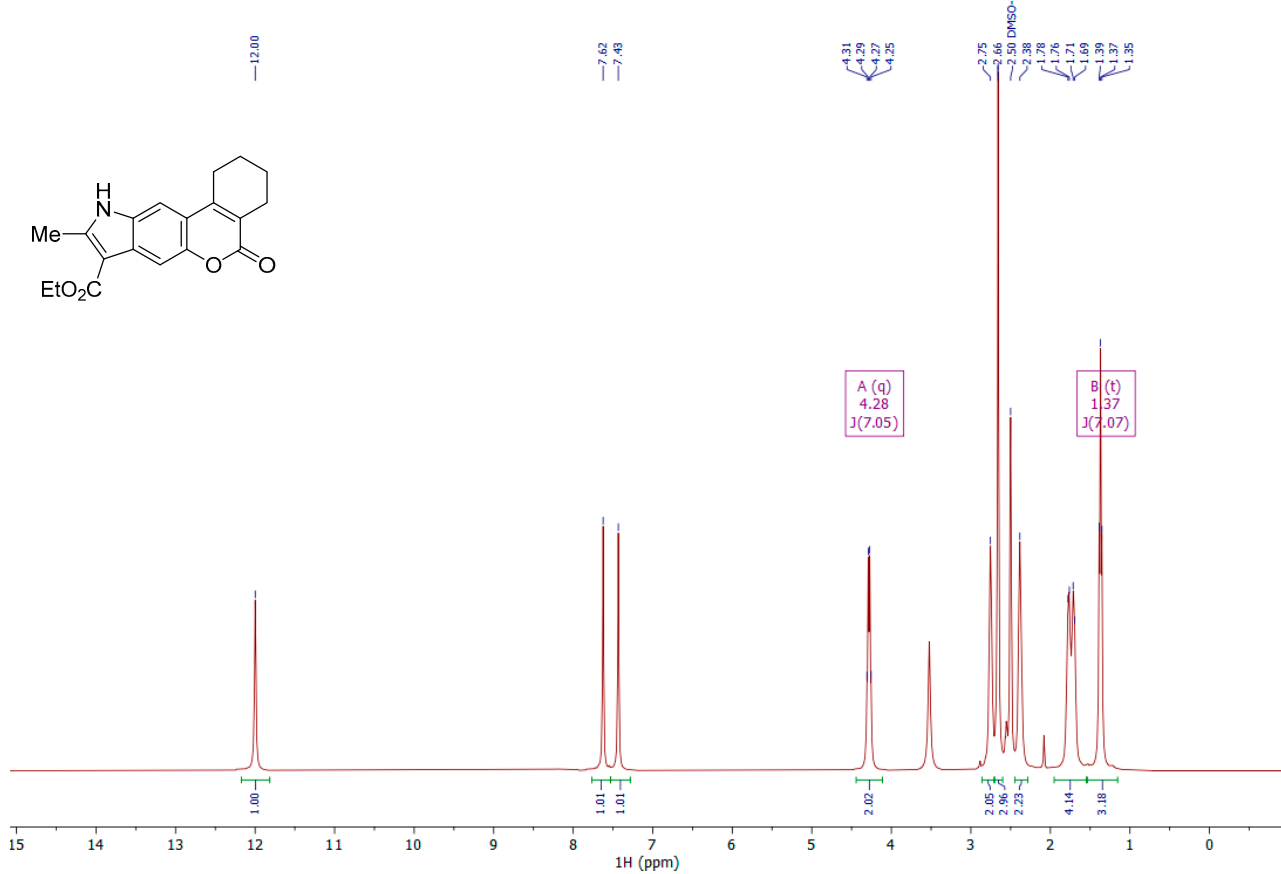


Figure S1. ¹H NMR spectrum of **2**.

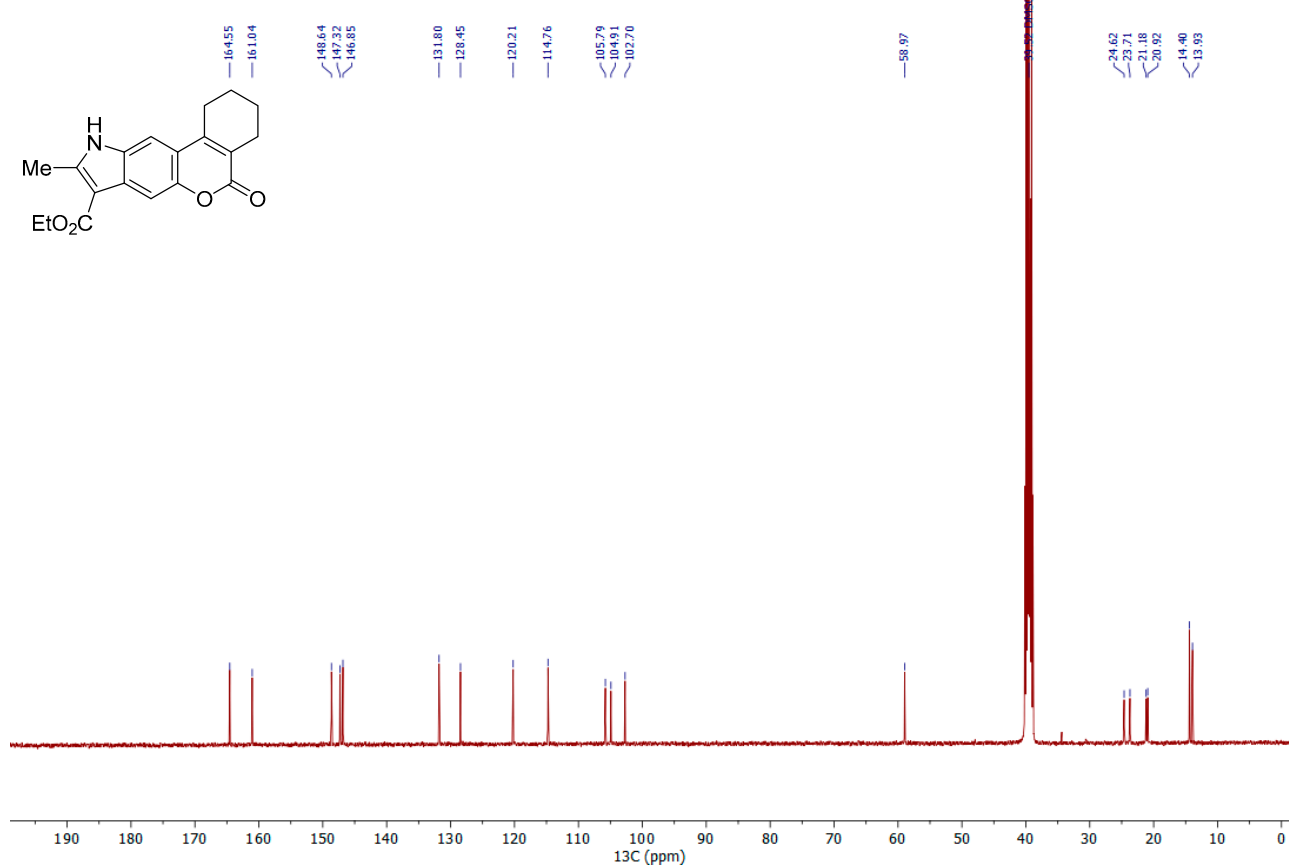


Figure S2. ¹³C NMR spectrum of **2**.

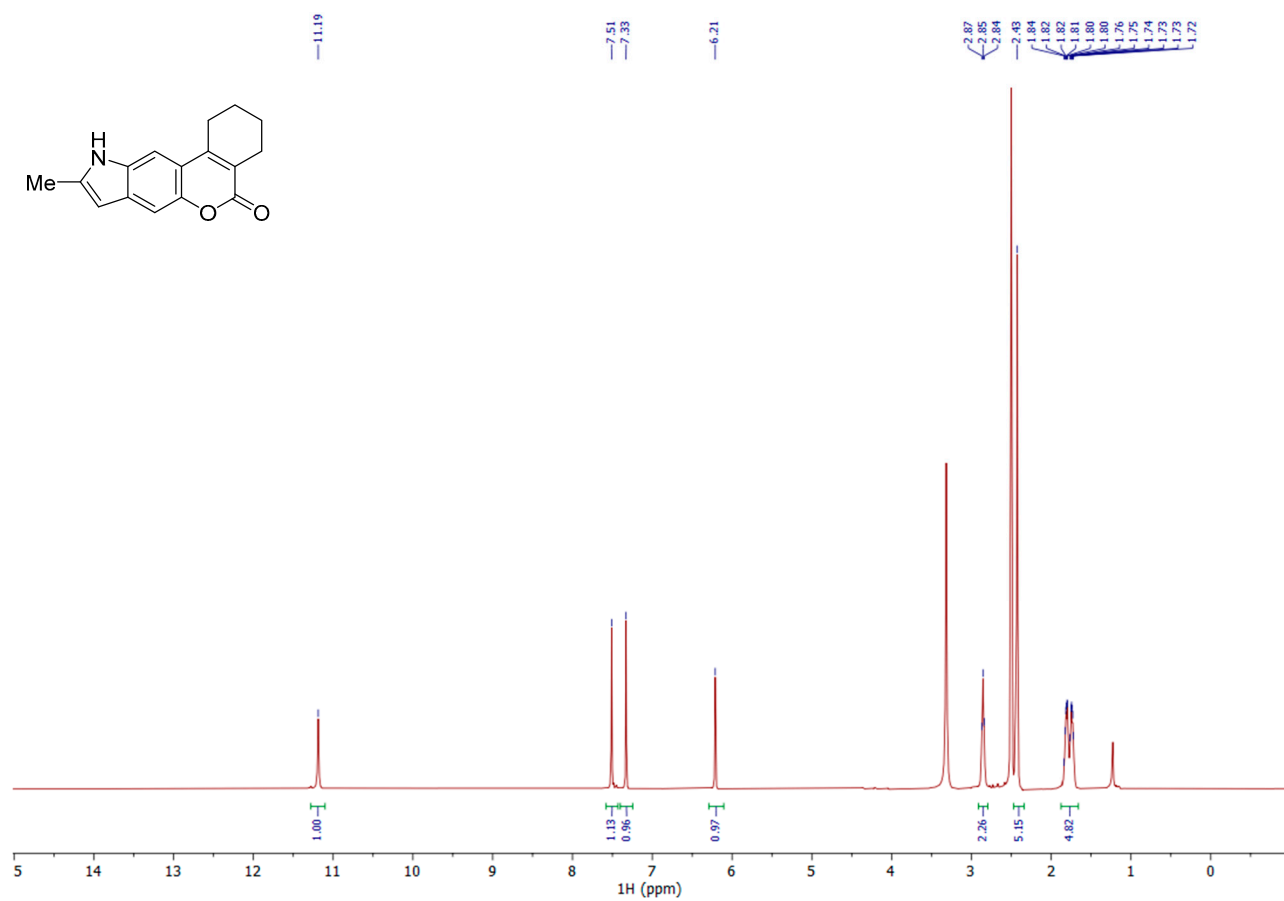


Figure S3. ¹H NMR spectrum of 3.

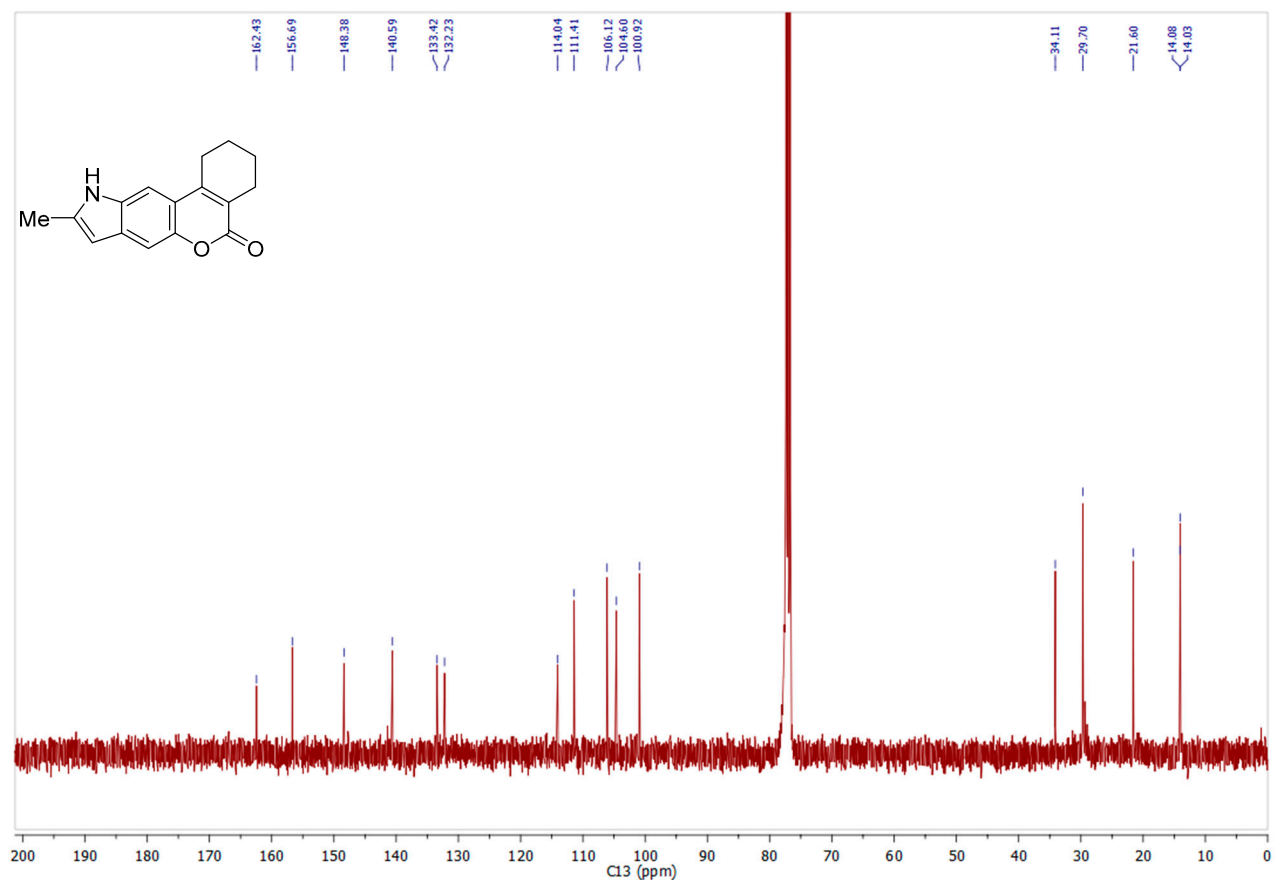


Figure S4. ¹³C NMR spectrum of 3.

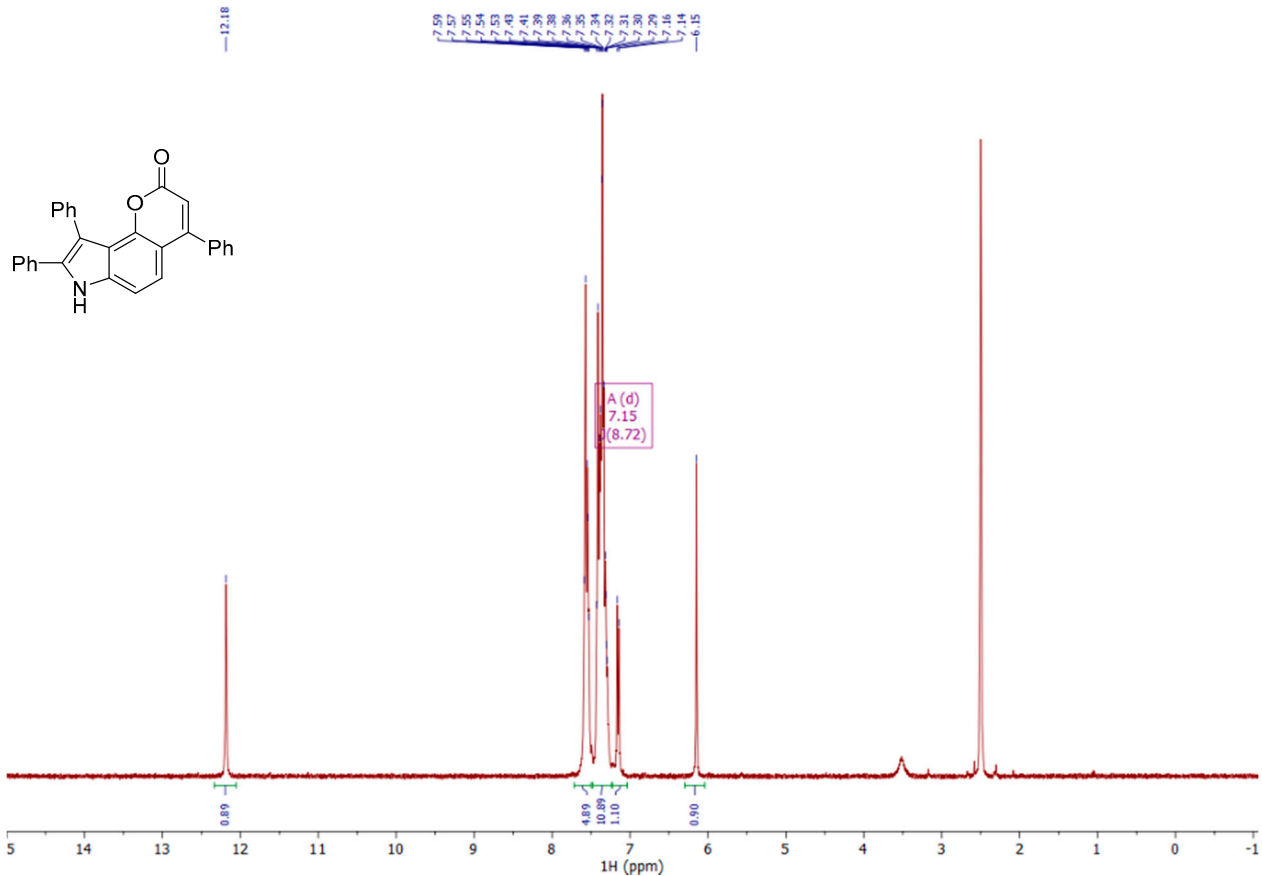


Figure S5. ¹H NMR spectrum of 6a.

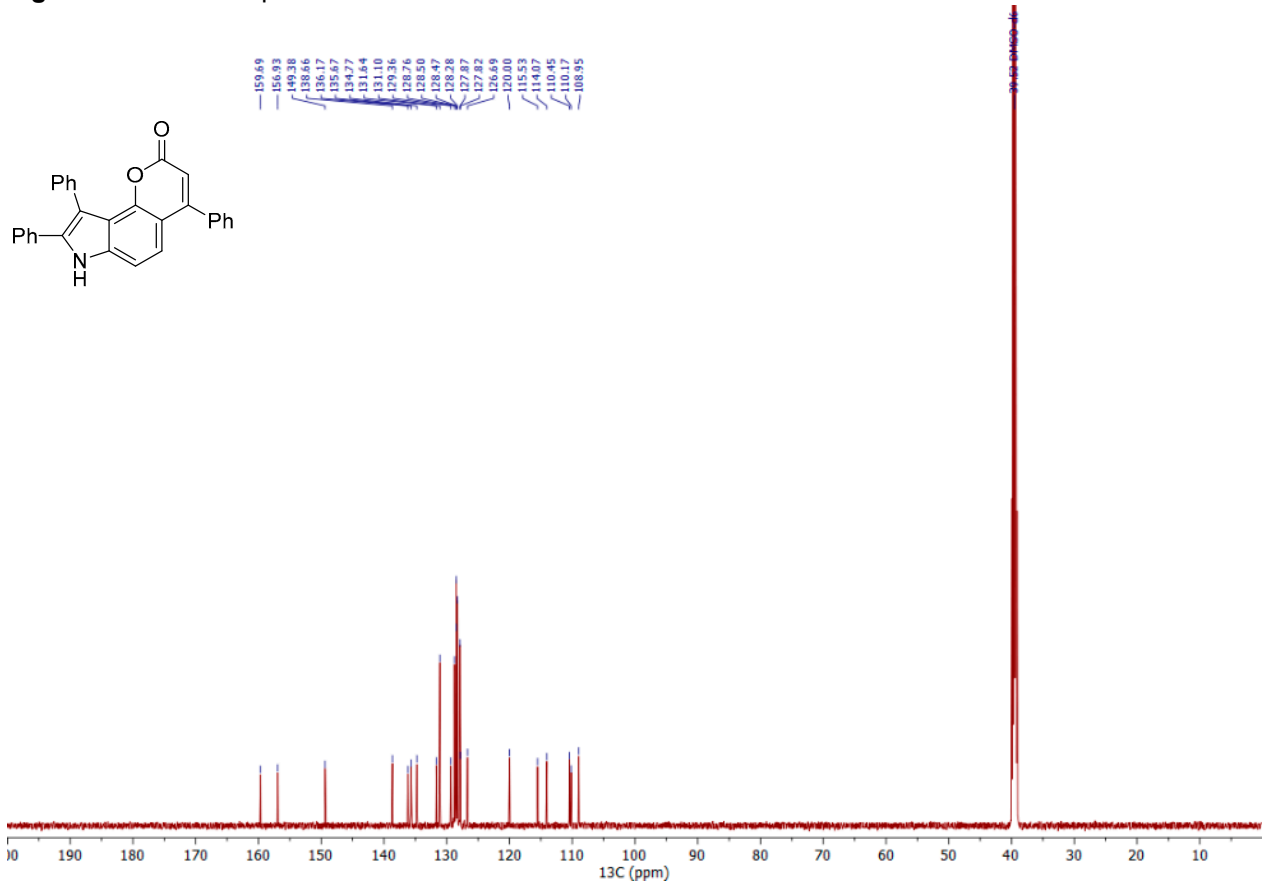


Figure S6. ¹³C NMR spectrum of 6a.

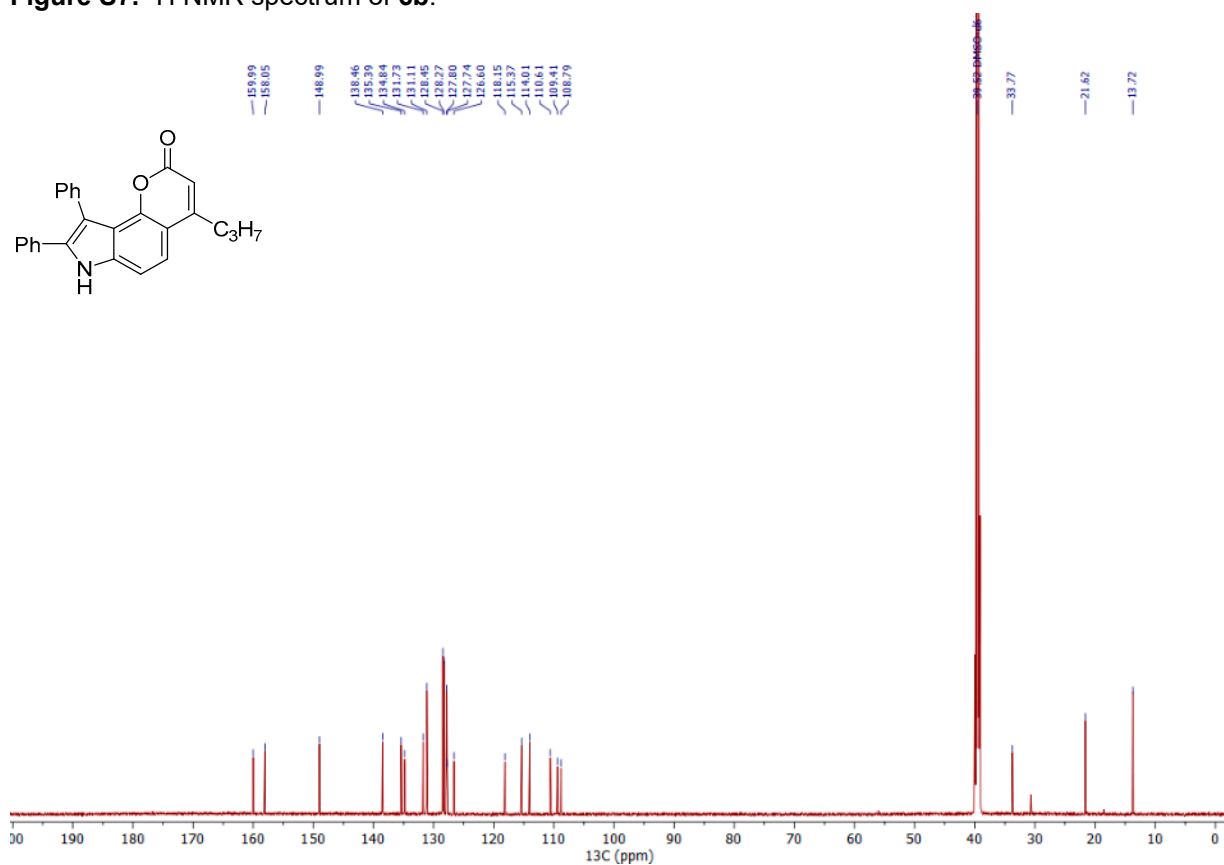
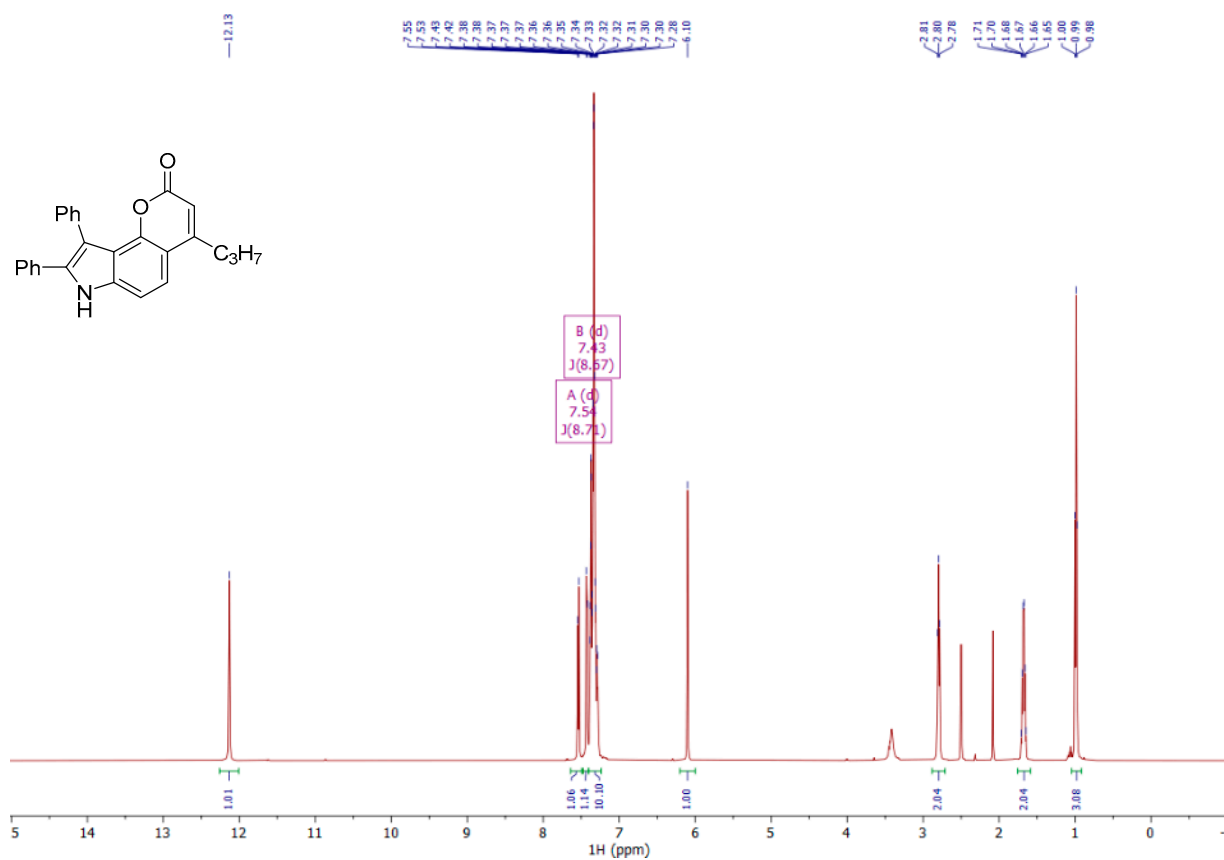


Figure S8. ^{13}C NMR spectrum of **6b**.

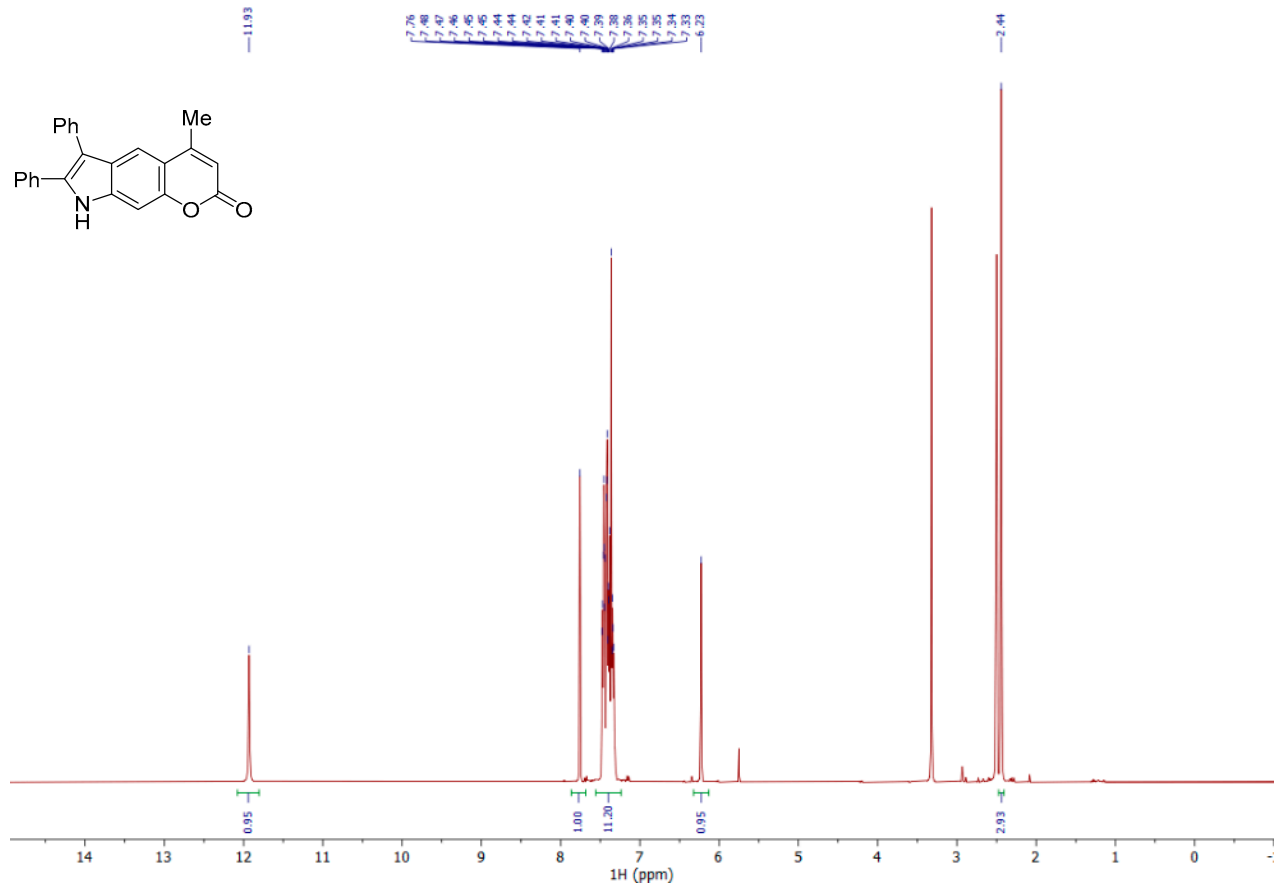


Figure S9. ¹H NMR spectrum of 7a.

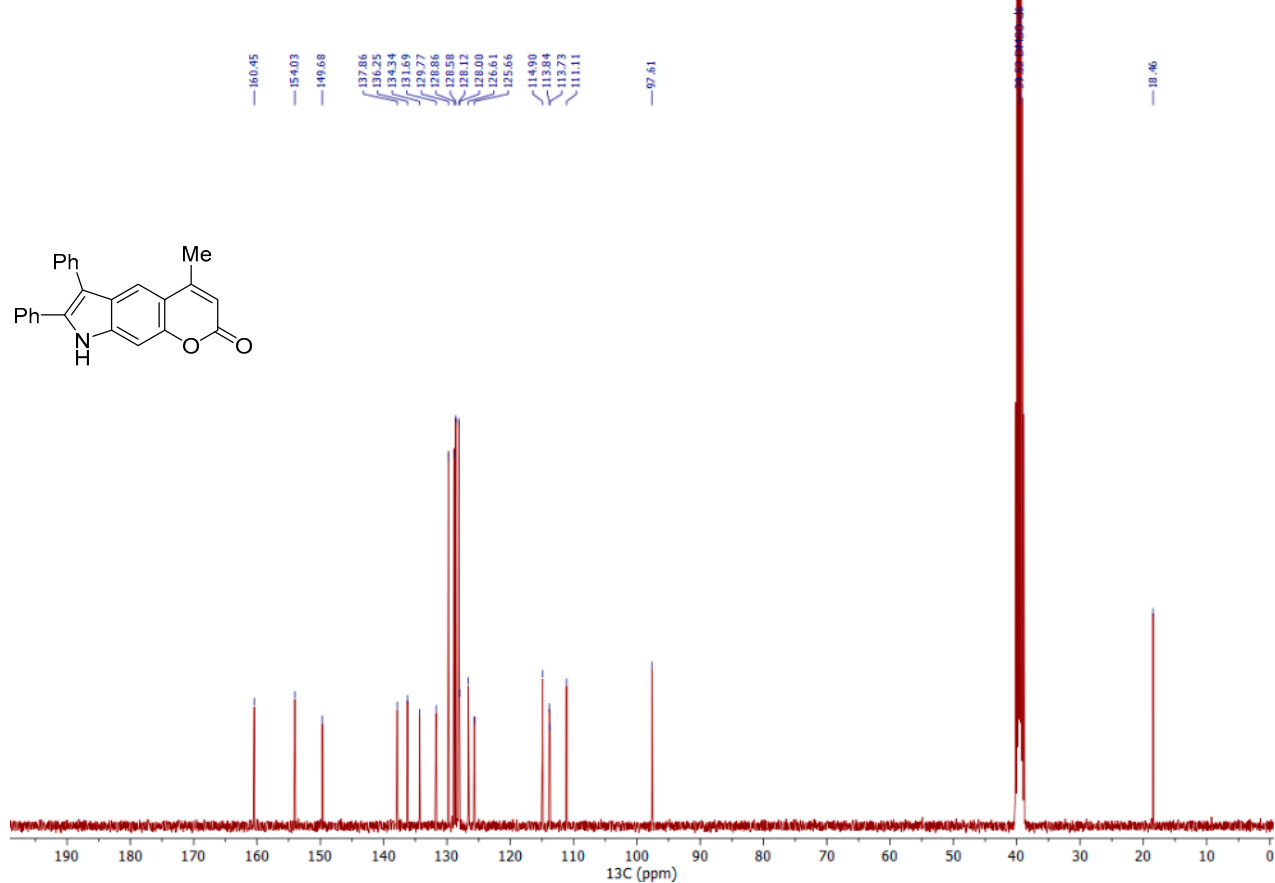


Figure S10. ¹³C NMR spectrum of 7a.

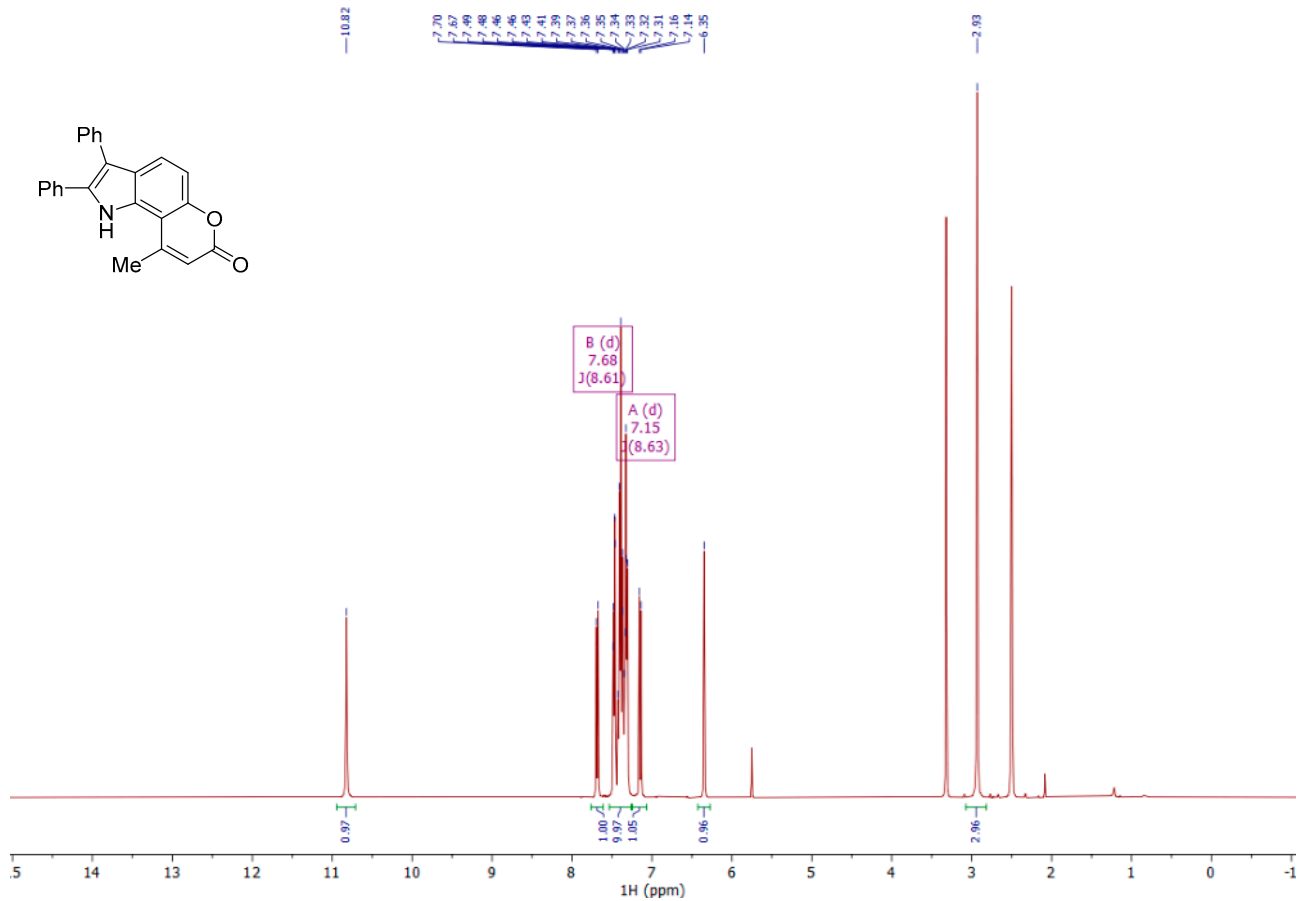


Figure S11. ^1H NMR spectrum of **8a**.

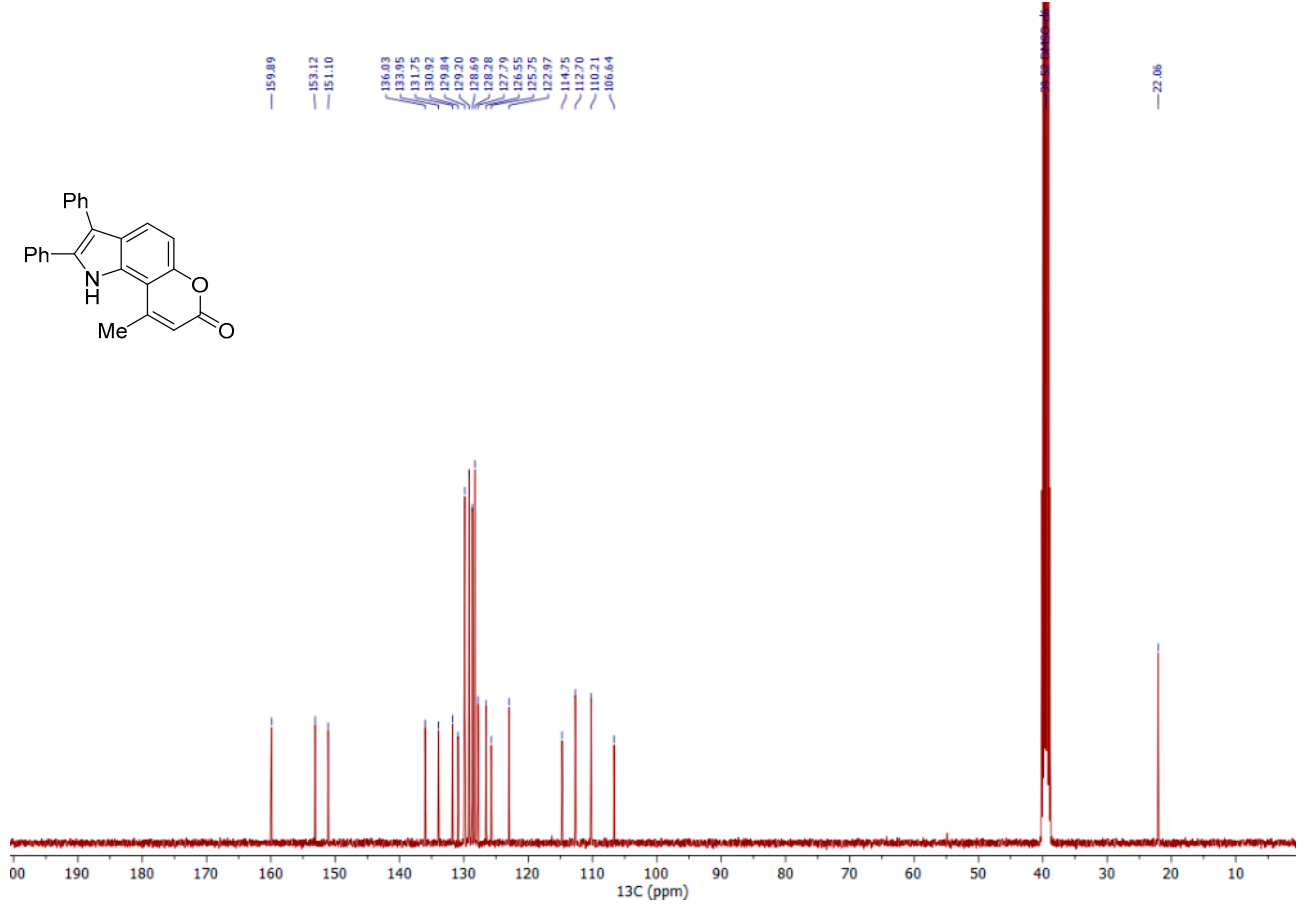


Figure S12. ^{13}C NMR spectrum of **8a**.

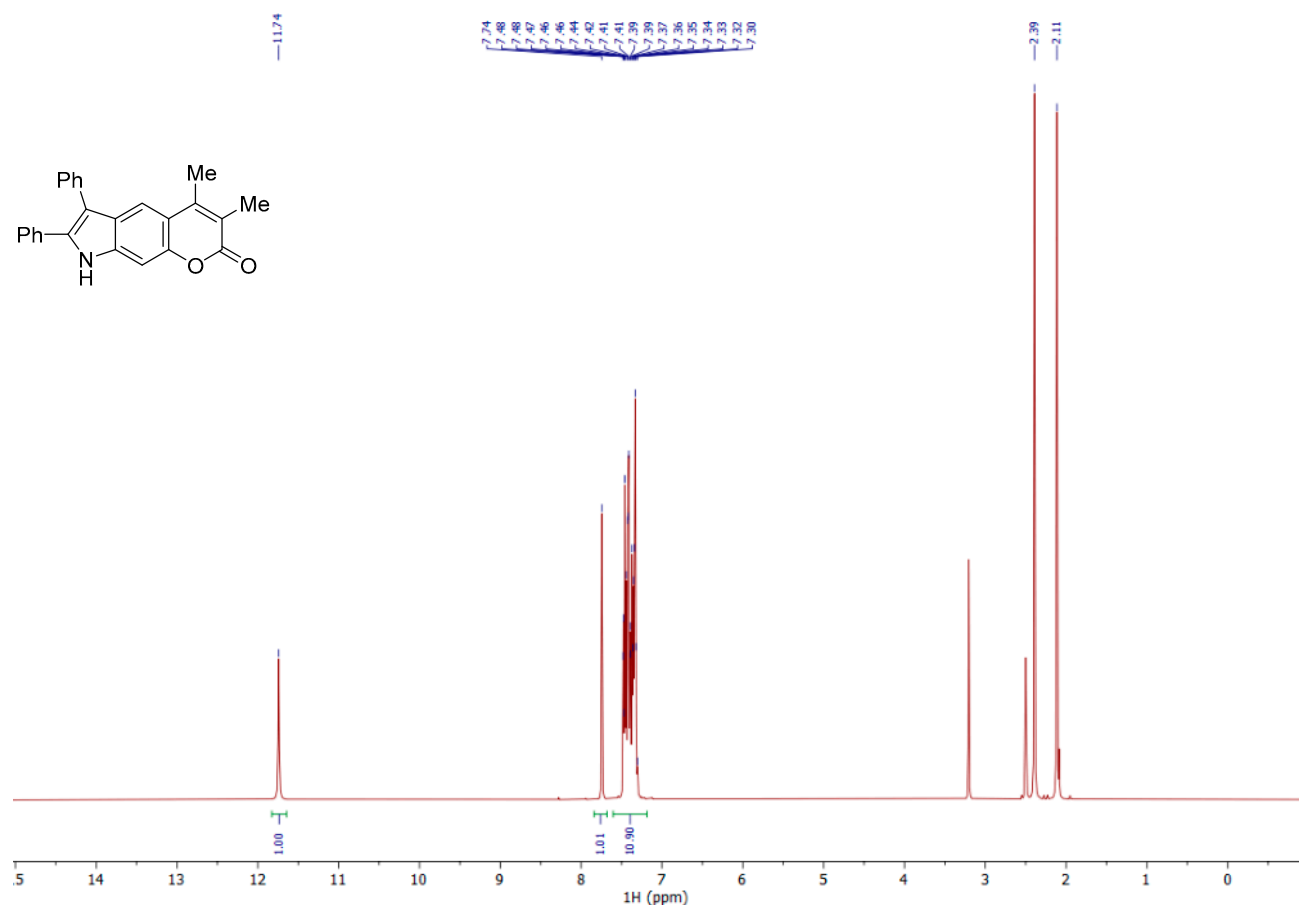


Figure S13. ^1H NMR spectrum of **7b**.

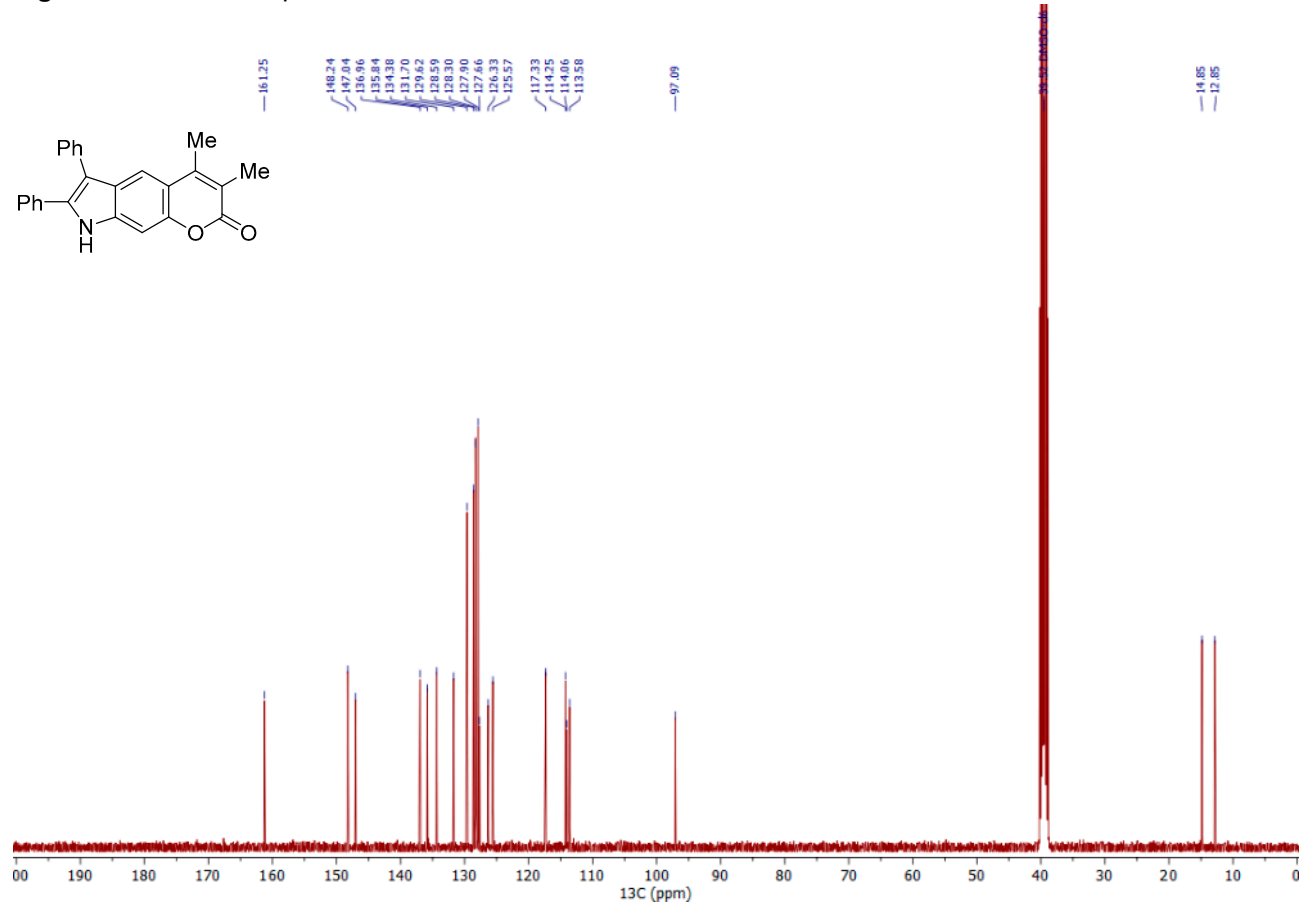


Figure S14. ^{13}C NMR spectrum of **7b**.

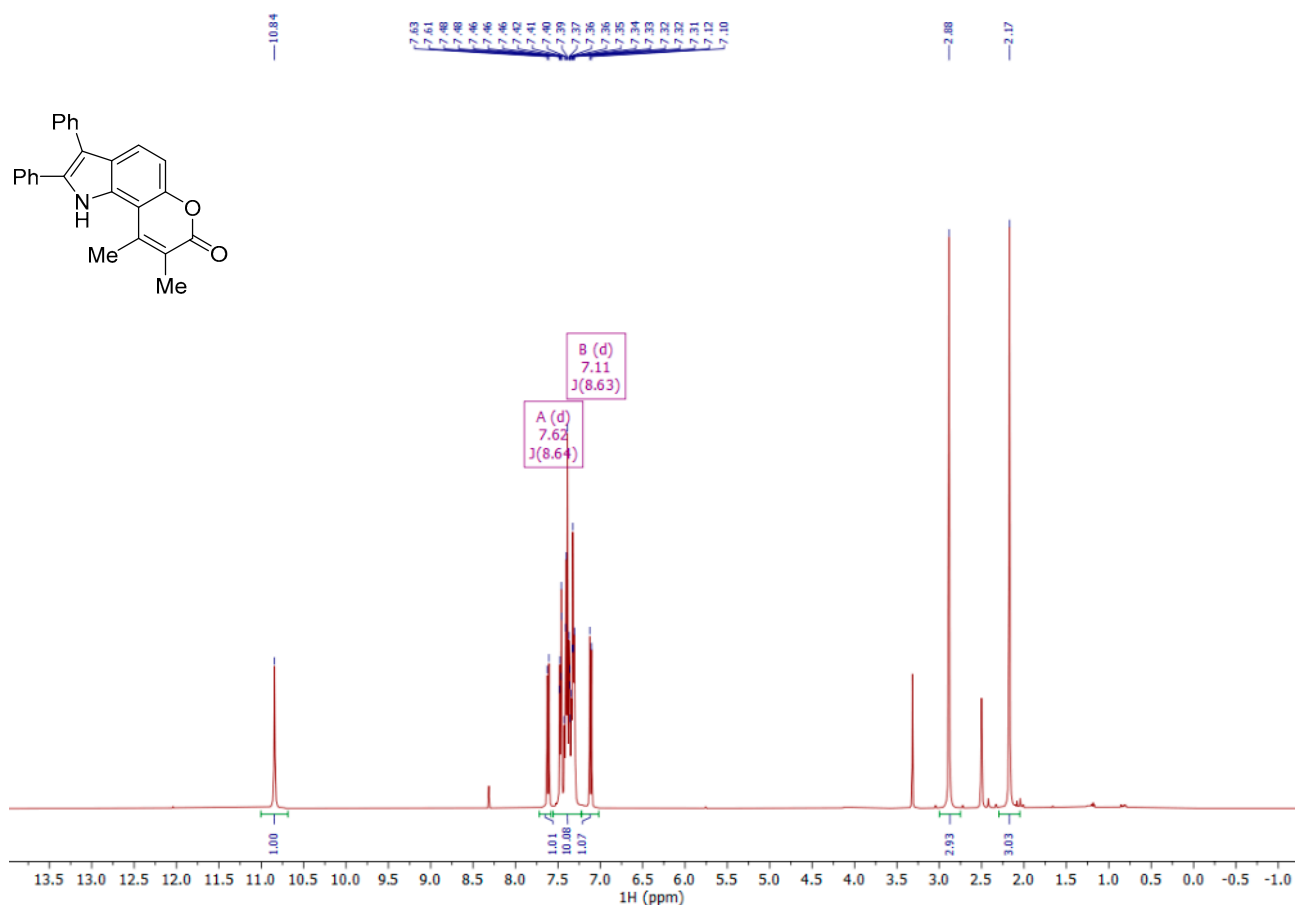


Figure S15. ¹H NMR spectrum of **8b**.

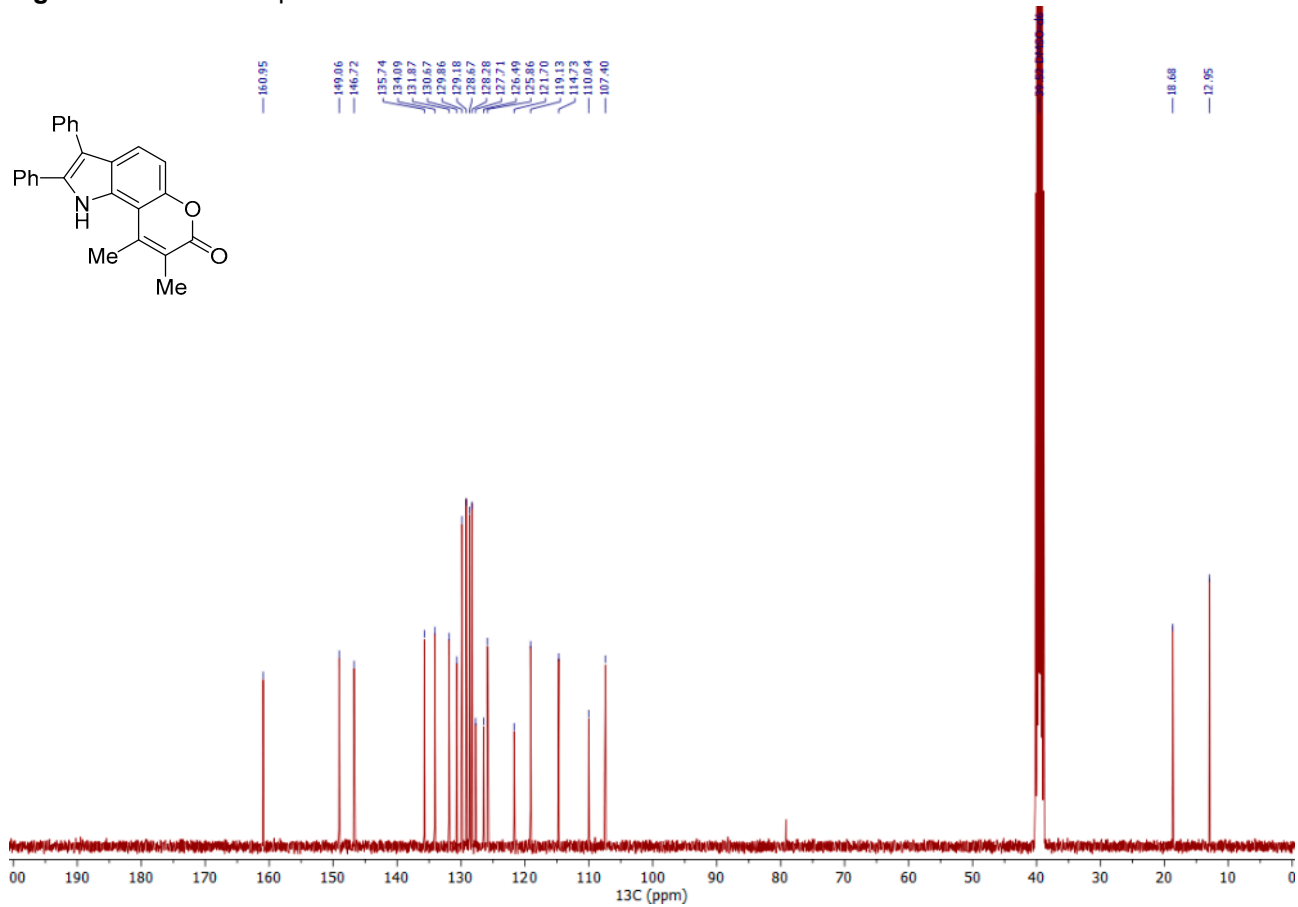


Figure S16. ¹³C NMR spectrum of **8b**.

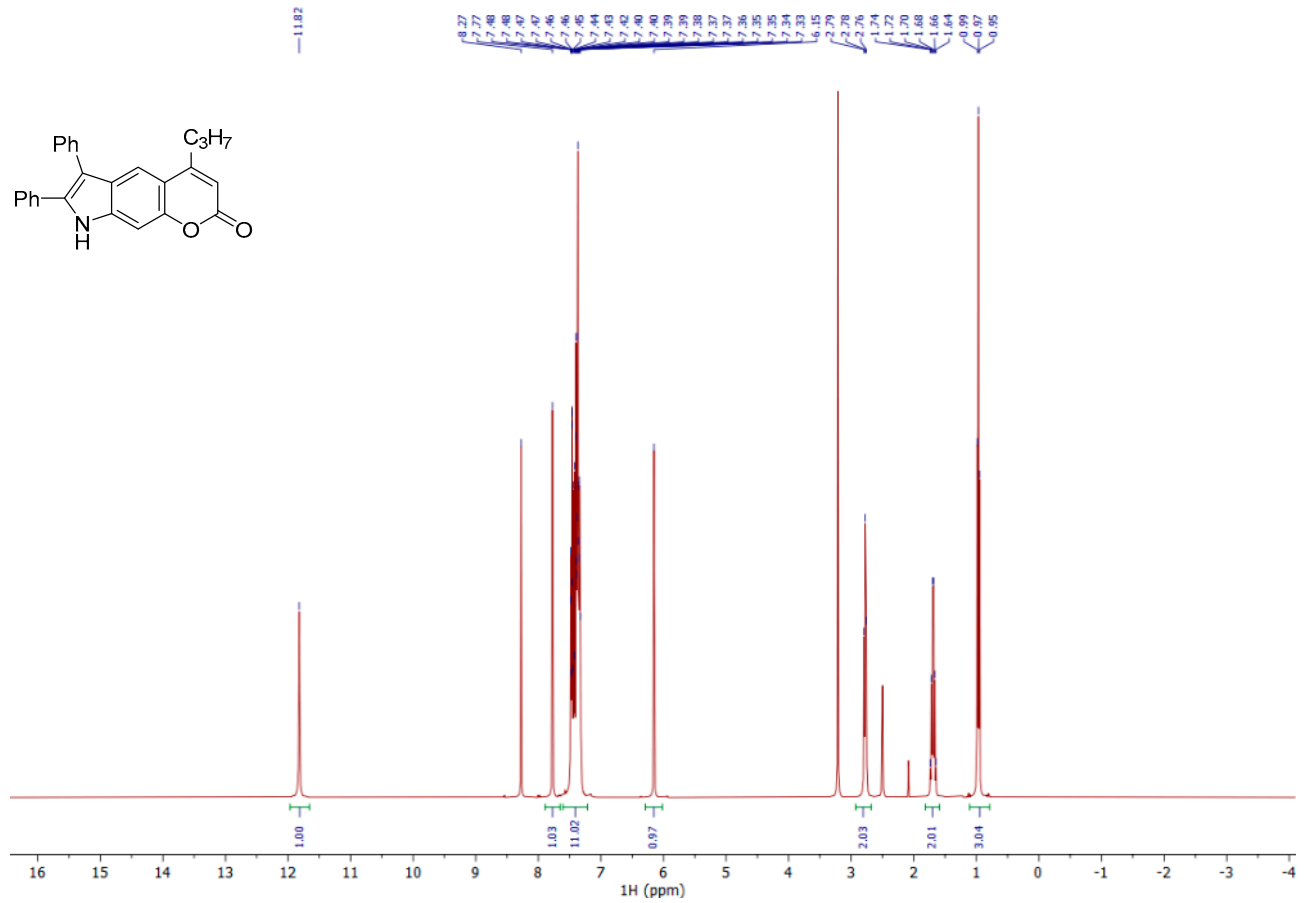


Figure S17. ¹H NMR spectrum of 7c.

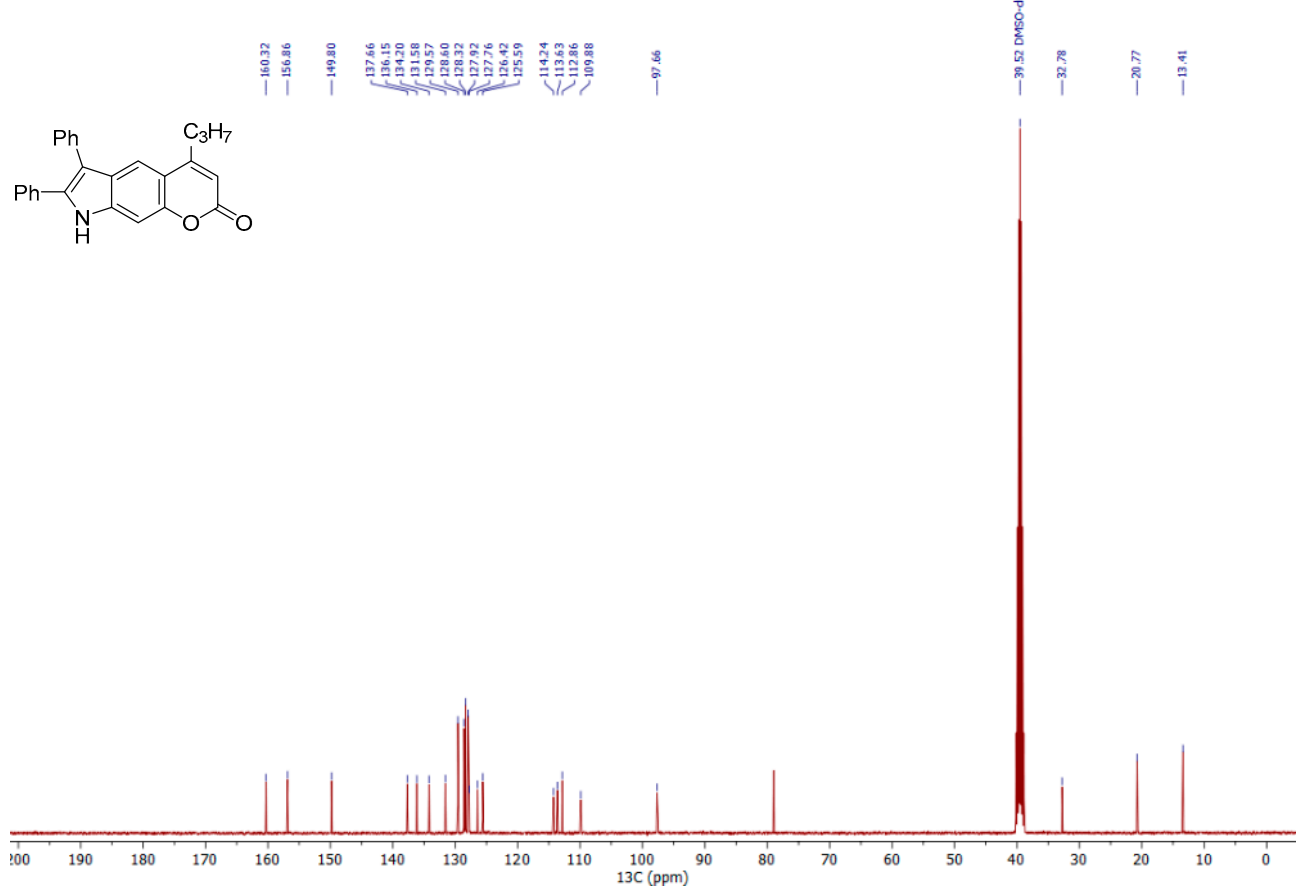
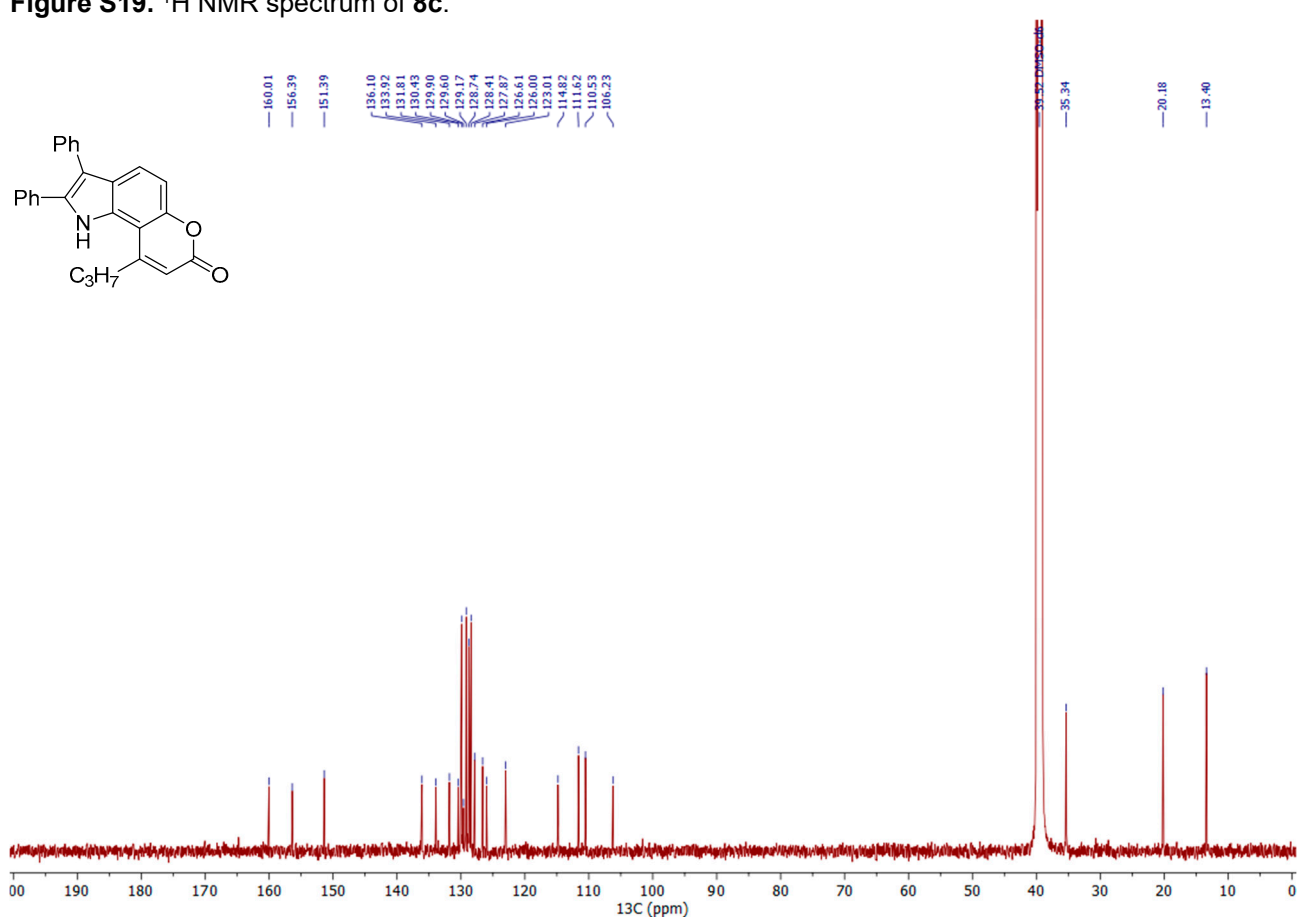
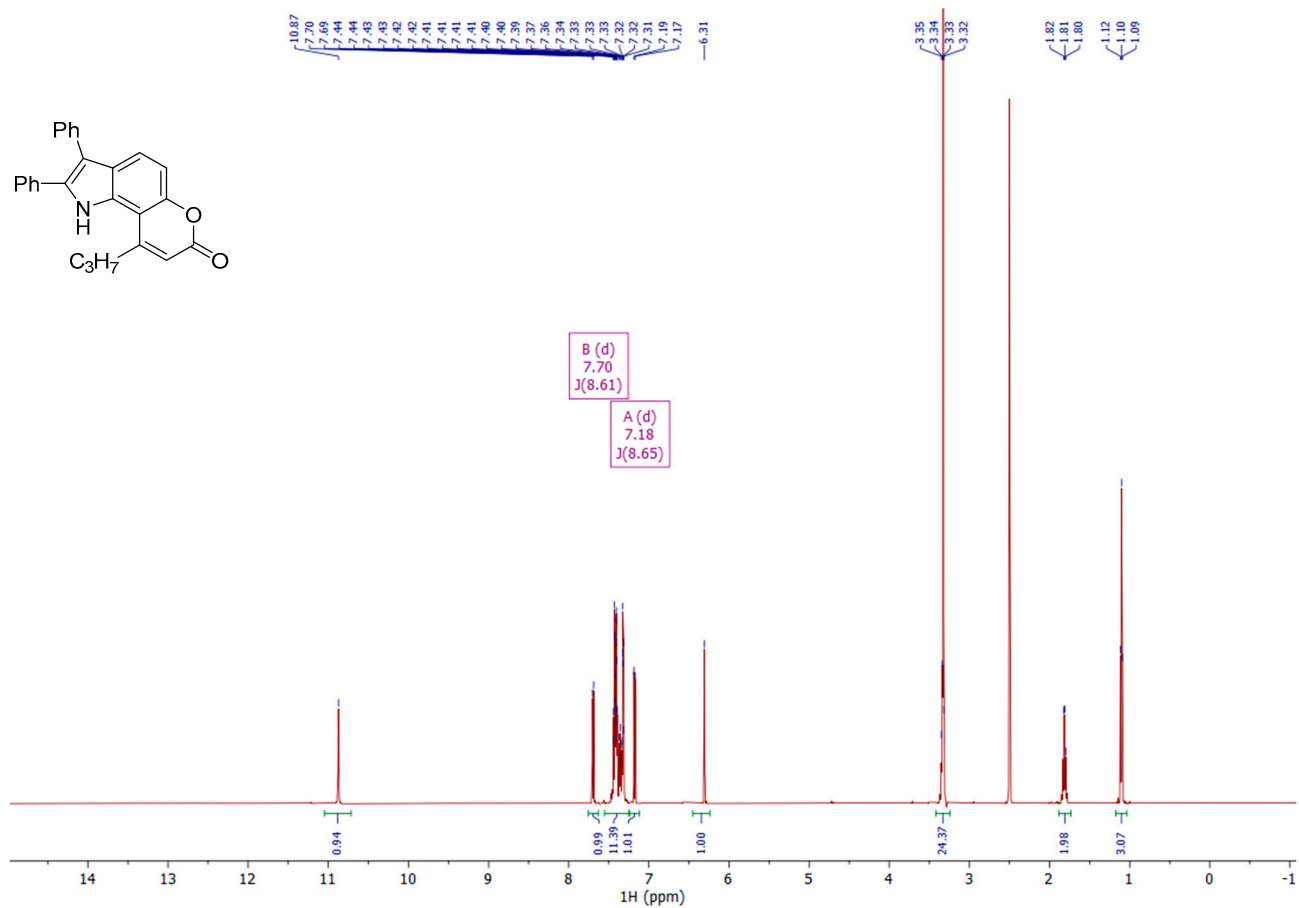


Figure S18. ¹³C NMR spectrum of 7c.



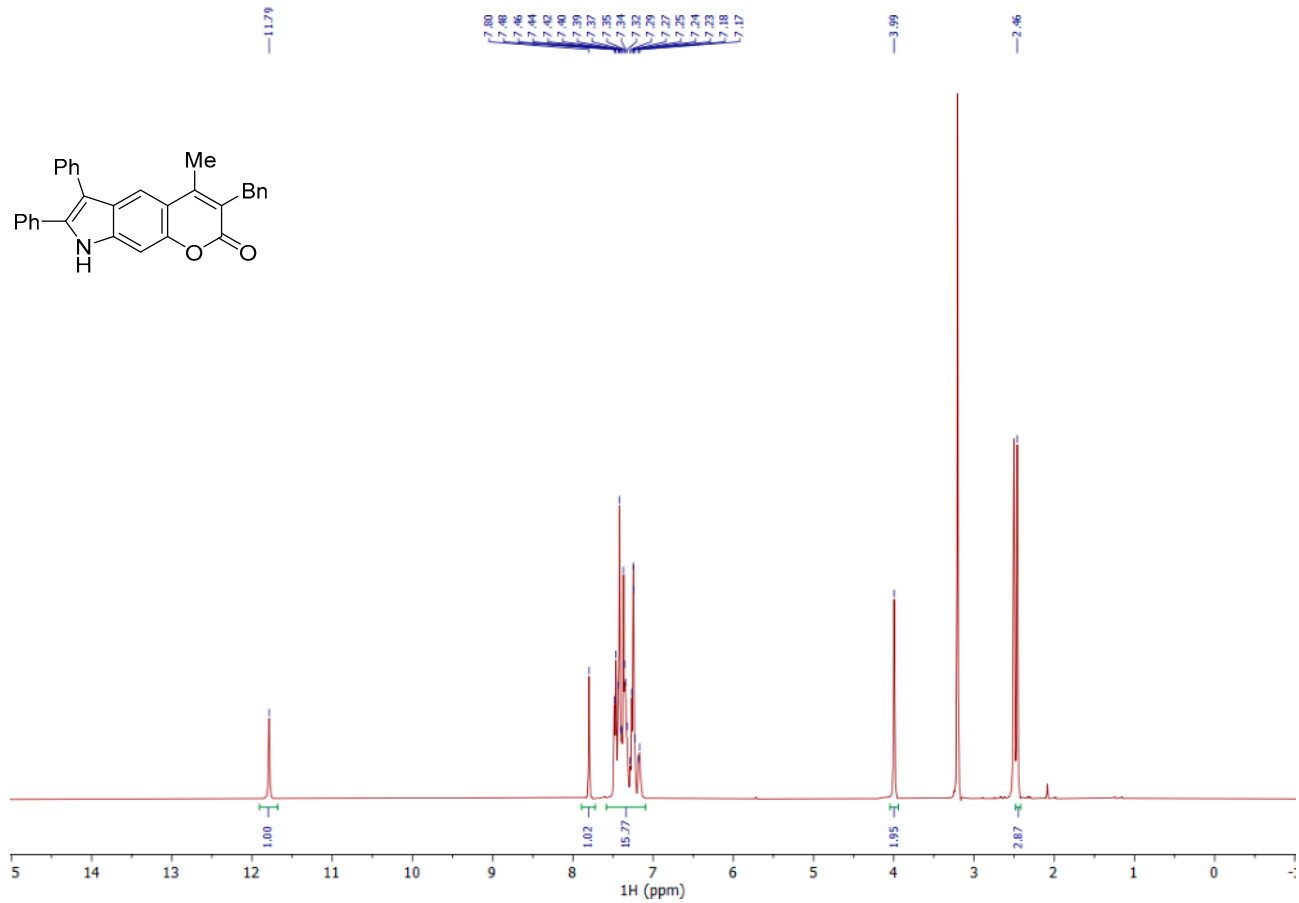


Figure S21. ^1H NMR spectrum of **7d**.

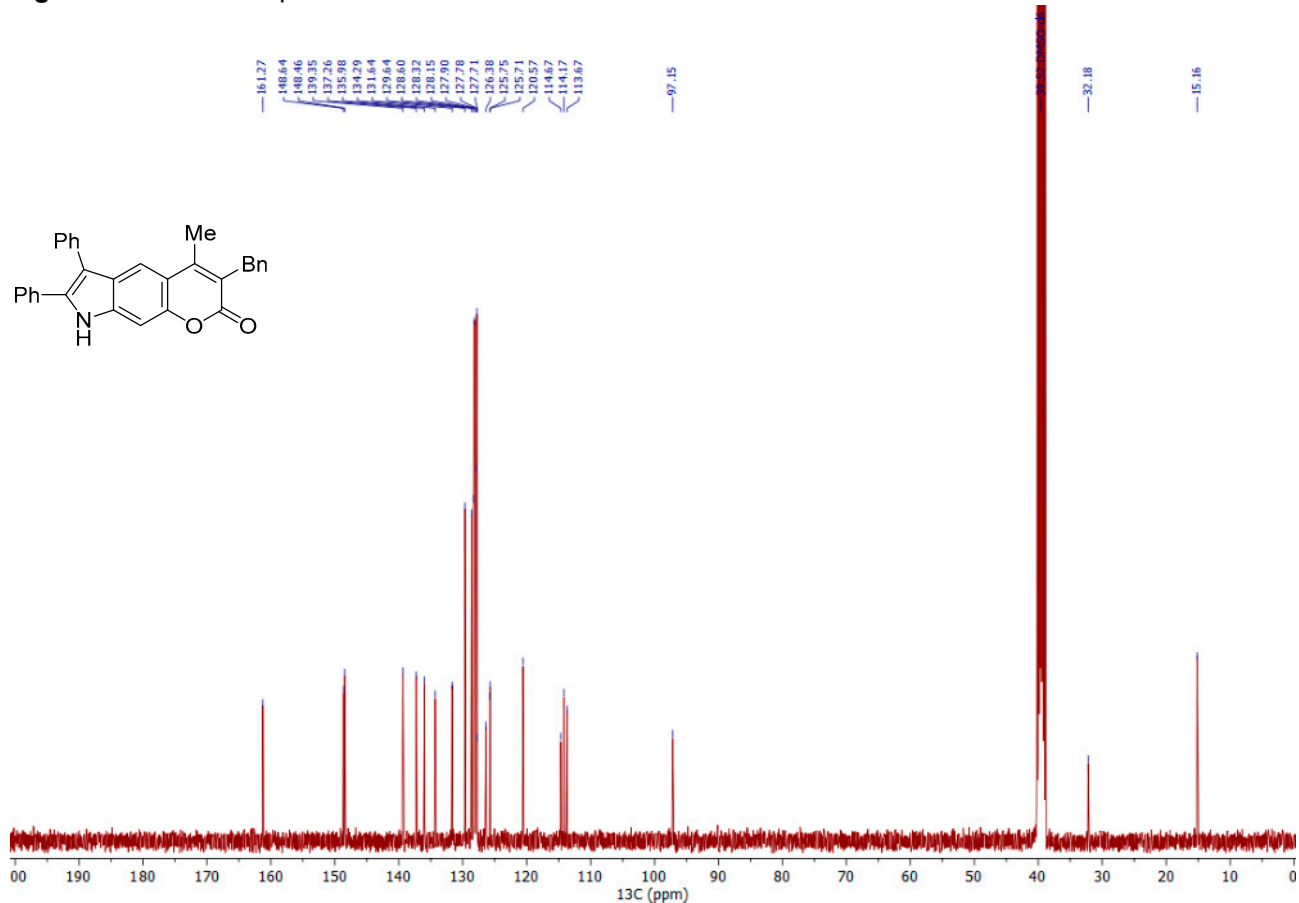


Figure S22. ^{13}C NMR spectrum of **7d**.

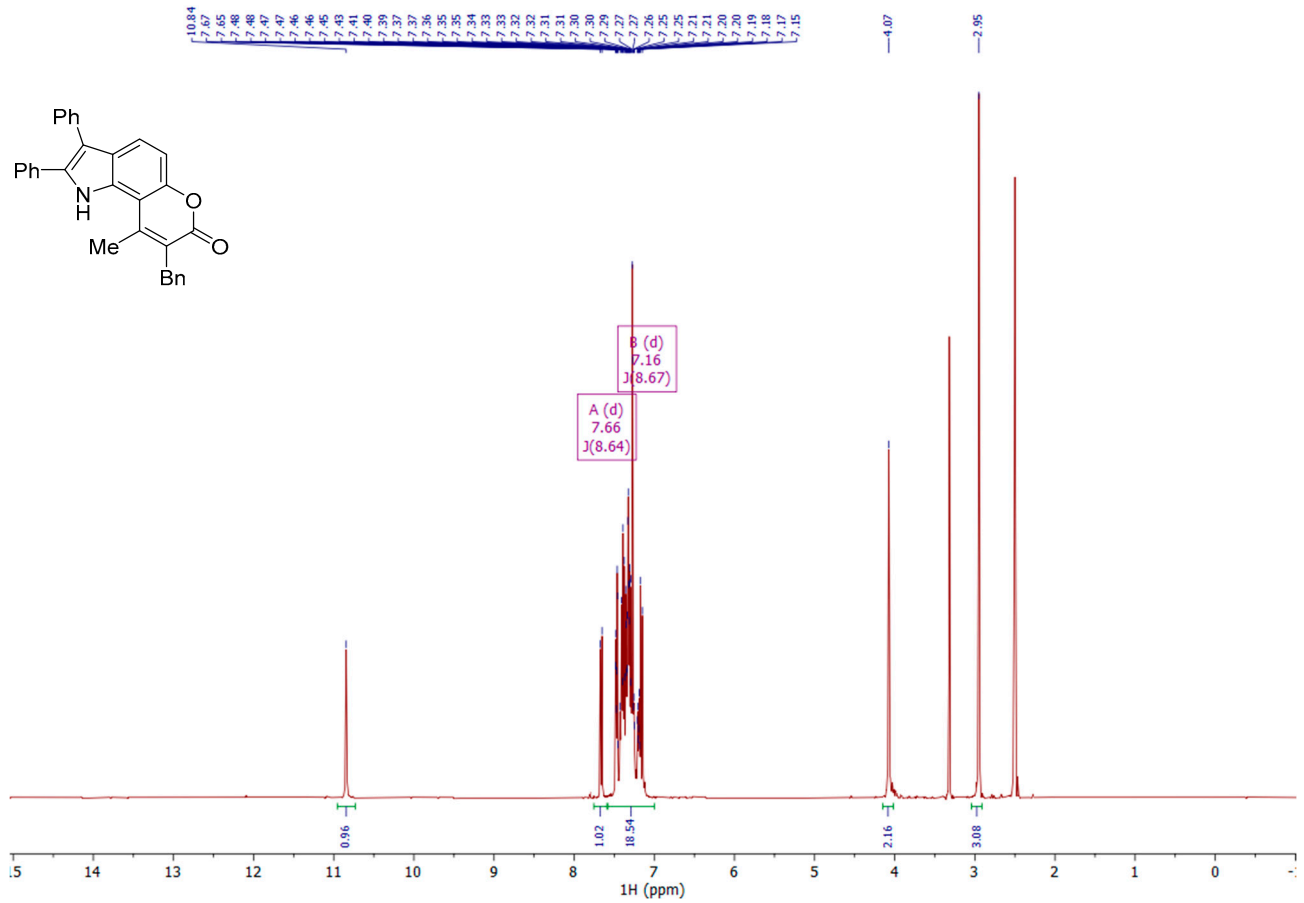


Figure S23. ¹H NMR spectrum of **8d**.

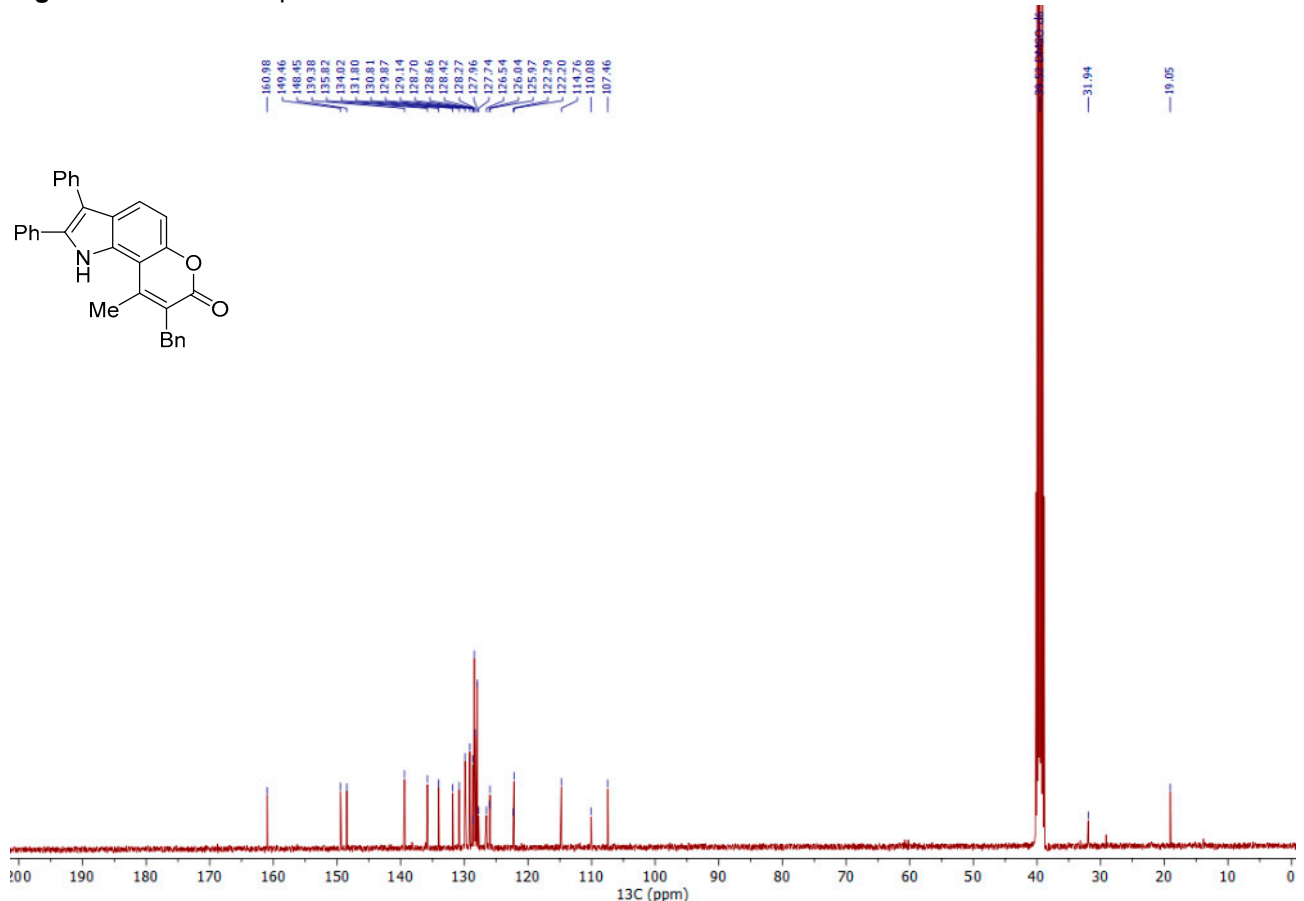


Figure S24. ¹³C NMR spectrum of **8d**.

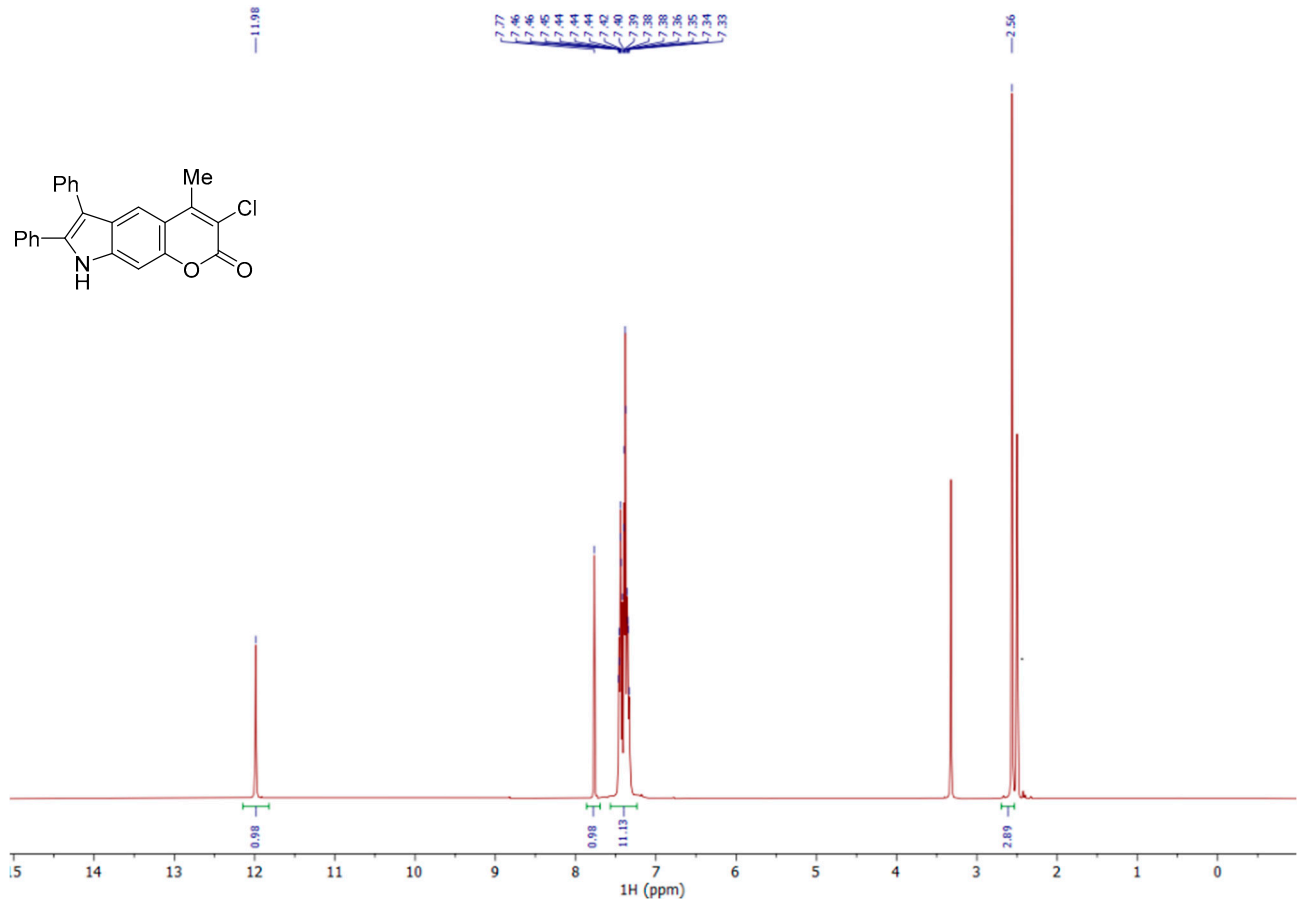


Figure S25. ^1H NMR spectrum of **7e**.

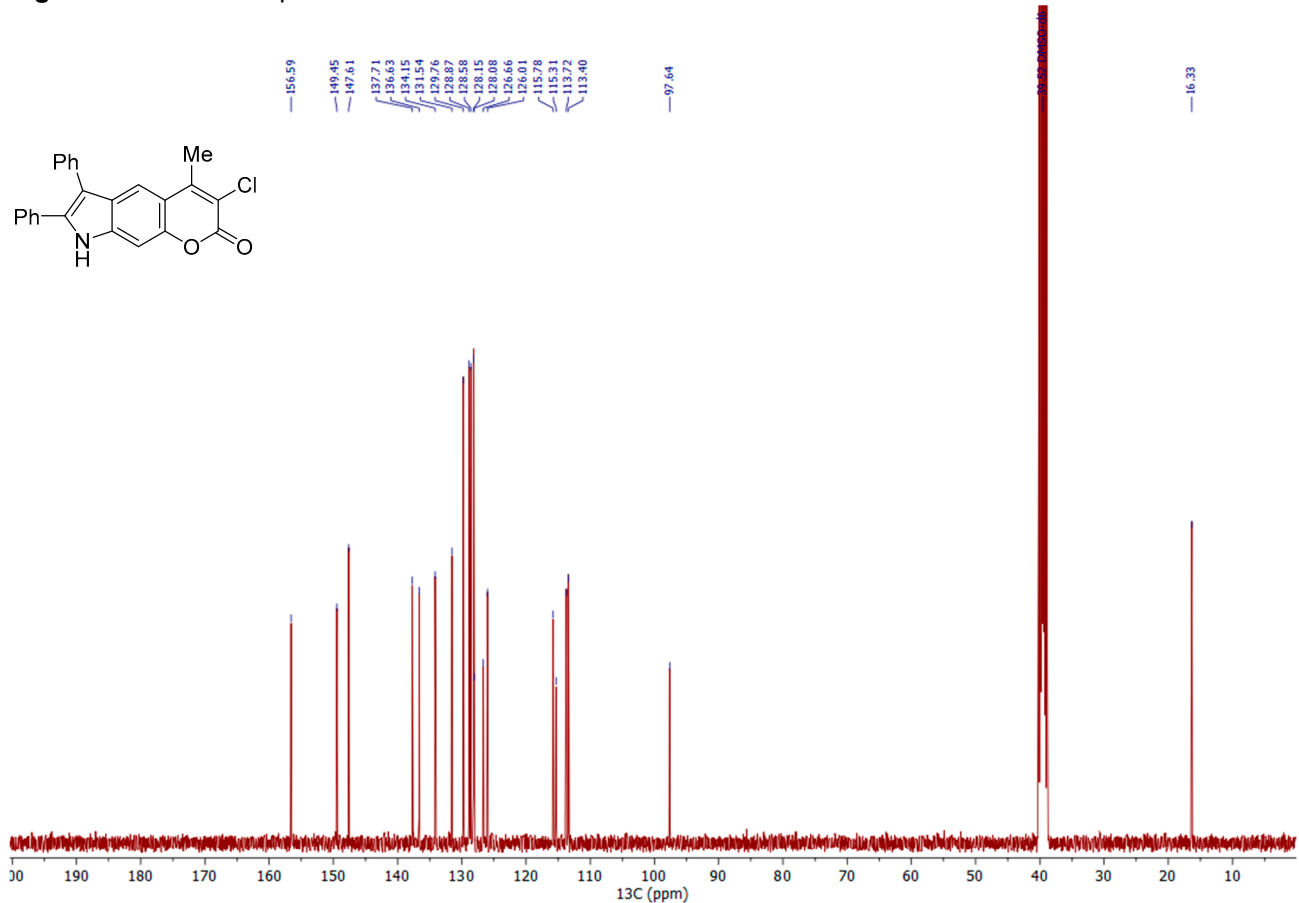


Figure S26. ^{13}C NMR spectrum of **7e**.

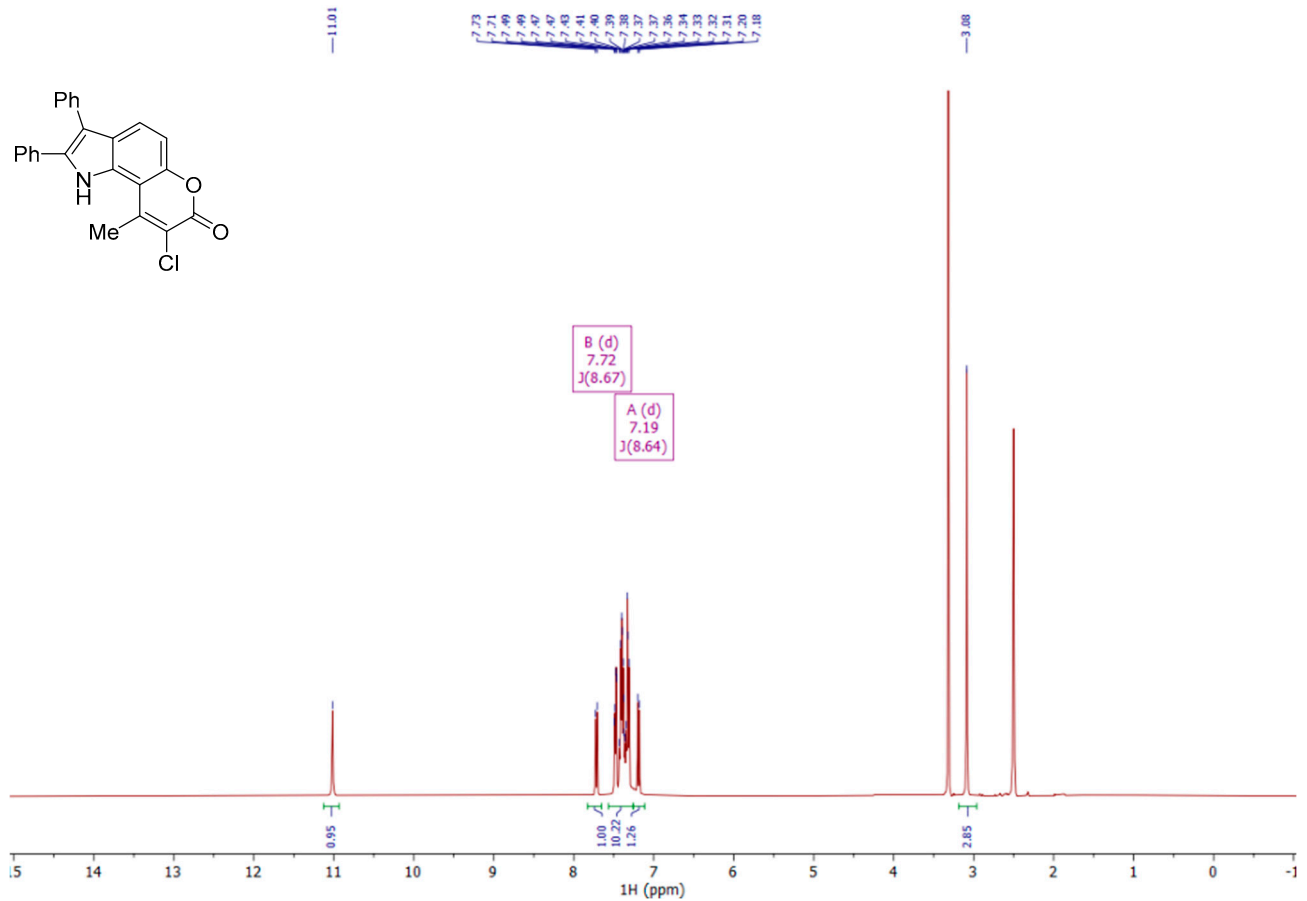


Figure S27. ^1H NMR spectrum of **8e**.

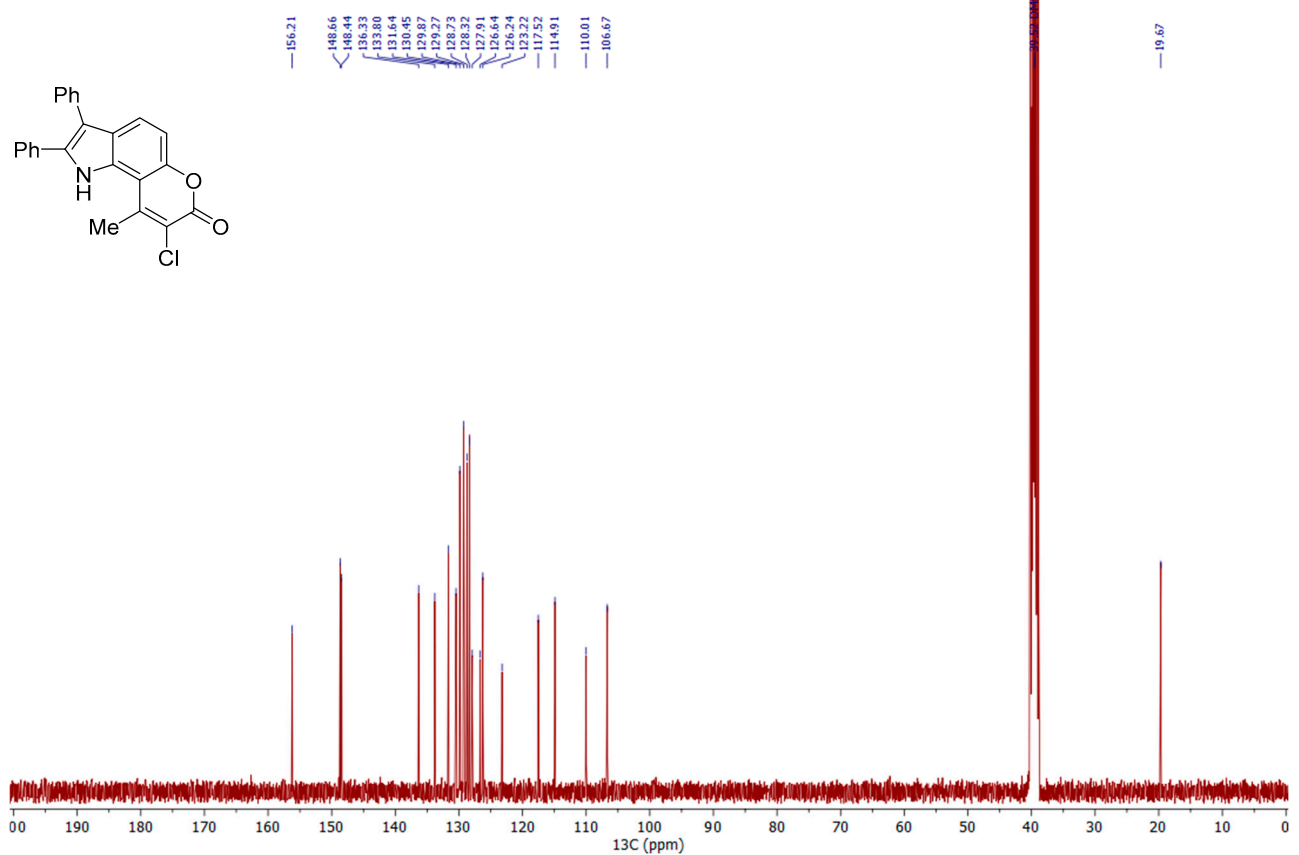


Figure S28. ^{13}C NMR spectrum of **8e**.

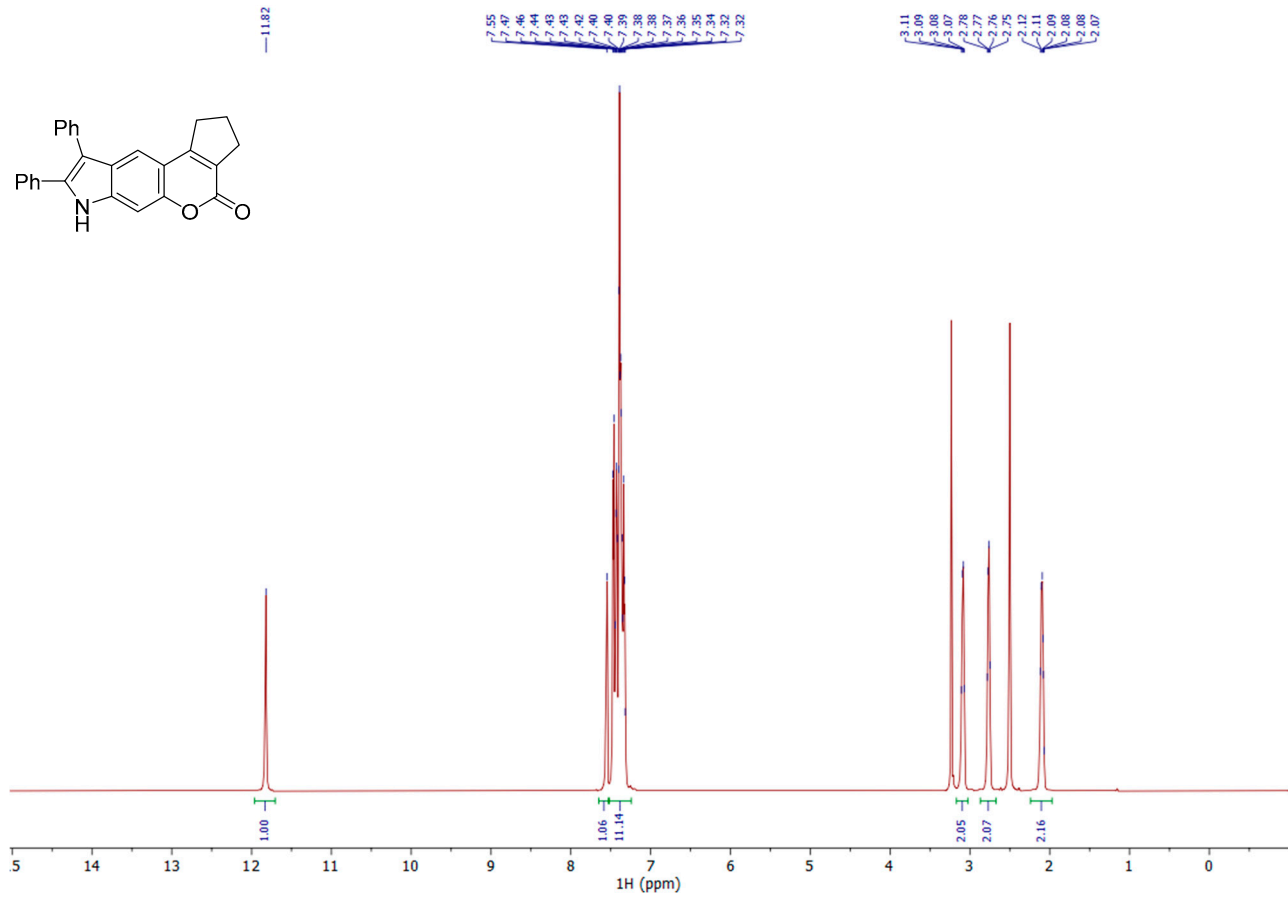


Figure S29. ^1H NMR spectrum of **7f**.

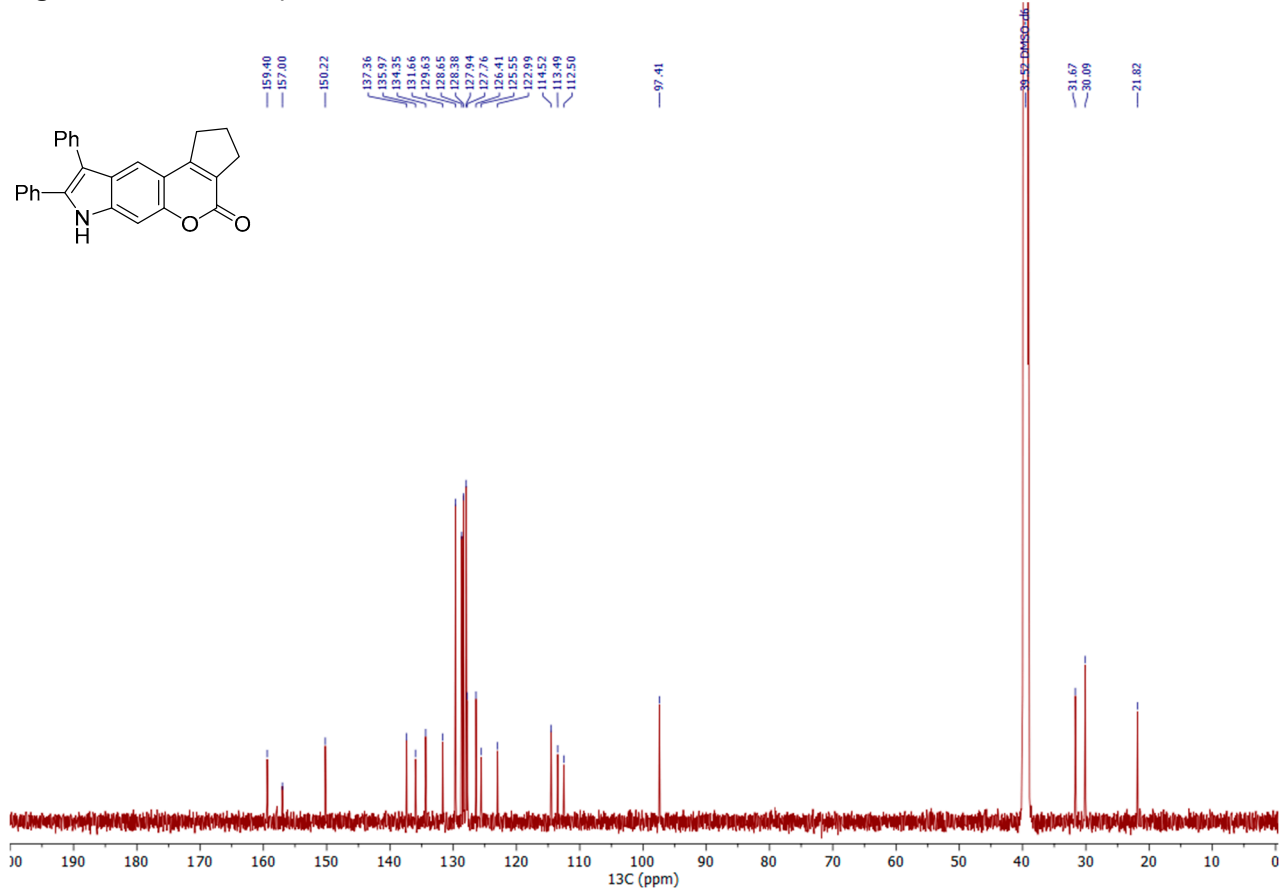


Figure S30. ^{13}C NMR spectrum of **7f**.

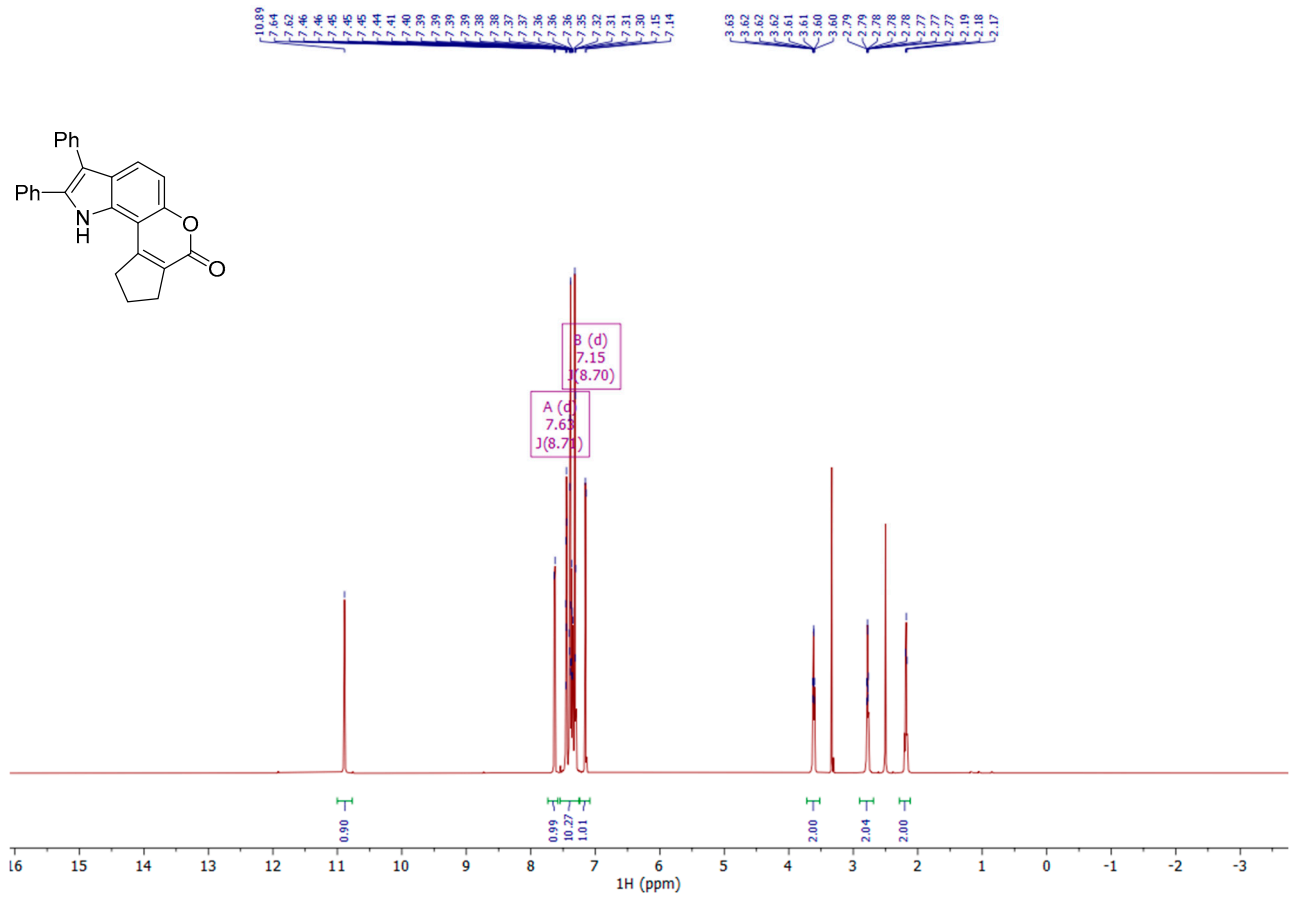


Figure S31. ^1H NMR spectrum of **8f**.

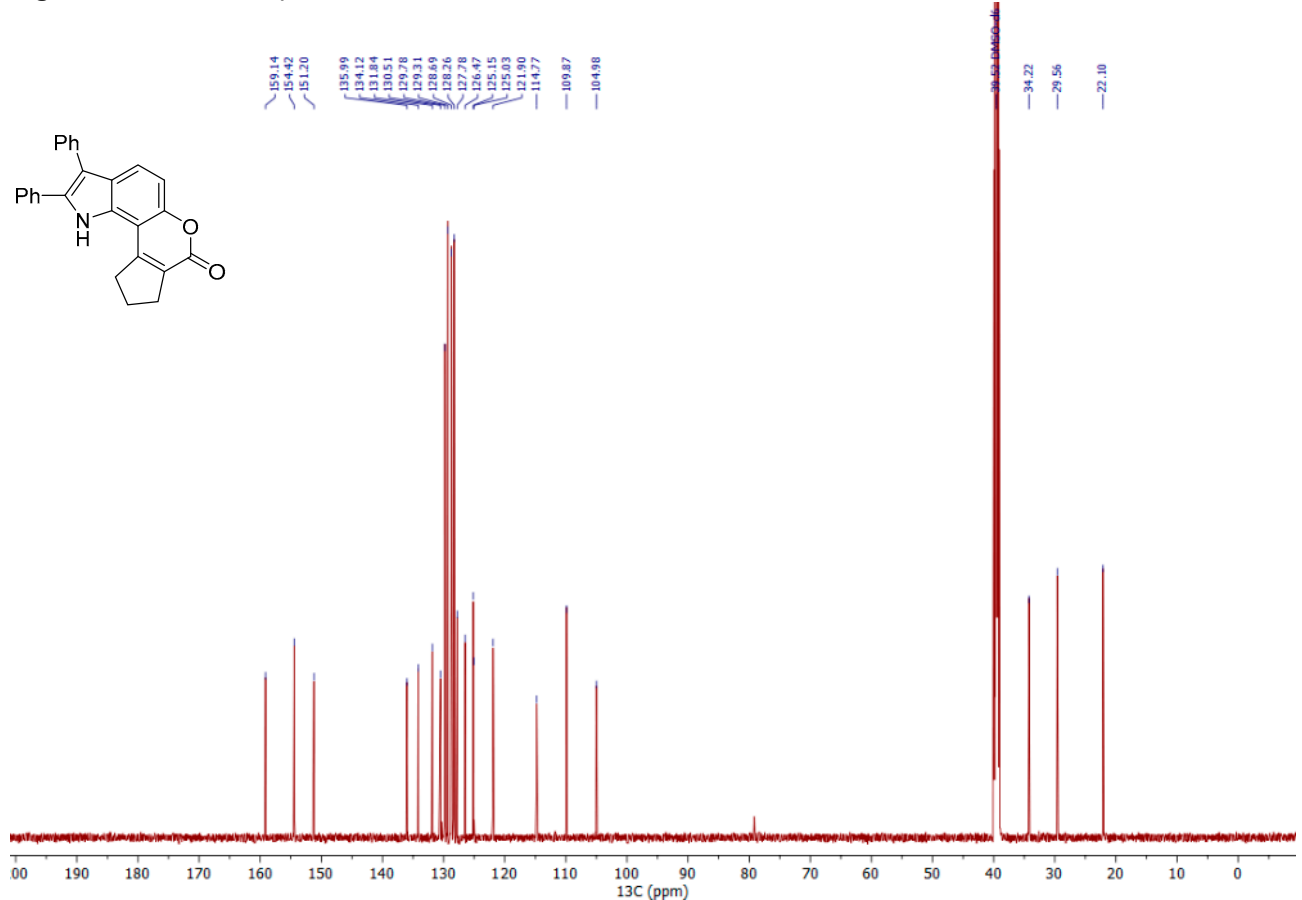


Figure S32. ^{13}C NMR spectrum of **8f**.

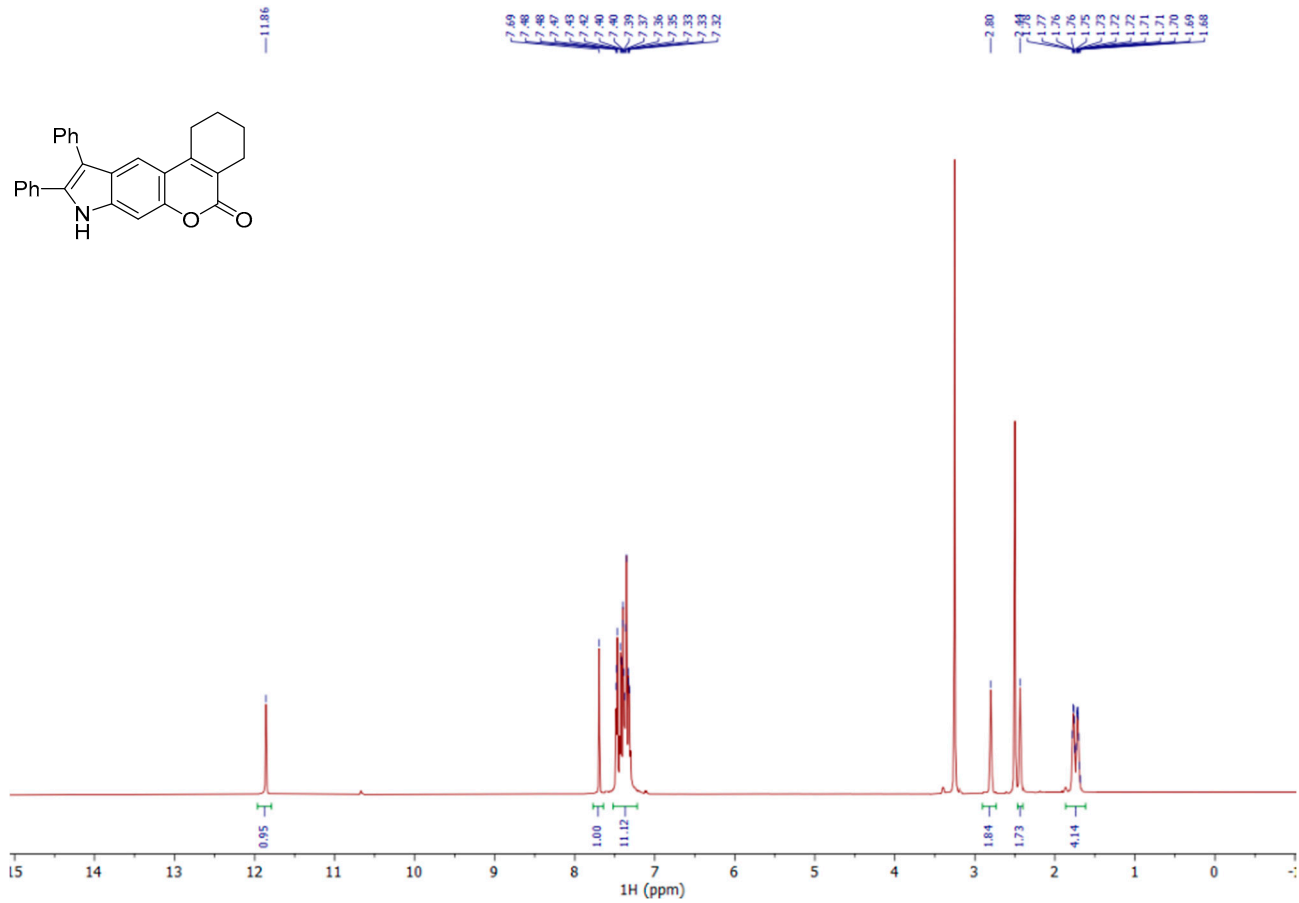


Figure S33. ¹H NMR spectrum of 7g.

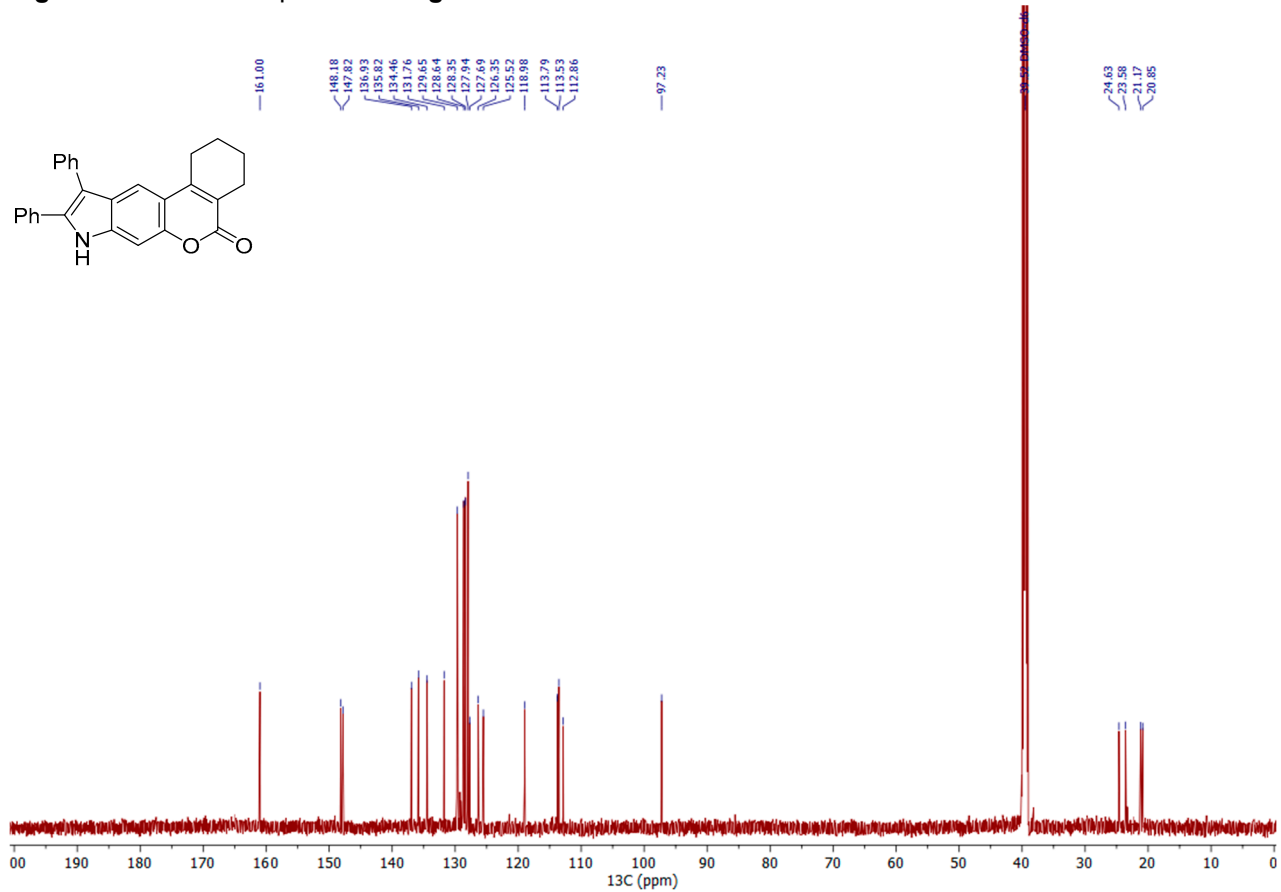


Figure S34. ¹³C NMR spectrum of 7g.

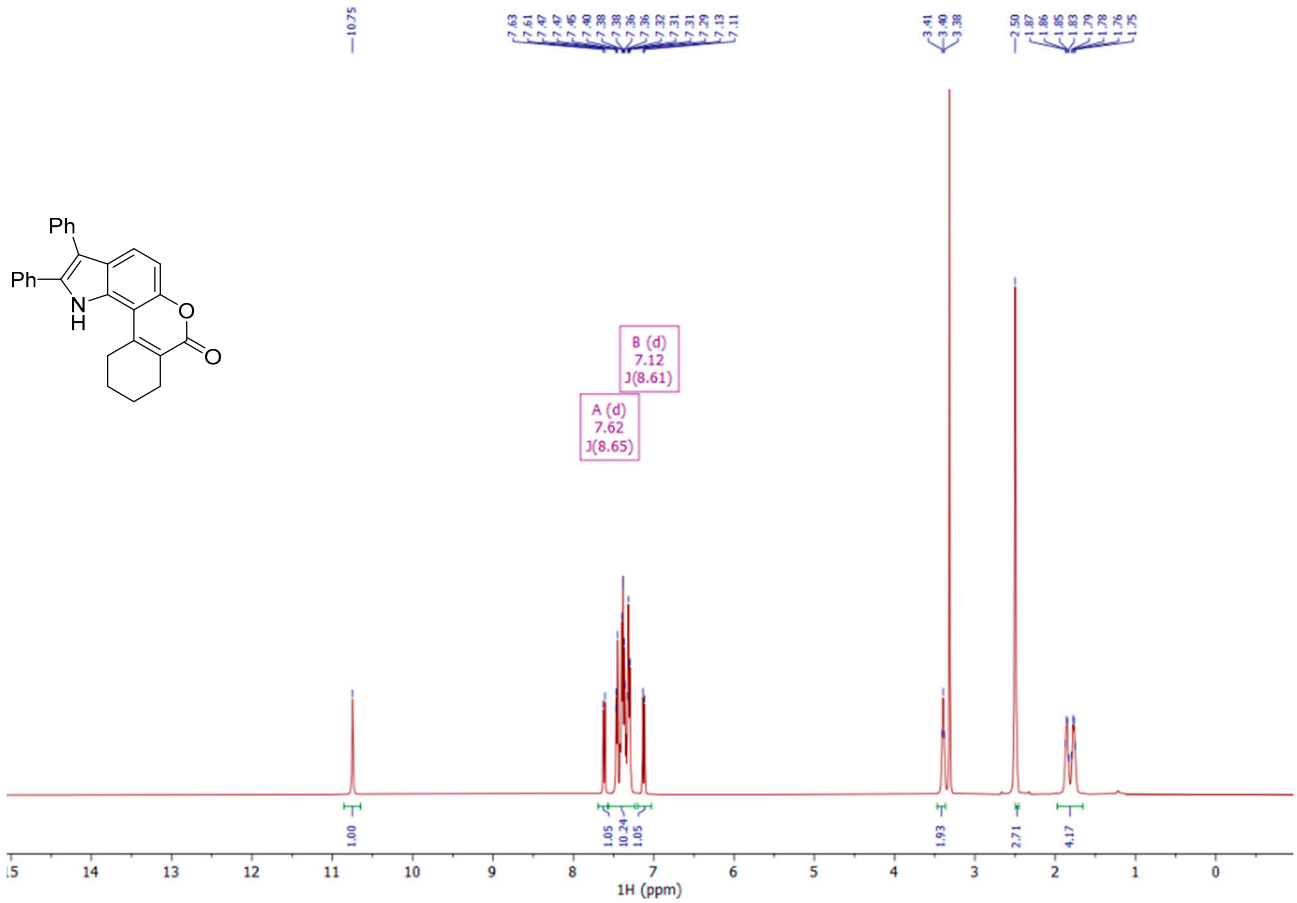


Figure S35. ^1H NMR spectrum of **8g**.

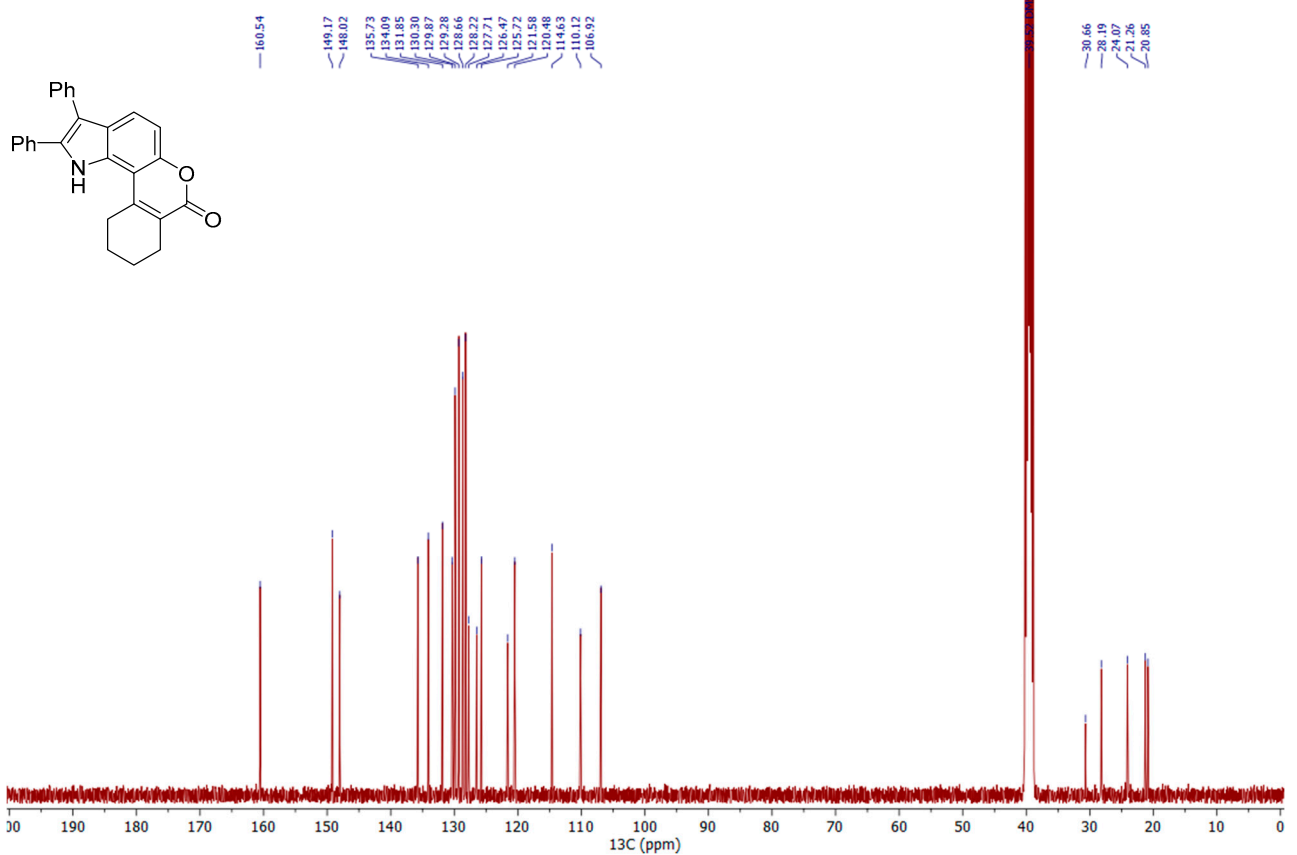


Figure S36. ^{13}C NMR spectrum of **8g**.

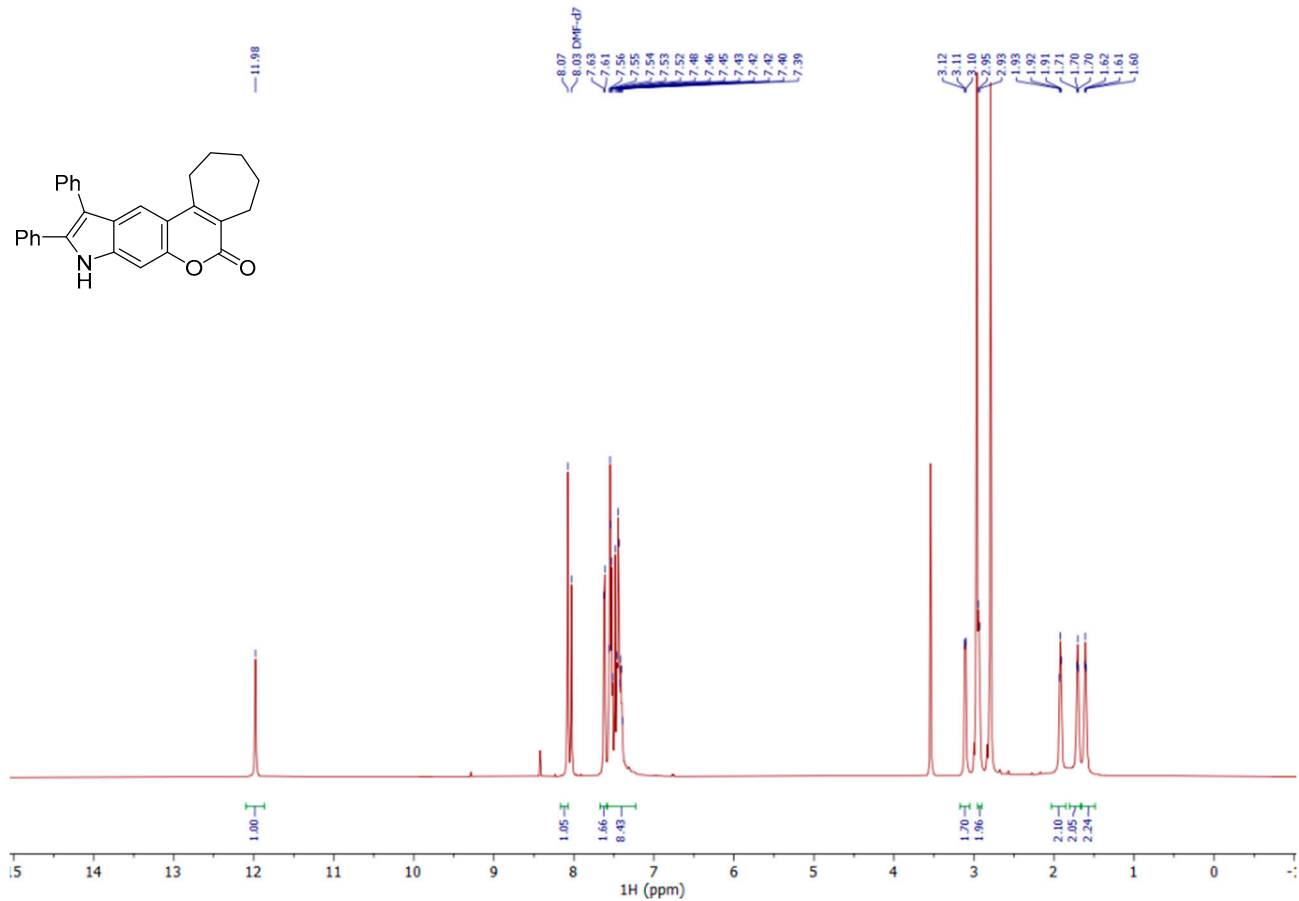


Figure S37. ^1H NMR spectrum of **7h**.

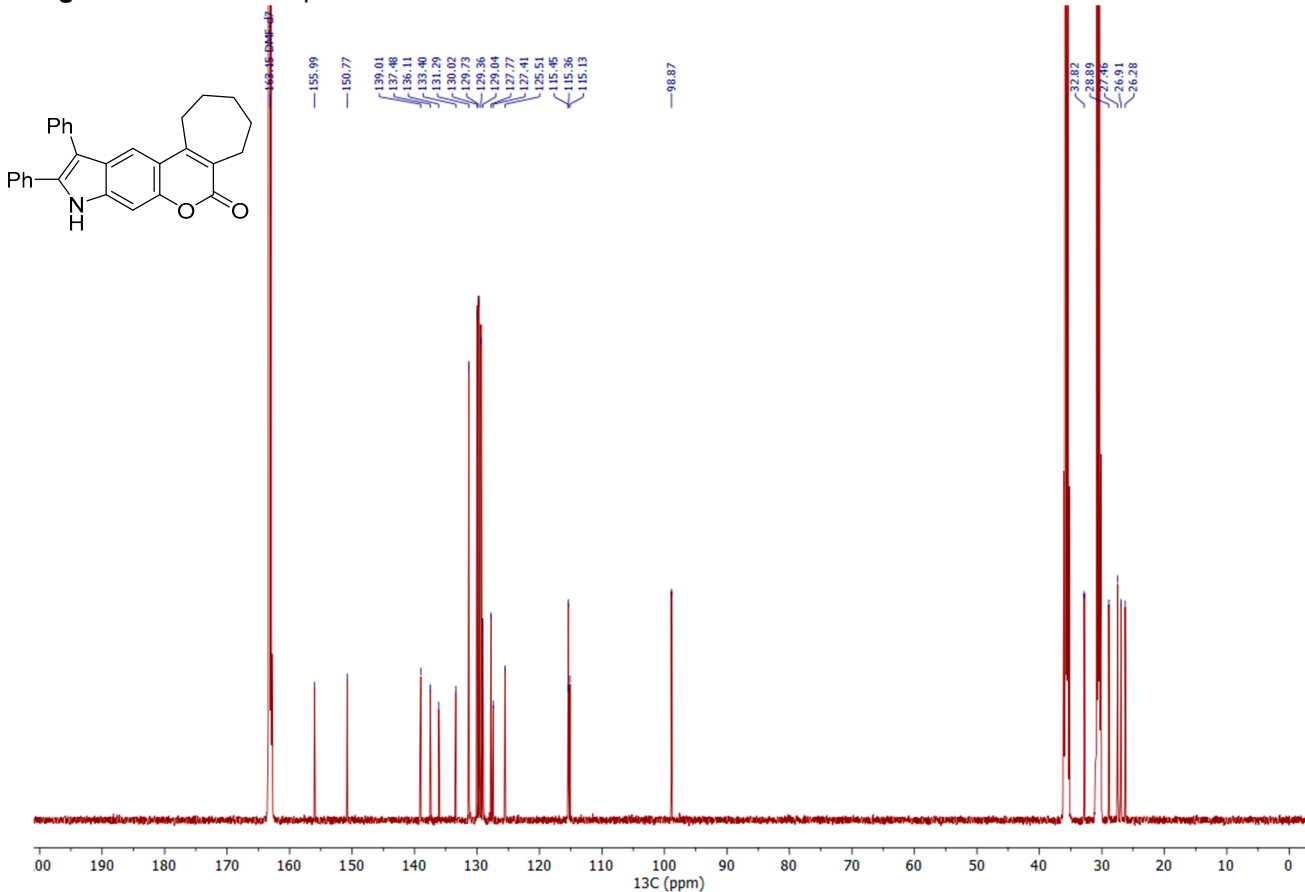


Figure S38. ^{13}C NMR spectrum of **7h**.

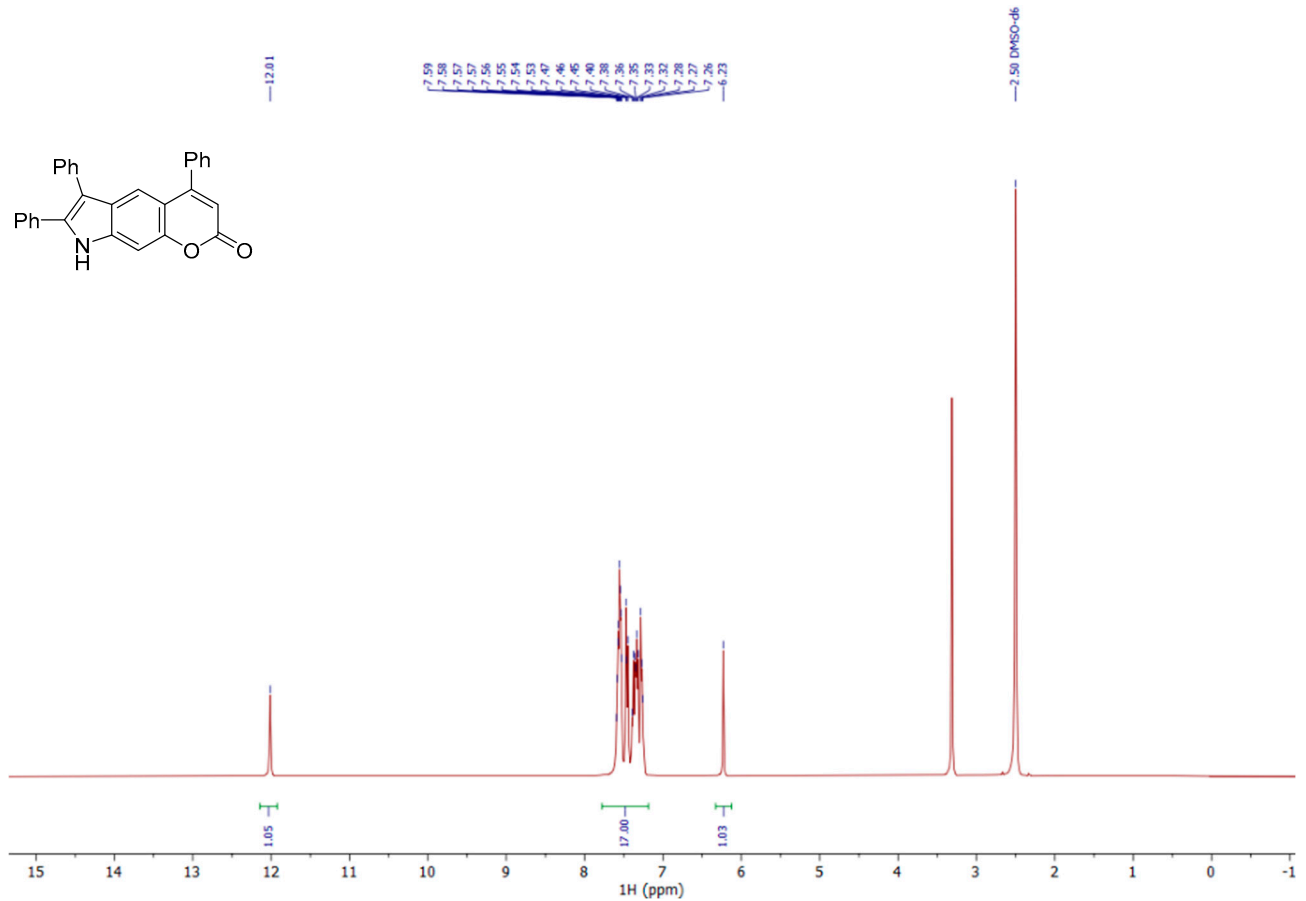


Figure S39. ^1H NMR spectrum of **7i**.

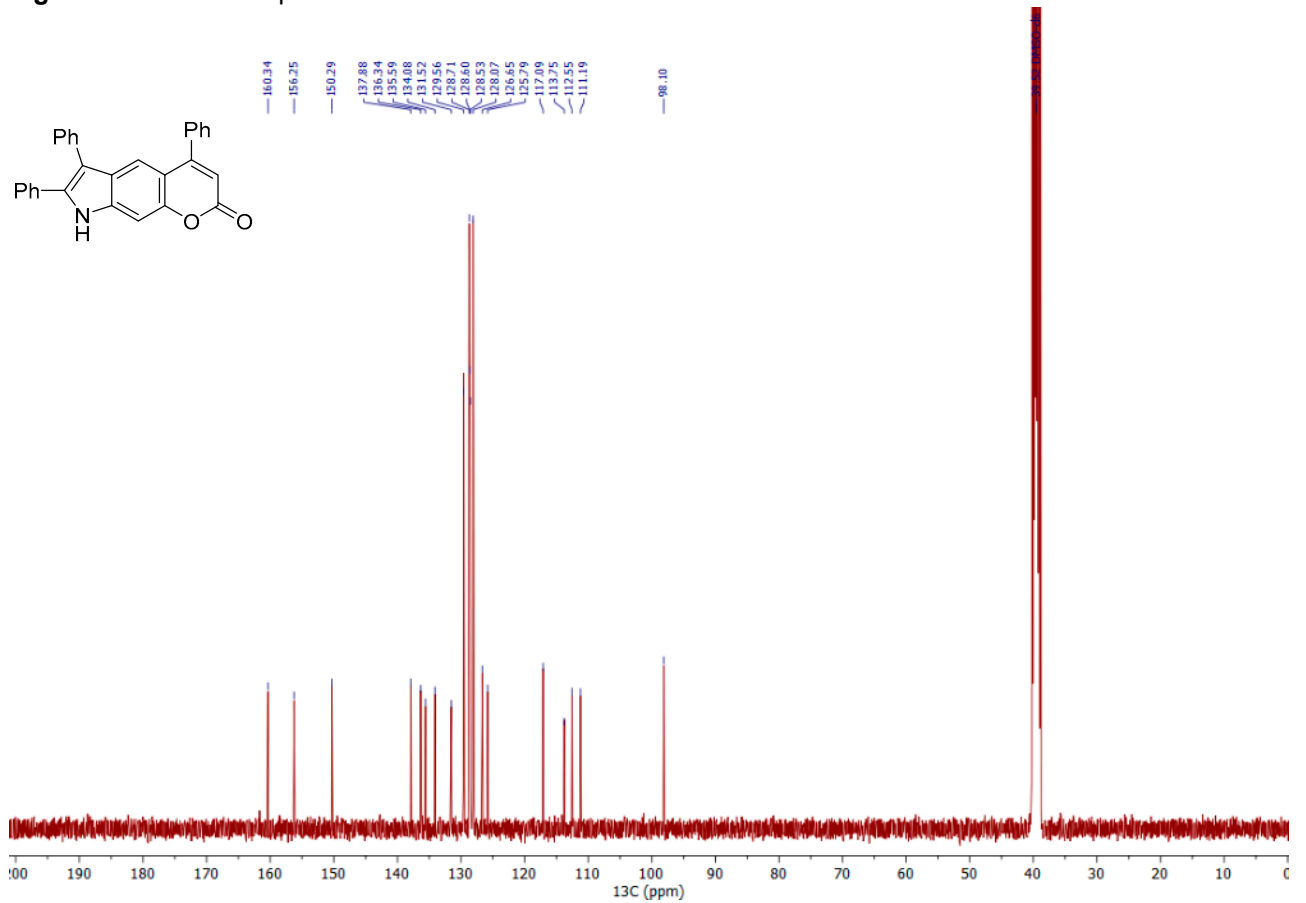


Figure S40. ^{13}C NMR spectrum of **7i**.

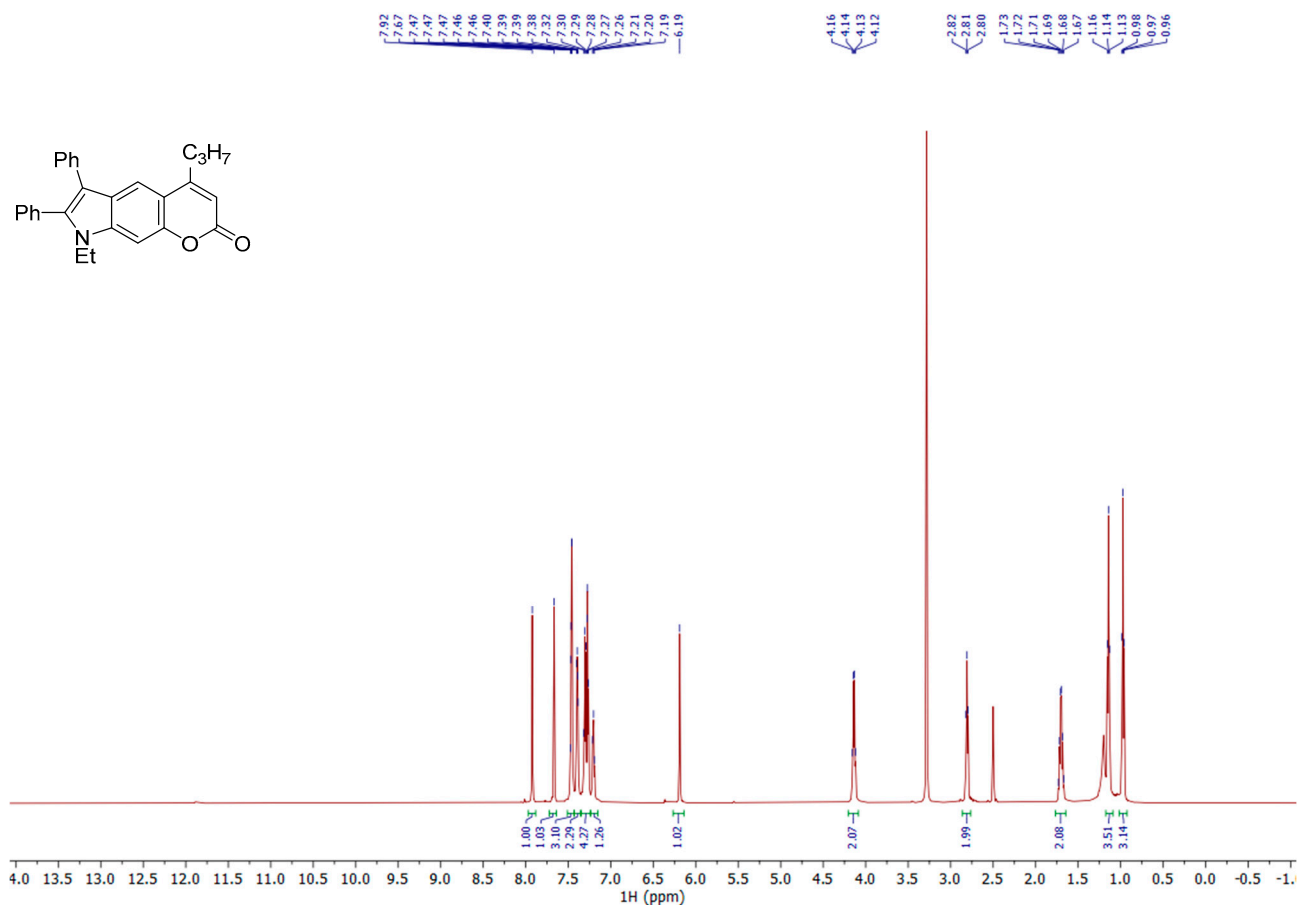


Figure S41. ¹H NMR spectrum of 9a.

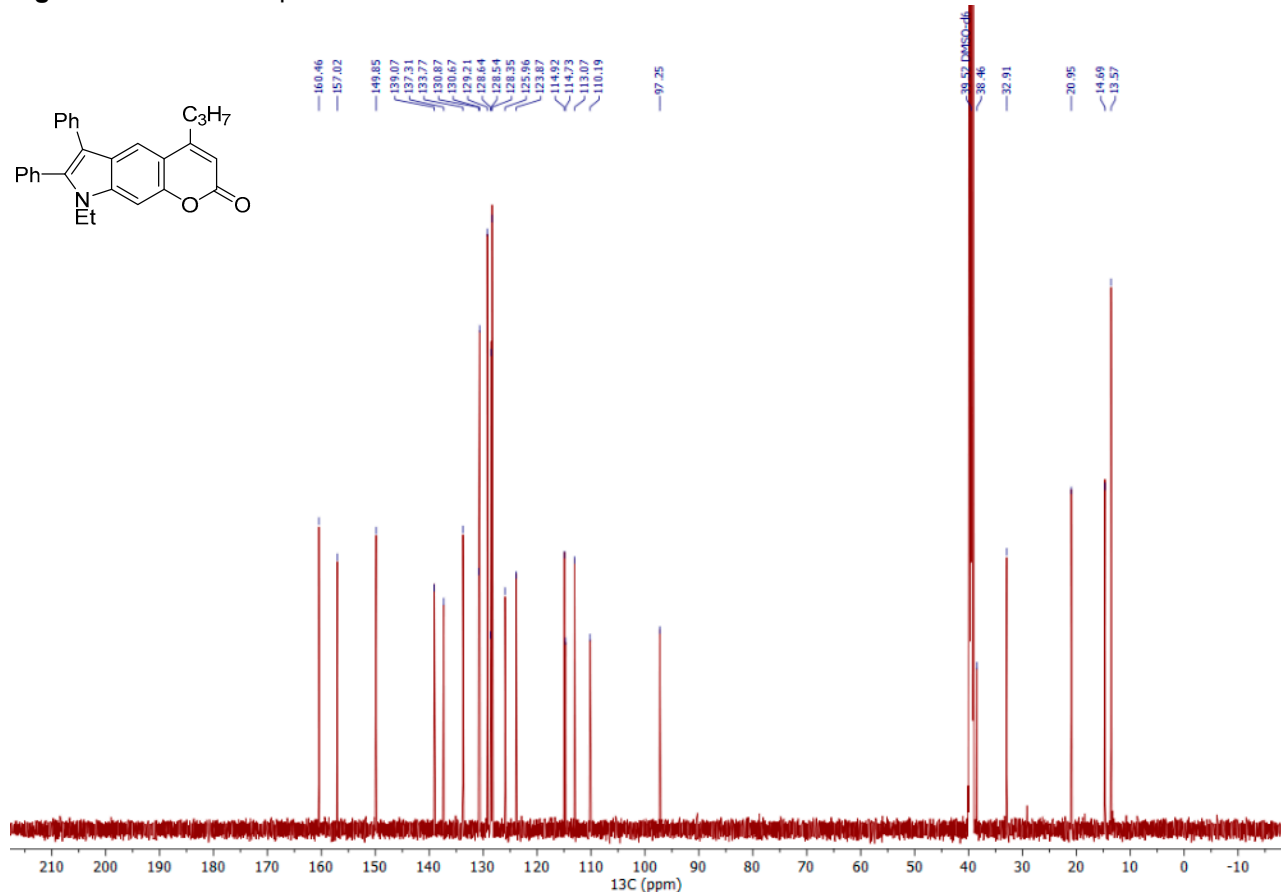


Figure S42. ¹³C NMR spectrum of 9a.

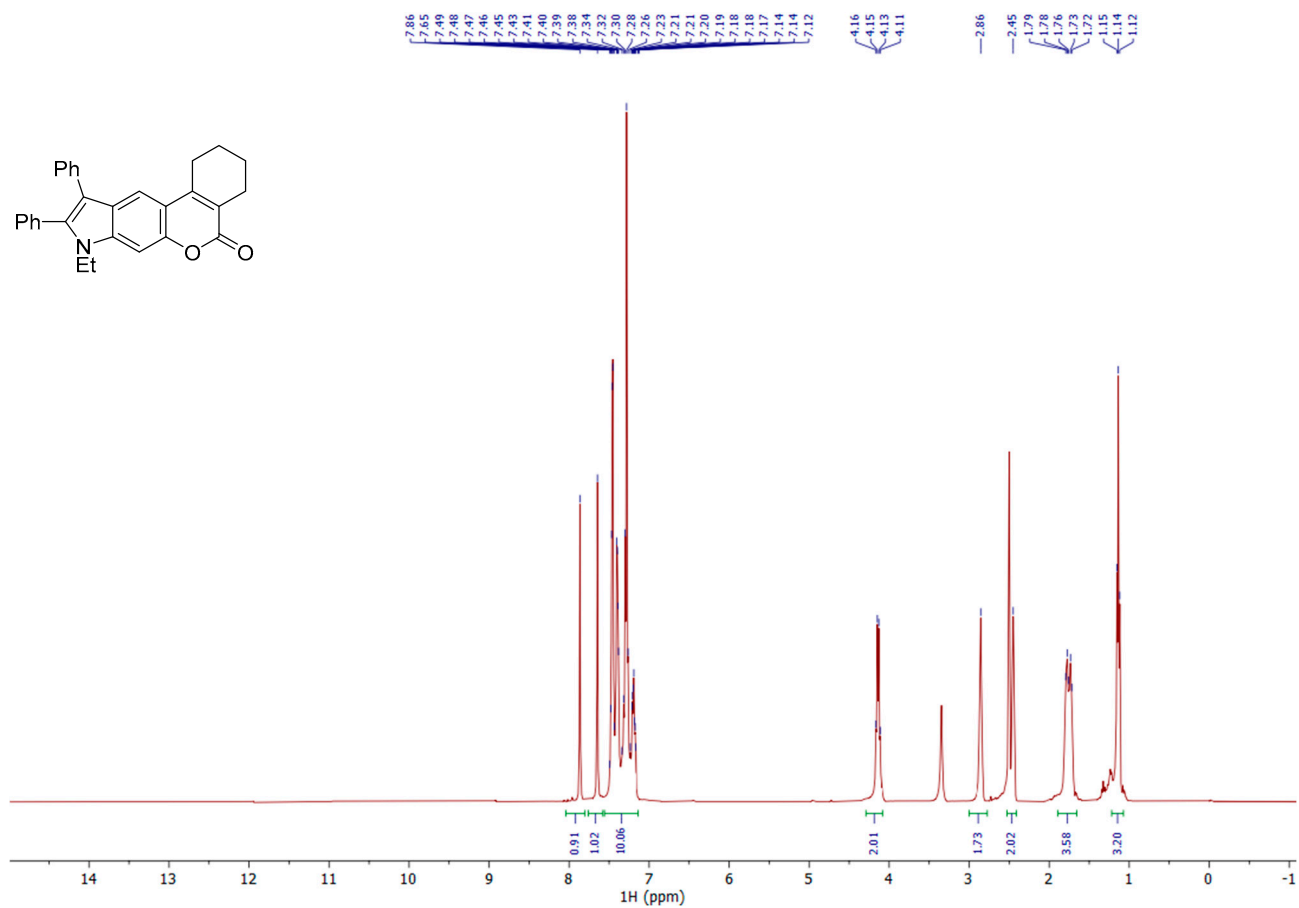


Figure S43. ¹H NMR spectrum of 9b.

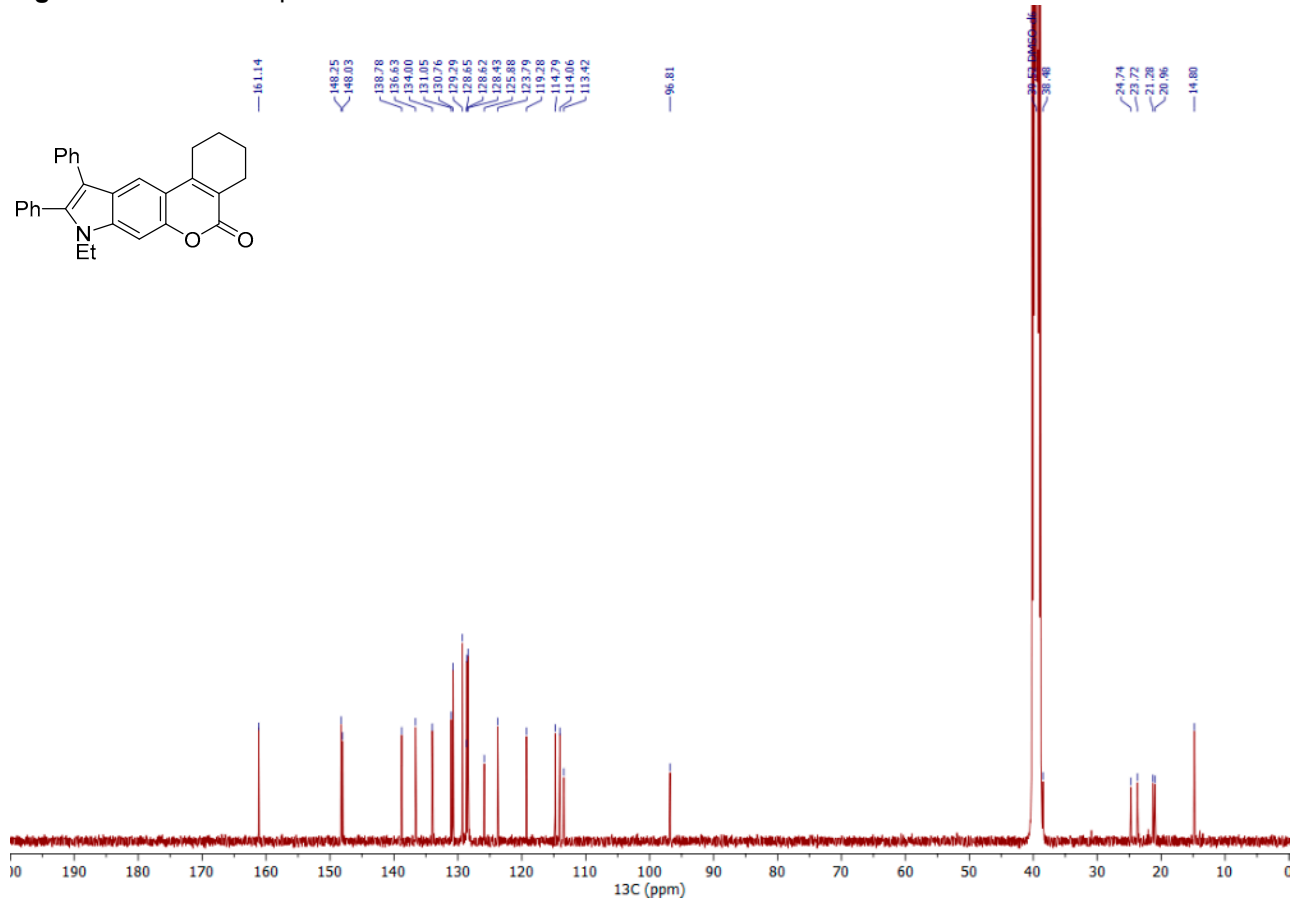


Figure S44. ¹³C NMR spectrum of 9b.

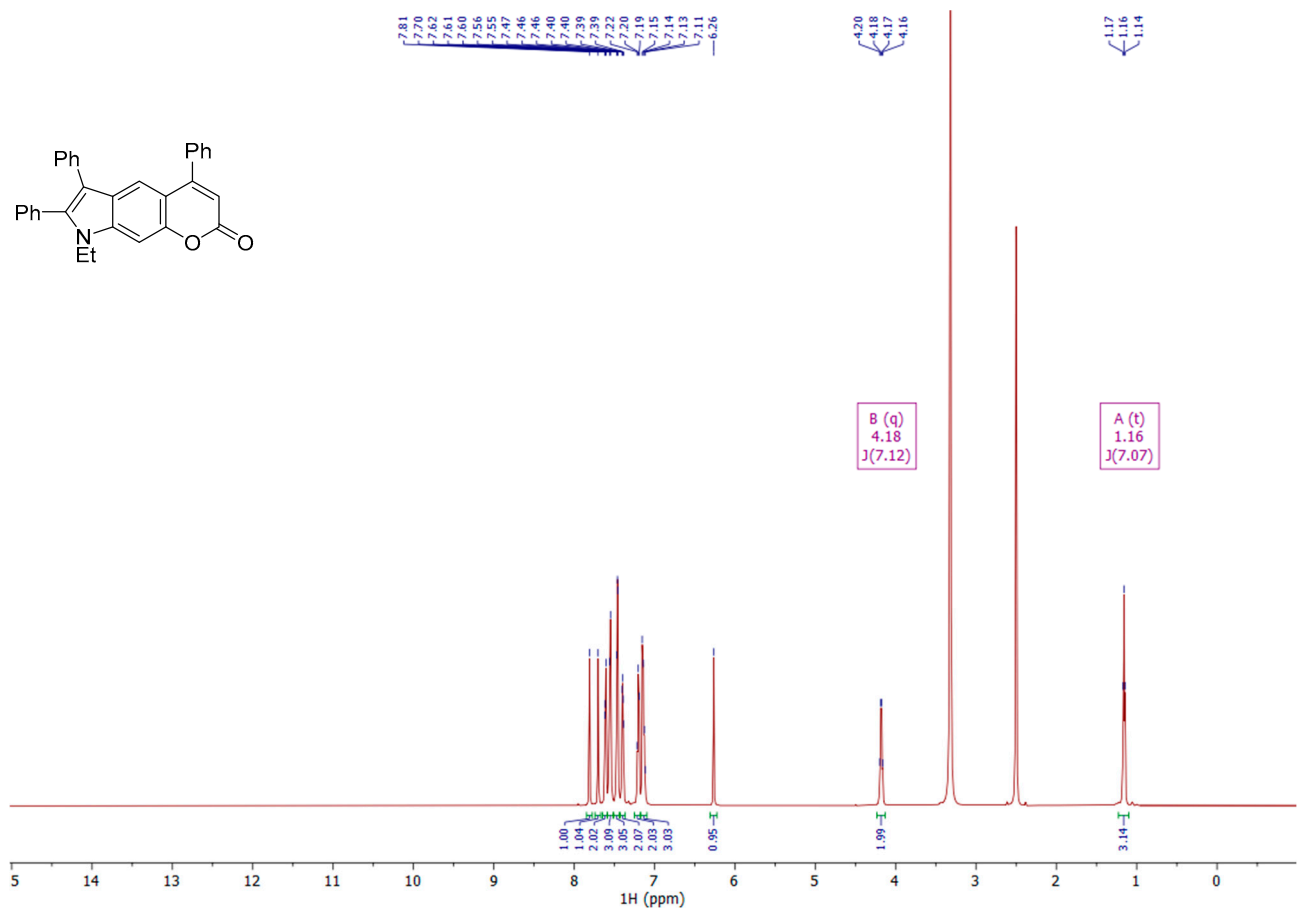


Figure S45. ^1H NMR spectrum of **9c**.

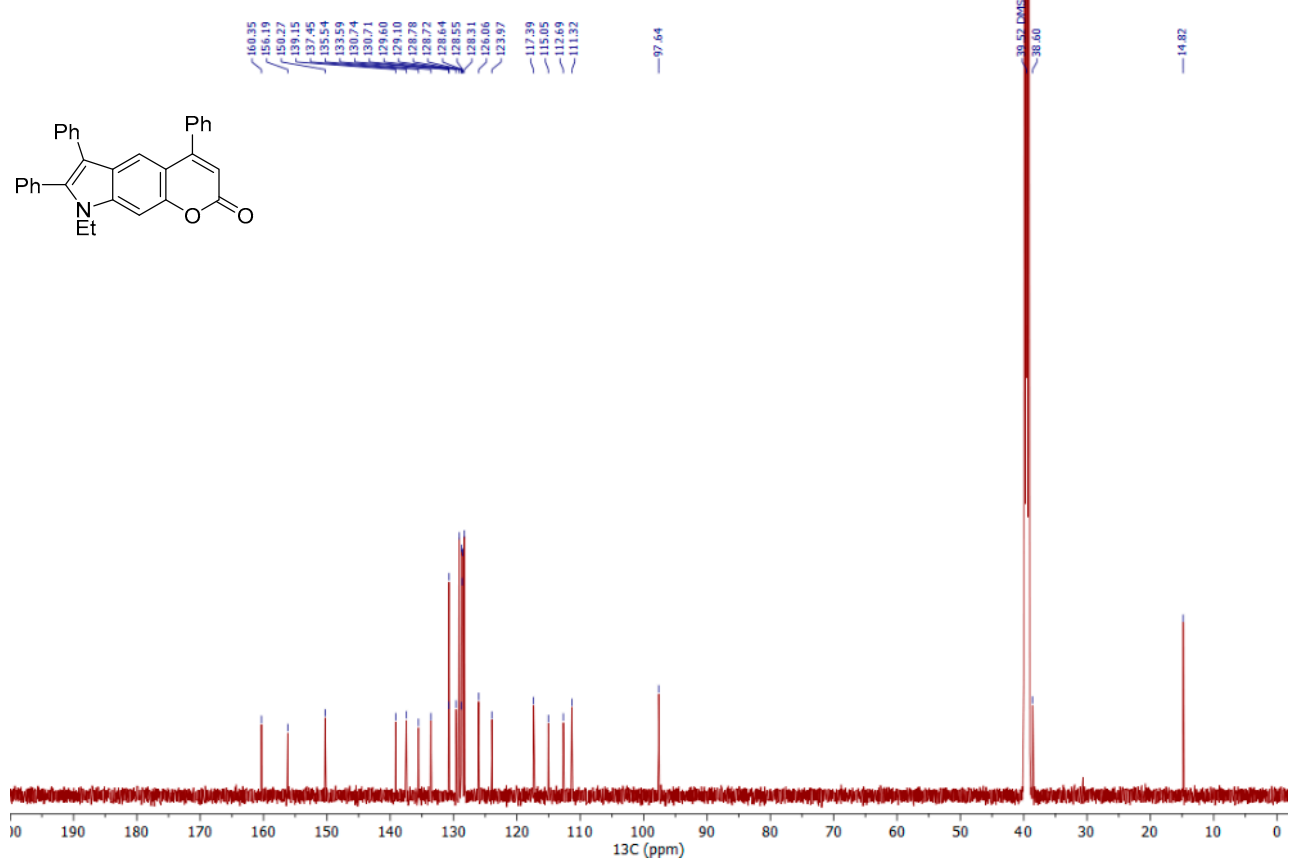


Figure S46. ^{13}C NMR spectrum of **9c**.

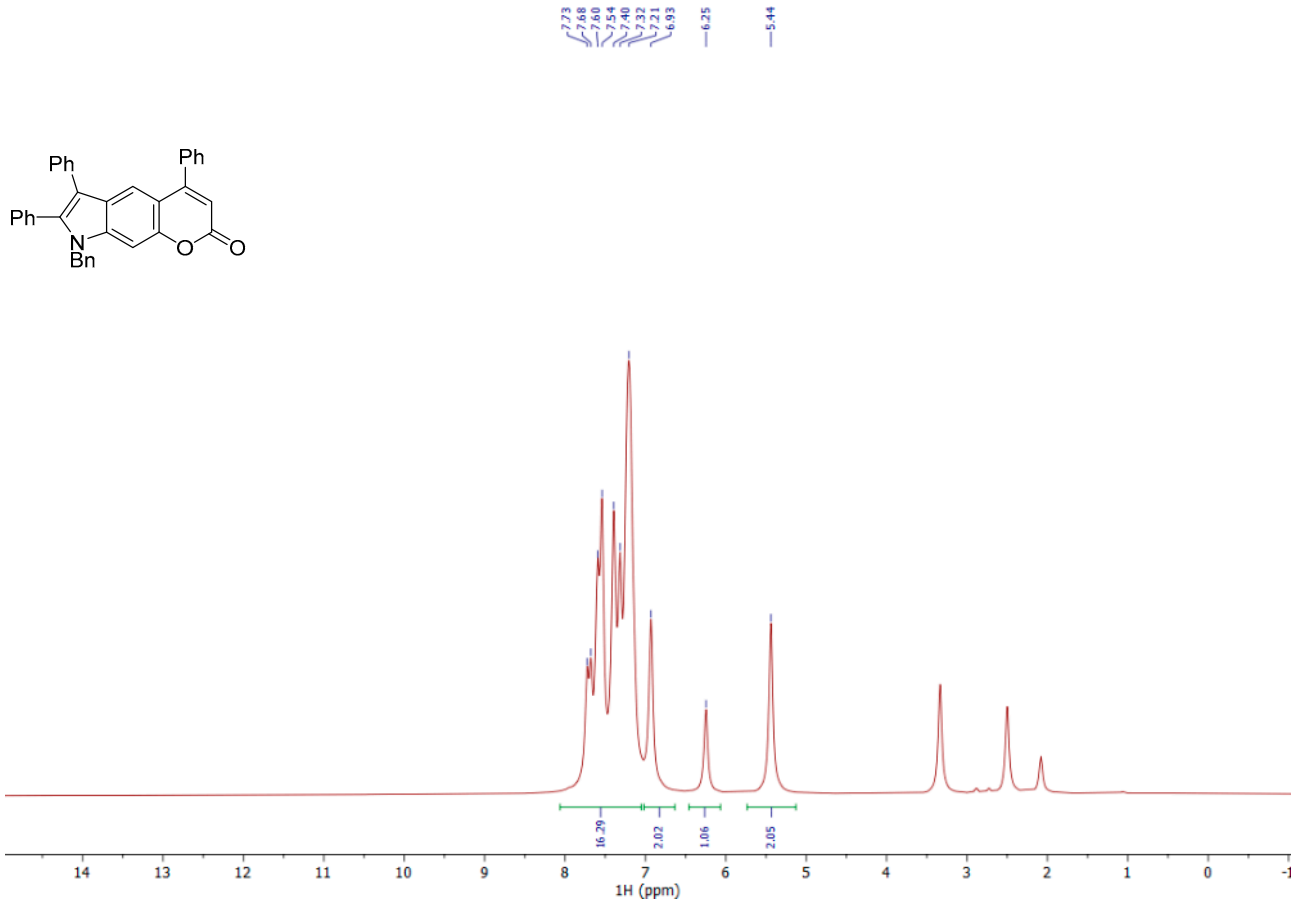


Figure S47. ¹H NMR spectrum of 9d.

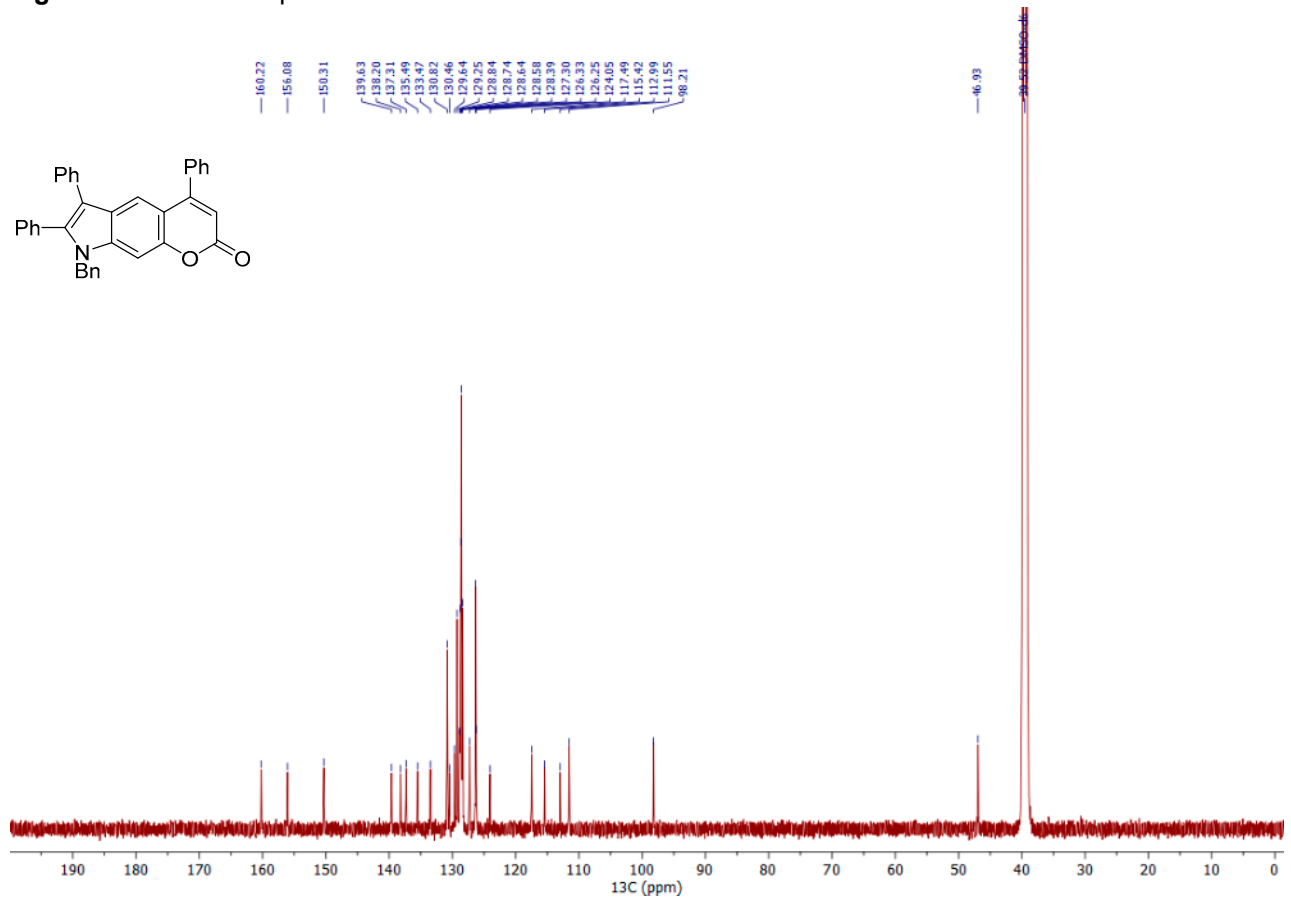


Figure S48. ¹³C NMR spectrum of 9d.

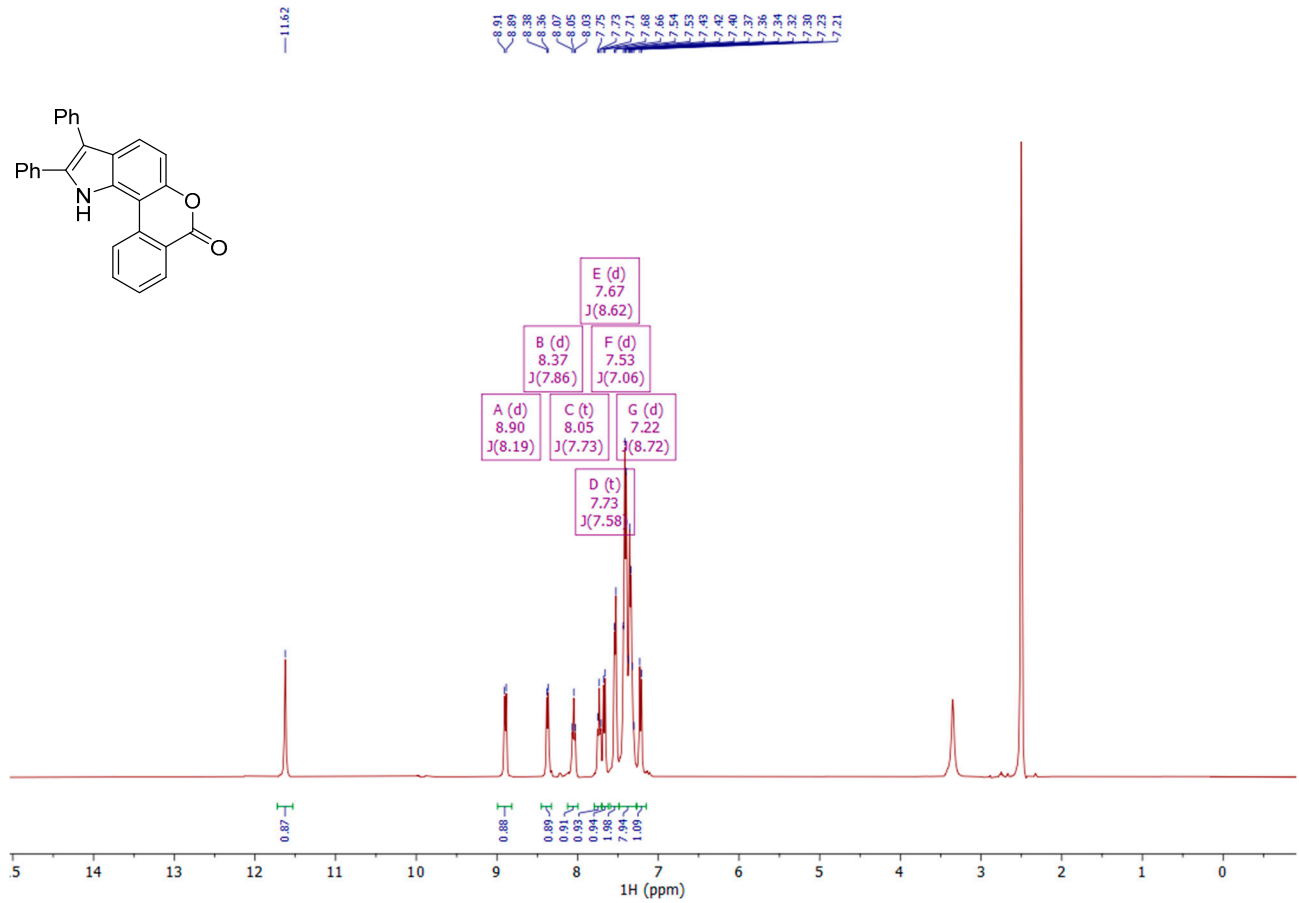


Figure S49. ^1H NMR spectrum of **10**.

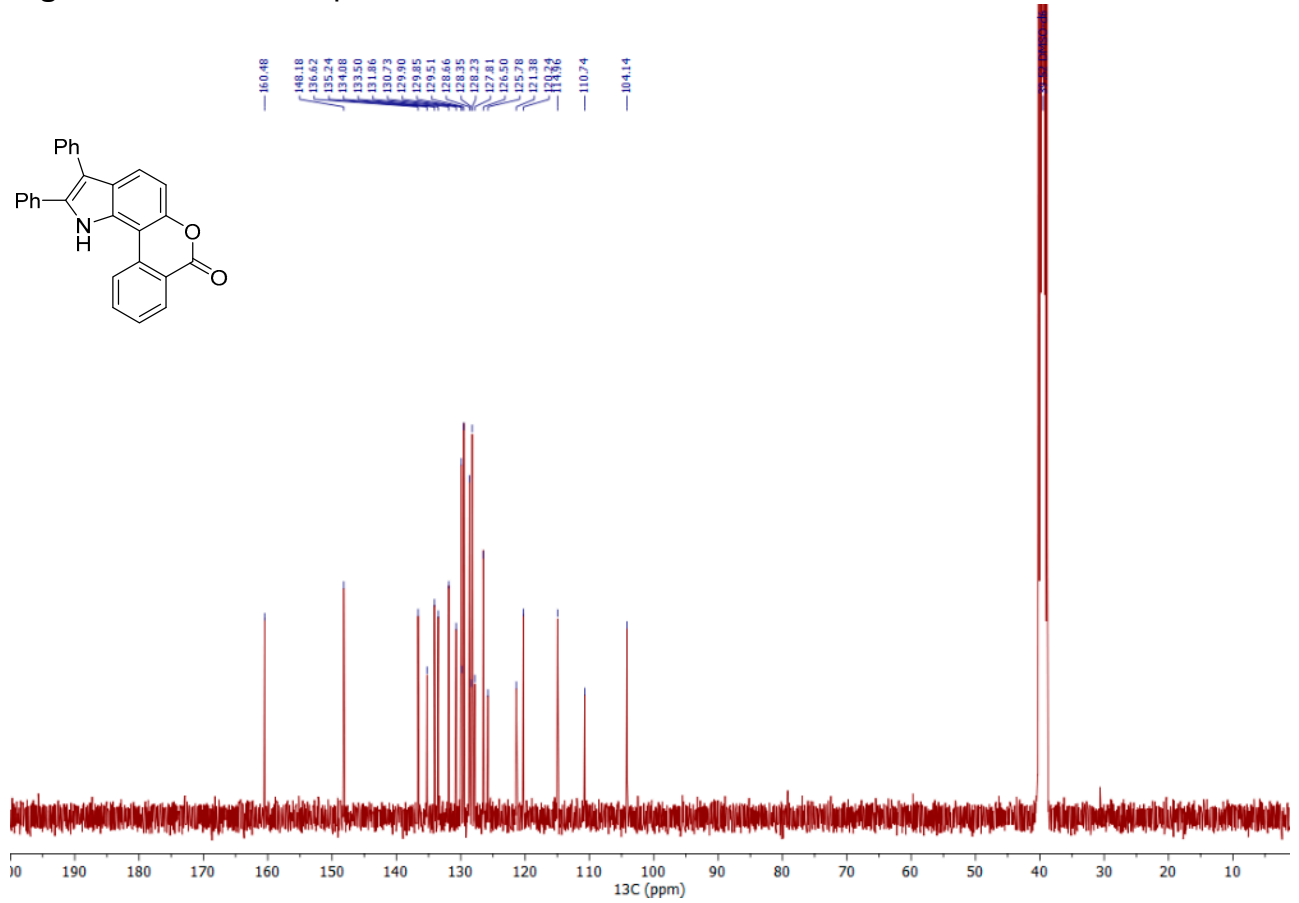


Figure S50. ^{13}C NMR spectrum of **10**.

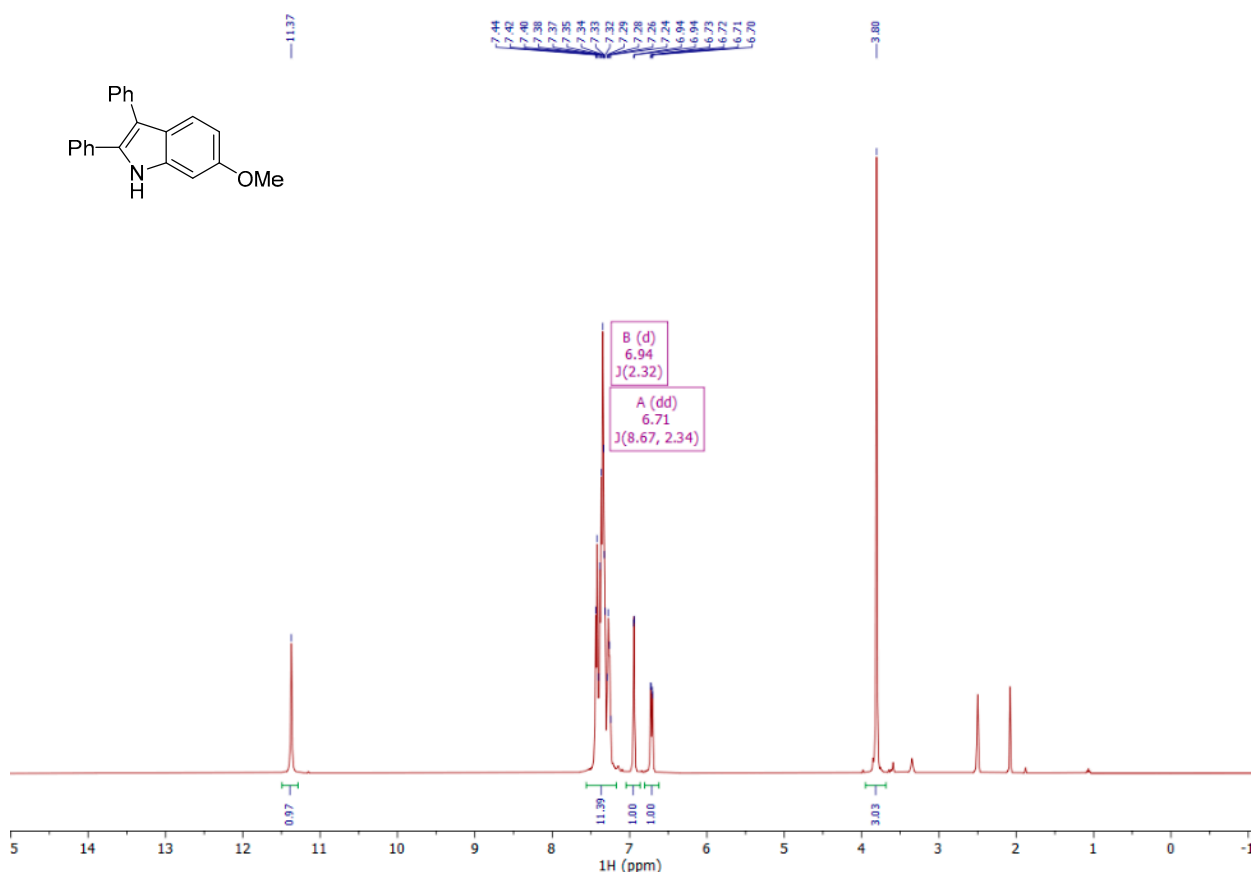


Figure S51. ^1H NMR spectrum of 2,3-diphenyl-6-methoxyindole **13**.

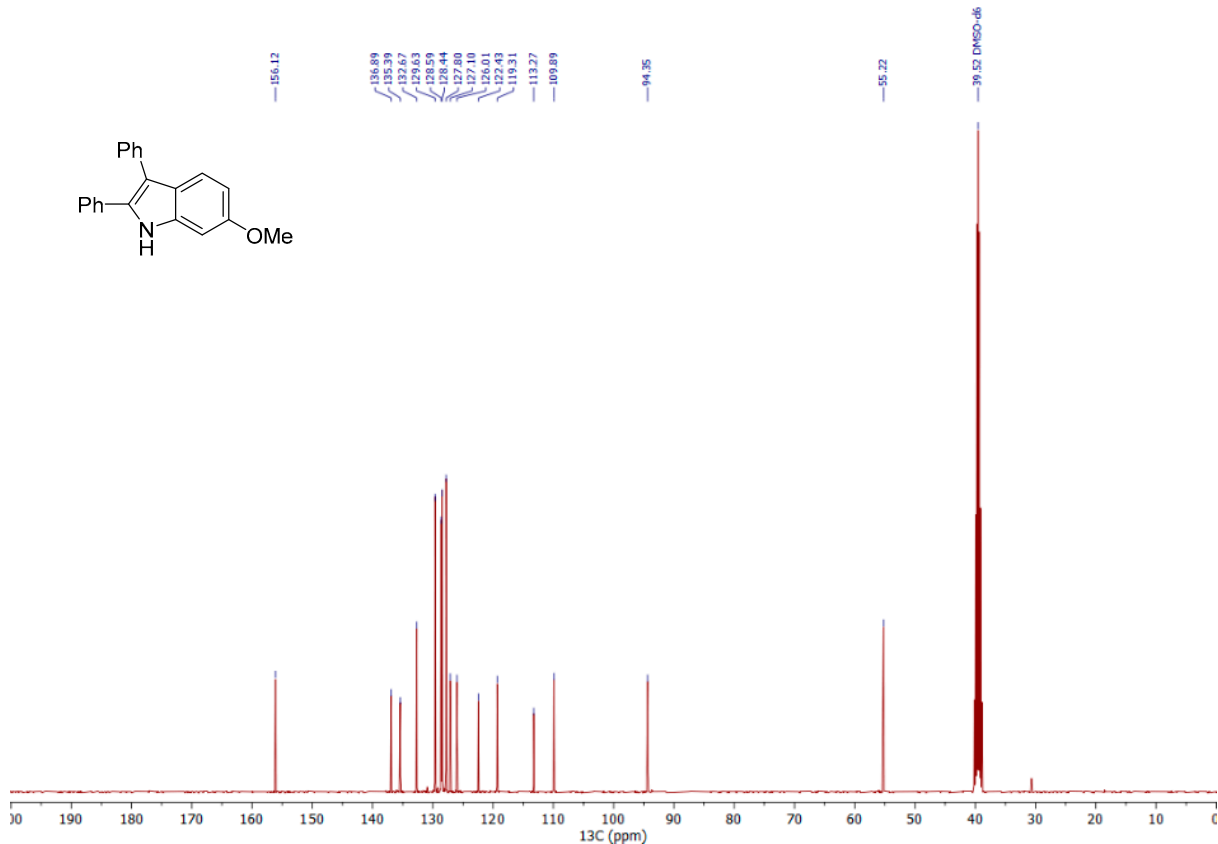


Figure S52. ^1H NMR spectrum of 2,3-diphenyl-6-methoxyindole **13**.

Photophysical data

Materials and Methods

Starting materials are commercially available. Water used throughout was Milli-Q water.

Equipment, measurements and characterization methods

UV-Vis absorption spectra were recorded on the spectrophotometer Shimadzu UV-1800.

Spectrophotometer using quartz cells with 1 cm path length at room temperature. Emission and excitation spectra were measured on the Horiba FluoroMax-4 using quartz cells with 1 cm path length at room temperature (wavelength range from 350 to 800 nm, slit 2-3 nm, λ_{ex} corresponds to $\lambda_{\text{abs}}^{\text{max}}$). Absolute quantum yields for oxadiazoles were by using the Integrating Sphere Quanta- ϕ of the Horiba-Fluoromax-4. Time-resolved fluorescence measurements were carried out using time-correlated single-photon counting (TCSPC) with a nanosecond LED (370 nm).

Photoluminescence Absolute quantum yield (PLQY) measurement

For each sensor was measured of absorption spectrum so that the concentration of solution was less 0,1 of optical density at selected wavelength to minimize inner-filter effect. For blank (naked solvent) and sensor solution were recorded of emission and Rayleigh scattering spectra by using Integrating Sphere of HORIBA FluoroMax-4. PLQY was calculated by equation: $\phi = (E_c - E_a) / (L_a - L_c)$, where E_c and L_c are the integrated luminescence of the sensor and blank, E_a and L_a are the integrated excitation profile of the sensor and blank.

Solvatochromic behavior of pyranoindole compounds

Table S2. Orientation polarizability for solvents (Δf), absorption and fluorescence emission maxima (λ_{abs} , λ_{em} , nm) and Stokes shift (nm, cm^{-1}) of **2** in different solvents.

| Solvent | Δf | λ_{abs} , nm | λ_{em} , nm | Stokes shift, nm | Stokes shift, cm^{-1} |
|-----------|------------|-----------------------------|----------------------------|------------------|--------------------------------|
| n-Heptane | 0.0001 | 335 | 397 | 62 | 4661 |
| Toluene | 0.0126 | 335 | 401 | 66 | 4913 |
| THF | 0.21 | 328 | 409 | 81 | 6038 |
| DCM | 0.22 | 329 | 410 | 81 | 6005 |
| MeCN | 0.3 | 328 | 420 | 92 | 6678 |

Table S3. Orientation polarizability for solvents (Δf), absorption and fluorescence emission maxima (λ_{abs} , λ_{em} , nm) and Stokes shift (nm, cm^{-1}) of **6b** in different solvents.

| Solvent | Δf | λ_{abs} , nm | λ_{em} , nm | Stokes shift, nm | Stokes shift, cm^{-1} |
|-----------|------------|-----------------------------|----------------------------|------------------|--------------------------------|
| n-Heptane | 0.0001 | 318 | 424 | 106 | 7862 |
| Toluene | 0.0126 | 309 | 442 | 133 | 9738 |
| THF | 0.21 | 304 | 453 | 149 | 10820 |
| DCM | 0.22 | 298 | 463 | 165 | 11959 |
| MeCN | 0.3 | 280 | 474 | 194 | 14617 |

Table S4. Orientation polarizability for solvents (Δf), absorption and fluorescence emission maxima (λ_{abs} , λ_{em} , nm) and Stokes shift (nm, cm^{-1}) of **7a** in different solvents.

| Solvent | Δf | λ_{abs} , nm | λ_{em} , nm | Stokes shift, nm | Stokes shift, cm^{-1} |
|-----------|------------|-----------------------------|----------------------------|------------------|--------------------------------|
| n-Heptane | 0.0001 | 336 | 440 | 104 | 7034 |
| Toluene | 0.0126 | 340 | 454 | 114 | 7385 |
| THF | 0.21 | 340 | 477 | 137 | 8447 |
| DCM | 0.22 | 340 | 486 | 146 | 8836 |
| MeCN | 0.3 | 335 | 502 | 167 | 9930 |

Table S5. Orientation polarizability for solvents (Δf), absorption and fluorescence emission maxima (λ_{abs} , λ_{em} , nm) and Stokes shift (nm, cm^{-1}) of **7c** in different solvents.

| Solvent | Δf | λ_{abs} , nm | λ_{em} , nm | Stokes shift, nm | Stokes shift, cm^{-1} |
|-----------|------------|-----------------------------|----------------------------|------------------|--------------------------------|
| n-Heptane | 0.0001 | 307 | 428 | 121 | 9209 |
| Toluene | 0.0126 | 285 | 439 | 154 | 12309 |
| THF | 0.21 | 280 | 465 | 185 | 14209 |
| DCM | 0.22 | 275 | 478 | 203 | 15443 |
| MeCN | 0.3 | 280 | 499 | 219 | 15674 |

Table S6. Orientation polarizability for solvents (Δf), absorption and fluorescence emission maxima (λ_{abs} , λ_{em} , nm) and Stokes shift (nm, cm^{-1}) of **7e** in different solvents.

| Solvent | Δf | λ_{abs} , nm | λ_{em} , nm | Stokes shift, nm | Stokes shift, cm^{-1} |
|-----------|------------|-----------------------------|----------------------------|------------------|--------------------------------|
| n-Heptane | 0.0001 | 296 | 438 | 142 | 10953 |
| Toluene | 0.0126 | 301 | 452 | 151 | 11099 |
| THF | 0.21 | 306 | 474 | 168 | 11583 |
| DCM | 0.22 | 306 | 500 | 194 | 12680 |
| DMSO | 0.276 | 304 | 516 | 212 | 13514 |
| MeCN | 0.3 | 303 | 526 | 223 | 13992 |
| MeOH | 0.31 | 305 | 541 | 236 | 14302 |

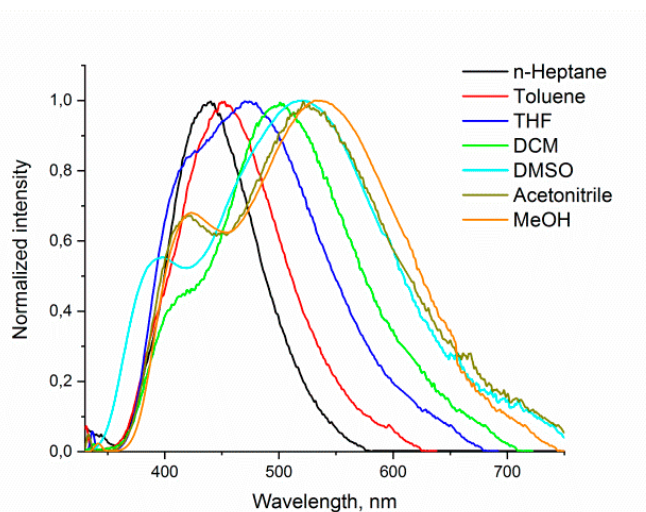


Figure S53. Normalized fluorescence spectra of **7e** in different solvents ($C = 10^{-5} \text{ M}^{-1}$).

Table S7. Orientation polarizability for solvents (Δf), absorption and fluorescence emission maxima (λ_{abs} , λ_{em} , nm) and Stokes shift (nm, cm^{-1}) of **8a** in different solvents.

| Solvent | Δf | λ_{abs} , nm | λ_{em} , nm | Stokes shift, nm | Stokes shift, cm^{-1} |
|-----------|------------|-----------------------------|----------------------------|------------------|--------------------------------|
| n-Heptane | 0.0001 | 306 | 437 | 131 | 9796 |
| Toluene | 0.0126 | 301 | 446 | 145 | 10801 |
| THF | 0.21 | 277 | 462 | 185 | 14456 |
| DCM | 0.22 | 276 | 477 | 201 | 15267 |
| MeCN | 0.3 | 287 | 496 | 209 | 14682 |

Table S8. Orientation polarizability for solvents (Δf), absorption and fluorescence emission maxima (λ_{abs} , λ_{em} , nm) and Stokes shift (nm, cm^{-1}) of **8c** in different solvents.

| Solvent | Δf | λ_{abs} , nm | λ_{em} , nm | Stokes shift, nm | Stokes shift, cm^{-1} |
|-----------|------------|-----------------------------|----------------------------|------------------|--------------------------------|
| n-Heptane | 0.0001 | 306 | 396 | 90 | 7427 |
| Toluene | 0.0126 | 325 | 432 | 107 | 7621 |
| THF | 0.21 | 306 | 458 | 152 | 10846 |
| DCM | 0.22 | 312 | 478 | 166 | 11131 |
| DMF | 0.274 | 318 | 493 | 175 | 11163 |
| MeCN | 0.3 | 300 | 494 | 194 | 13090 |
| MeOH | 0.31 | 302 | 531 | 229 | 14280 |

Table S9. Orientation polarizability for solvents (Δf), absorption and fluorescence emission maxima (λ_{abs} , λ_{em} , nm) and Stokes shift (nm, cm^{-1}) of **8d** in different solvents.

| Solvent | Δf | λ_{abs} , nm | λ_{em} , nm | Stokes shift, nm | Stokes shift, cm^{-1} |
|-----------|------------|-----------------------------|----------------------------|------------------|--------------------------------|
| n-Heptane | 0.0001 | 308 | 419 | 111 | 8601 |
| Toluene | 0.0126 | 329 | 441 | 112 | 7719 |
| THF | 0.21 | 315 | 458 | 143 | 9912 |
| DCM | 0.22 | 323 | 470 | 147 | 9683 |
| MeCN | 0.3 | 306 | 489 | 183 | 12229 |



Figure S54. Fluorescence photograph of pyranoindole **7e** (1 mM, excitation with 365 nm Hg lamp) in different solvents (left to right: *n*-heptane, toluene, tetrahydrofuran, dichloromethane, DMSO, acetonitrile, methanol).

Table S10. Orientation polarizability for solvents (Δf), absorption and fluorescence emission maxima (λ_{abs} , λ_{em} , nm) and Stokes shift (nm, cm^{-1}) of **8e** in different solvents.

| Solvent | Δf | λ_{abs} , nm | λ_{em} , nm | Stokes shift, nm | Stokes shift, cm^{-1} |
|-----------|------------|-----------------------------|----------------------------|------------------|--------------------------------|
| n-Heptane | 0.0001 | 308 | 431 | 123 | 9266 |
| Toluene | 0.0126 | 314 | 448 | 134 | 9526 |
| THF | 0.21 | 306 | 478 | 172 | 11759 |
| DCM | 0.22 | 305 | 499 | 194 | 12747 |
| DMSO | 0.276 | 303 | 523 | 218 | 13598 |
| MeCN | 0.3 | 305 | 524 | 219 | 13703 |
| MeOH | 0.31 | 306 | 530 | 224 | 13812 |

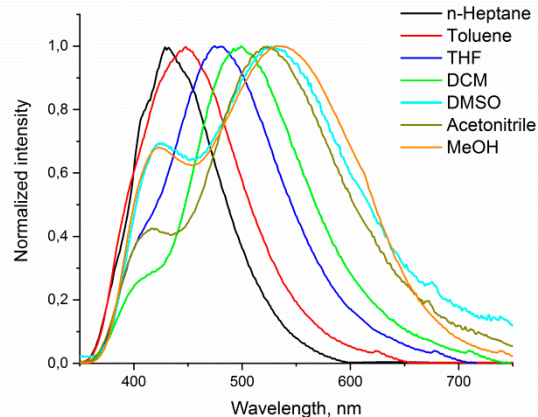


Figure S55. Normalized fluorescence spectra of **8e** in different solvents ($C = 10^{-5} \text{ M}^{-1}$).

Table S11. Orientation polarizability for solvents (Δf), absorption and fluorescence emission maxima (λ_{abs} , λ_{em} , nm) and Stokes shift (nm, cm^{-1}) of **8f** in different solvents.

| Solvent | Δf | λ_{abs} , nm | λ_{em} , nm | Stokes shift, nm | Stokes shift, cm^{-1} |
|-----------|------------|-----------------------------|----------------------------|------------------|--------------------------------|
| n-Heptane | 0.0001 | 305 | 364 | 59 | 5314 |
| Toluene | 0.0126 | 323 | 432 | 109 | 7812 |
| THF | 0.21 | 319 | 449 | 130 | 9076 |
| DCM | 0.22 | 321 | 465 | 144 | 9647 |
| MeCN | 0.3 | 294 | 473 | 179 | 12872 |

Table S12. Orientation polarizability for solvents (Δf), absorption and fluorescence emission maxima (λ_{abs} , λ_{em} , nm) and Stokes shift (nm, cm^{-1}) of **8g** in different solvents.

| Solvent | Δf | λ_{abs} , nm | λ_{em} , nm | Stokes shift, nm | Stokes shift, cm^{-1} |
|-----------|------------|-----------------------------|----------------------------|------------------|--------------------------------|
| n-Heptane | 0.0001 | 320 | 406 | 86 | 6619 |
| Toluene | 0.0126 | 320 | 426 | 106 | 7776 |
| THF | 0.21 | 306 | 444 | 138 | 10157 |
| DCM | 0.22 | 310 | 459 | 149 | 10472 |
| DMF | 0.274 | 318 | 472 | 154 | 10260 |
| MeCN | 0.3 | 304 | 474 | 170 | 11798 |
| MeOH | 0.31 | 305 | 522 | 217 | 13629 |

Table S13. Orientation polarizability for solvents (Δf), absorption and fluorescence emission maxima (λ_{abs} , λ_{em} , nm) and Stokes shift (nm, cm^{-1}) of **9a** in different solvents.

| Solvent | Δf | λ_{abs} , nm | λ_{em} , nm | Stokes shift, nm | Stokes shift, cm^{-1} |
|-----------|------------|-----------------------------|----------------------------|------------------|--------------------------------|
| n-Heptane | 0.0001 | 332 | 442 | 110 | 7496 |
| Toluene | 0.0126 | 335 | 455 | 120 | 7873 |
| THF | 0.21 | 334 | 475 | 141 | 8888 |
| DCM | 0.22 | 336 | 499 | 163 | 9722 |
| DMF | 0.274 | 337 | 516 | 179 | 10294 |
| MeCN | 0.3 | 334 | 522 | 188 | 10783 |
| MeOH | 0.31 | 339 | 550 | 211 | 11317 |

Table S14. Orientation polarizability for solvents (Δf), absorption and fluorescence emission maxima (λ_{abs} , λ_{em} , nm) and Stokes shift (nm, cm^{-1}) of **9b** in different solvents.

| Solvent | Δf | λ_{abs} , nm | λ_{em} , nm | Stokes shift, nm | Stokes shift, cm^{-1} |
|-----------|------------|-----------------------------|----------------------------|------------------|--------------------------------|
| n-Heptane | 0.0001 | 335 | 423 | 88 | 6210 |
| Toluene | 0.0126 | 333 | 429 | 96 | 6720 |
| THF | 0.21 | 330 | 429 | 99 | 6993 |
| DCM | 0.22 | 329 | 432 | 103 | 7247 |
| MeCN | 0.3 | 329 | 435 | 106 | 7406 |

Table S15. Orientation polarizability for solvents (Δf), absorption and fluorescence emission maxima (λ_{abs} , λ_{em} , nm) and Stokes shift (nm, cm^{-1}) of **10** in different solvents.

| Solvent | Δf | λ_{abs} , nm | λ_{em} , nm | Stokes shift, nm | Stokes shift, cm^{-1} |
|-----------|------------|-----------------------------|----------------------------|------------------|--------------------------------|
| n-Heptane | 0.0001 | 330 | 454 | 124 | 8277 |
| Toluene | 0.0126 | 327 | 460 | 133 | 8842 |
| THF | 0.21 | 328 | 477 | 149 | 9523 |
| DCM | 0.22 | 325 | 499 | 174 | 10729 |
| MeCN | 0.3 | 322 | 516 | 194 | 11676 |

Table S16. Orientation polarizability for solvents (Δf), absorption and fluorescence emission maxima (λ_{abs} , λ_{em} , nm) and Stokes shift (nm, cm^{-1}) of **12** in different solvents.

| Solvent | Δf | λ_{abs} , nm | λ_{em} , nm | Stokes shift, nm | Stokes shift, cm^{-1} |
|-----------|------------|-----------------------------|----------------------------|------------------|--------------------------------|
| n-Heptane | 0.0001 | 320 | 506 | 186 | 11487 |
| Toluene | 0.0126 | 314 | 504 | 190 | 12006 |
| THF | 0.21 | 320 | 542 | 222 | 12799 |
| DCM | 0.22 | 314 | 563 | 249 | 14085 |
| MeCN | 0.3 | 315 | 593 | 278 | 14883 |

Table S17. Lippert-Mataga plot for compounds **2**, **6**, **7**, **8**, **9**, **10**, and **12**.

| compound | Slopes | R ² | $\Delta\mu$, D |
|-----------|--------------|----------------|-----------------|
| 2 | 7792 | 0.89 | 9.9 |
| 6b | 17884 | 0.87 | 15.0 |
| 7a | 10606 | 0.87 | 11.6 |
| 7c | 21179 | 0.86 | 16.4 |
| 7e | 9806 | 0.87 | 11.1 |
| 8a | 20984 | 0.89 | 16.3 |
| 8c | 19962 | 0.97 | 15.9 |
| 8d | 15421 | 0.89 | 14.0 |
| 8e | 14906 | 0.97 | 13.8 |
| 8f | 18727 | 0.87 | 15.4 |
| 8g | 17850 | 0.93 | 15.1 |
| 9a | 9814 | 0.90 | 11.2 |
| 9b | 3879 | 0.86 | 7.0 |
| 10 | 11239 | 0.87 | 11.9 |
| 12 | 10707 | 0.89 | 11.7 |

Table S18. The photophysical properties of compounds in different solvents.

| Compound | <i>n</i> -Heptane | Toluene | THF | DCM | DMSO | MeCN | MeOH |
|-----------|-------------------|---------|-----|-----|------|------|------|
| 2 | 397 | 401 | 409 | 410 | 424 | 420 | 450 |
| 6b | 424 | 442 | 453 | 463 | 477 | 474 | 526 |
| 7a | 440 | 454 | 477 | 486 | 520 | 502 | 553 |
| 7c | 428 | 439 | 465 | 478 | 505 | 499 | 532 |
| 7e | 438 | 452 | 474 | 500 | 516 | 526 | 541 |
| 8a | 437 | 446 | 462 | 477 | 500 | 496 | 531 |
| 8c | 396 | 432 | 458 | 478 | 501 | 494 | 531 |
| 8d | 419 | 441 | 458 | 470 | 495 | 489 | 524 |
| 8e | 431 | 448 | 478 | 499 | 527 | 524 | 530 |
| 8f | 364 | 432 | 449 | 465 | 485 | 473 | 519 |
| 8g | 406 | 426 | 444 | 459 | 479 | 474 | 522 |
| 9a | 442 | 455 | 475 | 499 | 521 | 522 | 550 |
| 9b | 423 | 429 | 429 | 432 | 450 | 435 | 450 |
| 10 | 454 | 460 | 477 | 499 | 525 | 516 | 549 |
| 12 | 506 | 504 | 542 | 563 | 598 | 593 | 598 |

Lippert-Mataga equation:

$$\nu_A - \nu_F = \frac{2}{hc} \left(\frac{\varepsilon - 1}{2\varepsilon + 1} - \frac{n^2 - 1}{2n^2 + 1} \right) \frac{(\mu_E - \mu_G)^2}{a^3} \quad (\textbf{formula 1})$$

ν_A и ν_F – the wavenumbers (cm^{-1}) of the absorption and emission, respectively

$h = 6.6256 \times 10^{-34}$ – Planck's constant,

$c = 2.9979 \times 10^{10}$ cm/s – speed of light,

a – the radius of the cavity in which the fluorophore resides,

$a^3 = \text{Å}^3$ – the van der Waals volume,

ε – Relative permittivity of the solvent,

n – Refractive index of the solvent.

According to Abraham and co-workers, the van der Waals volume ($\text{Å}^3/\text{molecule}$) can be calculated from the following formula [1]:

$$V_{\text{vdW}} = (\text{all atom contributions}) - 5.92N_B - 14.7R_A - 3.8R_{NA} \quad (\textbf{formula 2})$$

where, N_B is the number of bonds, R_A is the number of aromatic rings, and R_{NA} is the number of non-aromatic rings.

Table S19. Fluorescence lifetime of probe **8c**, **8g**, **9a** ($C = 2 \times 10^{-6}$ M) in MeOH.

| Compound | τ_1 , ns ^a | α_1 ^b | τ_2 , ns ^a | α_2 ^b | τ_3 , ns ^a | α_3 ^b | τ , ns ^a | X^{2d} |
|--------------------|----------------------------|-------------------------|----------------------------|-------------------------|----------------------------|-------------------------|--------------------------|----------|
| 8c (420 nm) | 1.190024 | 34.70 | 3.754074 | 65.30 | - | - | 2.86 | 1.178404 |
| 8c (531 nm) | 3.506346 | 80.70 | 6.982067 | 19.30 | - | - | 4.18 | 1.118359 |
| 8g (522 nm) | 6.070119 | 100.00 | - | - | - | - | 6.07 | 1.062046 |
| 9a (398 nm) | 1.684421 | 36.47 | 1.281684 | 41.96 | 3.776949 | 21.57 | 1.15 | 1.091145 |
| 9a (564 nm) | 0.764980 | 76.30 | 4.506832 | 23.70 | - | - | 1.64 | 1.163146 |

^a Decay time, ^b Fractional contribution, ^c Weighted average decay time $\tau_{av} = \sum (\tau_i \times \alpha_i)$, ^d Quality of fitting

Table S20. Energies of HOMO and LUMO, and energy gap for compounds **7** and **8**.

| Compound | E(HOMO), eV | E(LUMO), eV | HOMO-LUMO energy gap, eV |
|----------------|-------------|-------------|-----------------------------|
| 7a | -6.99 | -0.74 | 6.25 |
| 7b | -6.93 | -0.66 | 6.27 |
| 7c | -6.96 | -0.70 | 6.26 |
| 7d | -6.96 | -0.72 | 6.24 |
| 7e | -7.10 | -0.91 | 6.19 |
| 7f | -6.94 | -0.65 | 6.29 |
| 7g | -6.91 | -0.61 | 6.30 |
| 7h | -6.92 | -0.63 | 6.29 |
| 8a | -6.99 | -0.76 | 6.23 |
| 8b | -6.90 | -0.65 | 6.25 |
| 8c | -6.96 | -0.69 | 6.27 |
| 8d | -6.93 | -0.71 | 6.22 |
| 8e | -7.09 | -0.94 | 6.15 |
| 8f | -6.91 | -0.65 | 6.26 |
| 8g | -6.88 | -0.59 | 6.29 |
| 7e_MeCN | -6.84 | -0.81 | 6.03 |
| 8e_MeCN | -6.86 | -0.81 | 6.05 |

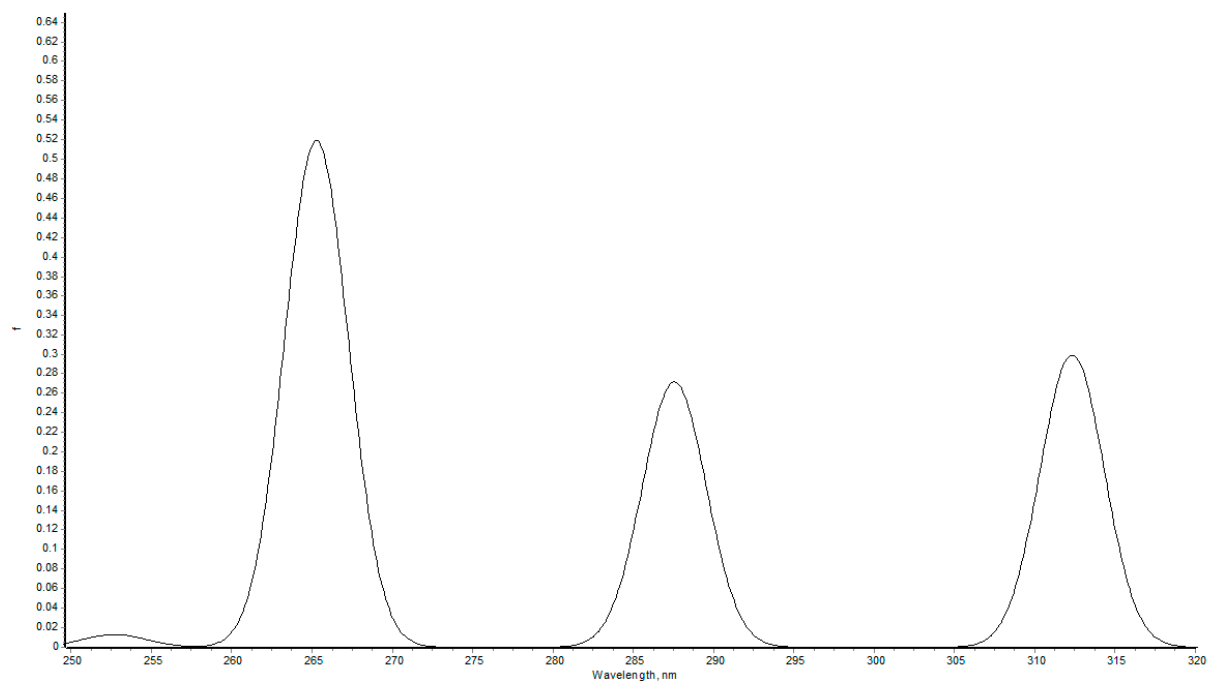


Figure S56. Calculated UV-Vis spectra for optimized equilibrium model structure **7c** (CAM-B3LYP/6-31+G* level of theory).

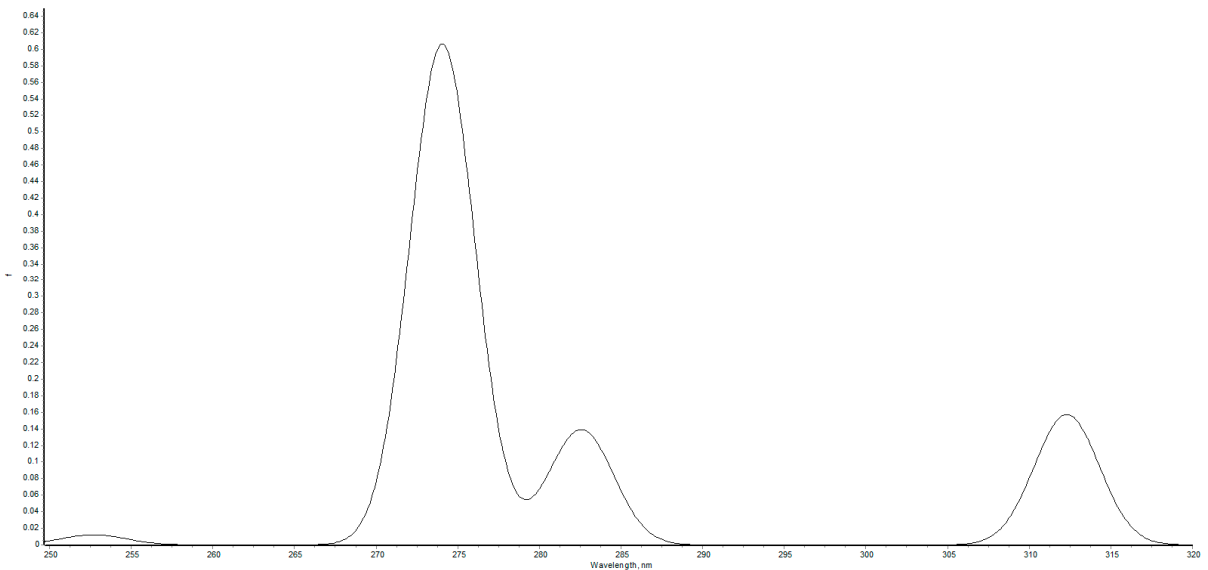


Figure S57. Calculated UV-Vis spectra for optimized equilibrium model structure **8c** (CAM-B3LYP/6-31+G* level of theory).

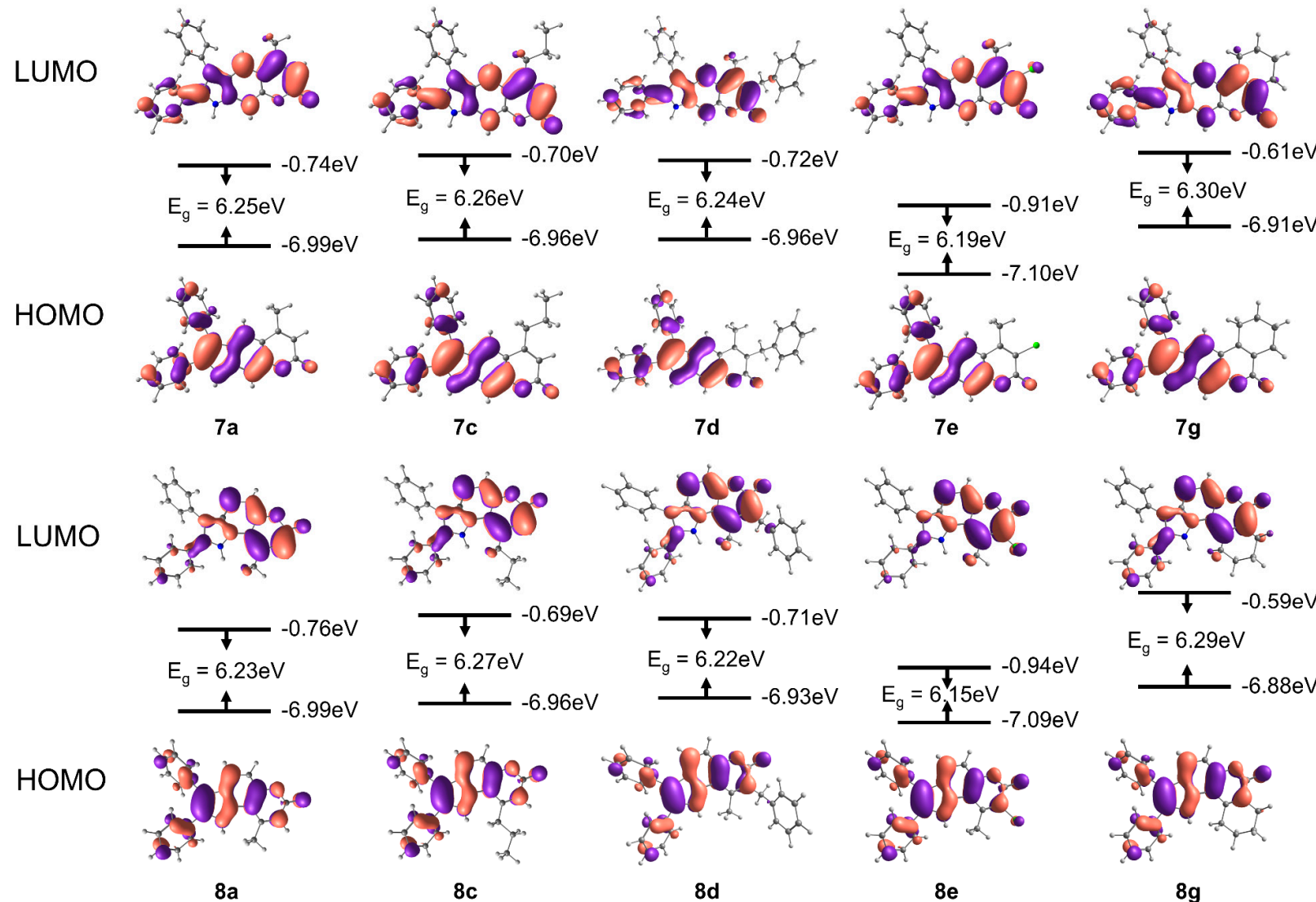


Figure S58. Molecular orbital and energy levels of **7a-8a**, **7c-8c**, **7d-8d**, **7e-8e**, **7g-8g** pyranoindole fluorophores, calculated at the CAM-B3LYP/6-31+G* level of theory.

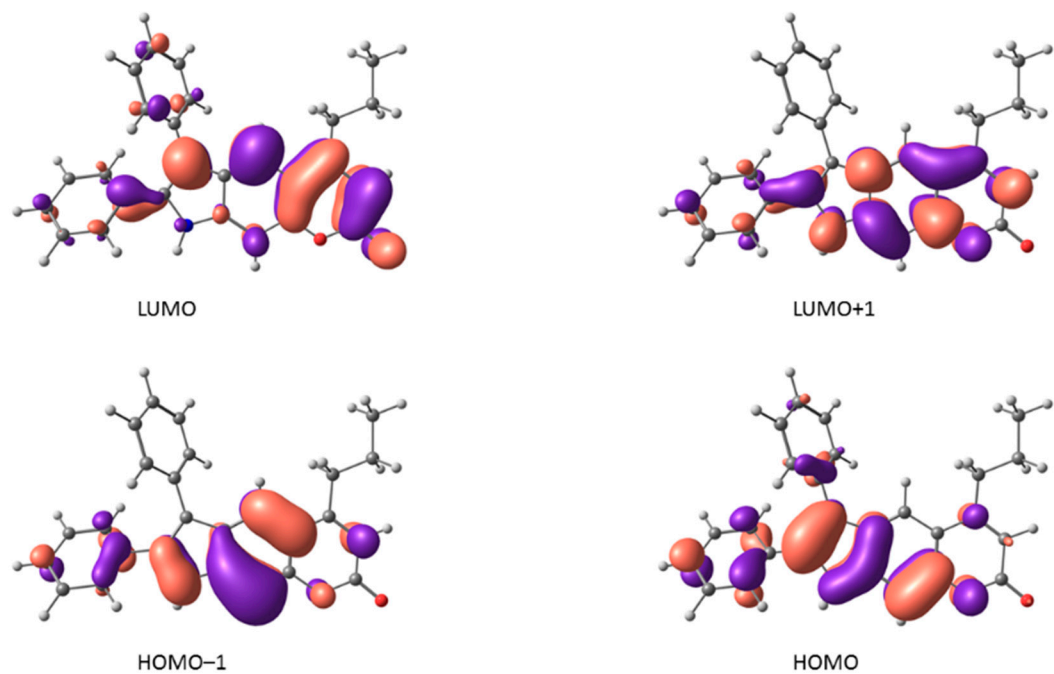


Figure S59. Visualization of HOMOs and LUMOs responsible for observed UV-Vis spectra in optimized equilibrium model structure **7c** (CAM-B3LYP/6-31+G* level of theory).

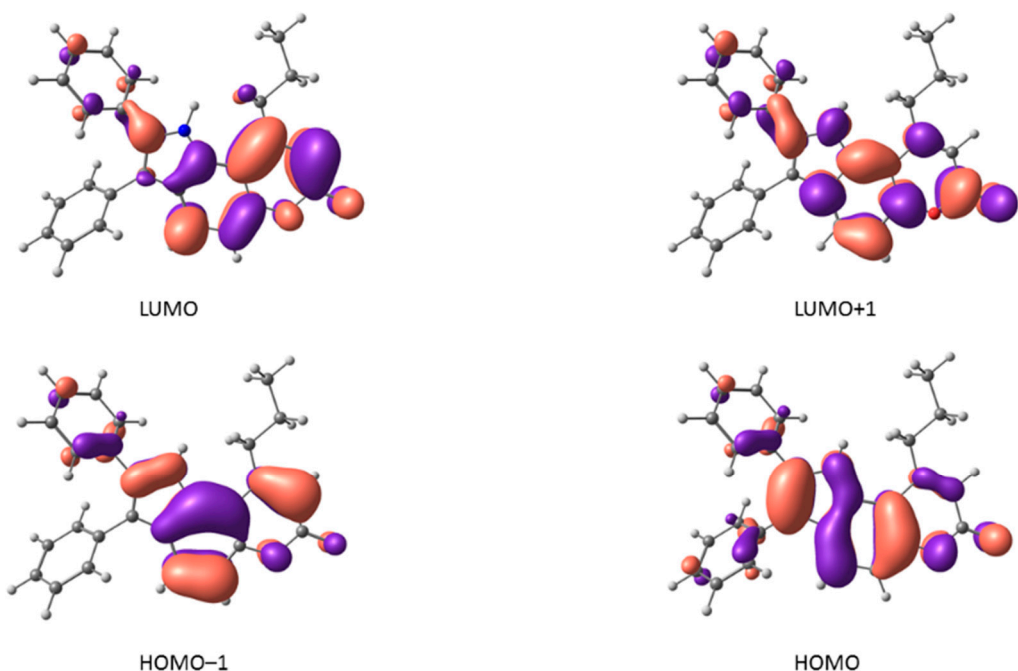
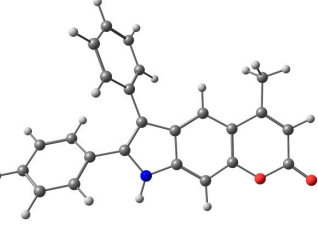
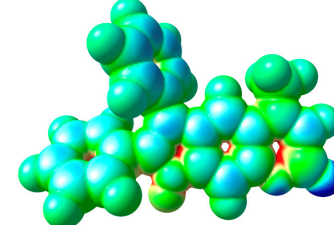
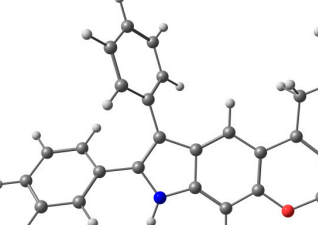
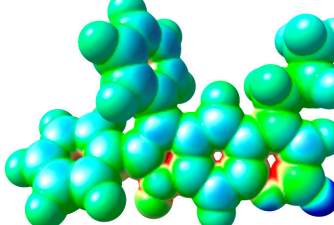
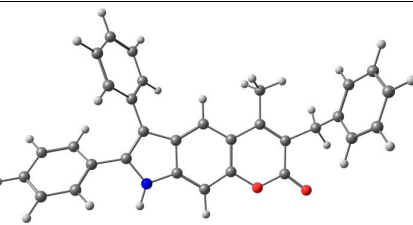
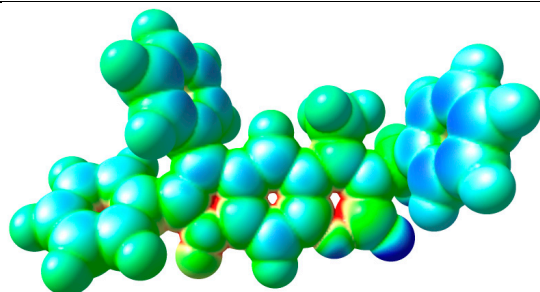
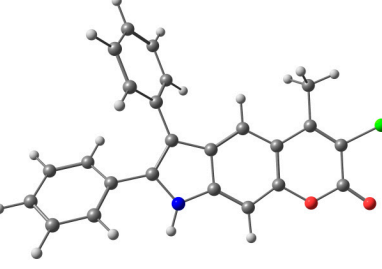
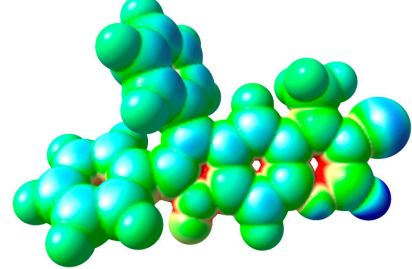
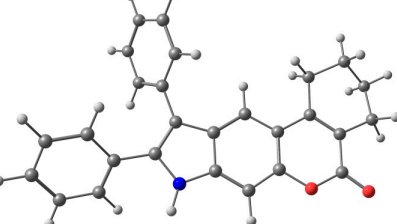
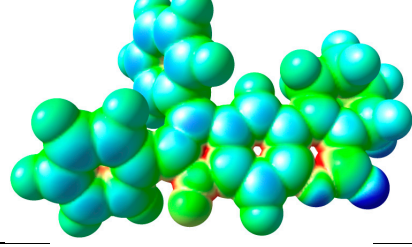
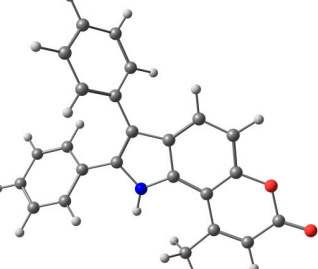
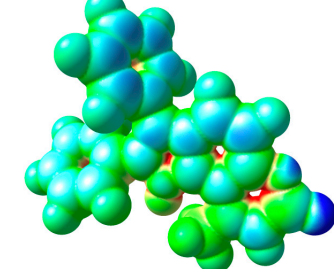


Figure S60. Visualization of HOMOs and LUMOs responsible for observed UV-Vis spectra in optimized equilibrium model structure **8c** (CAM-B3LYP/6-31+G* level of theory).

Table S21. Optimized structures in S_0 in gas phase and visualization of molecular electrostatic potential distribution.

| # | Optimized Structures in S_0 | Visualization of Molecular Electrostatic Potential Distribution 0.0  0.2 |
|----|---|---|
| 7a |  |  |
| 7c |  |  |
| 7d |  |  |
| 7e |  |  |
| 7g |  |  |
| 8a |  |  |

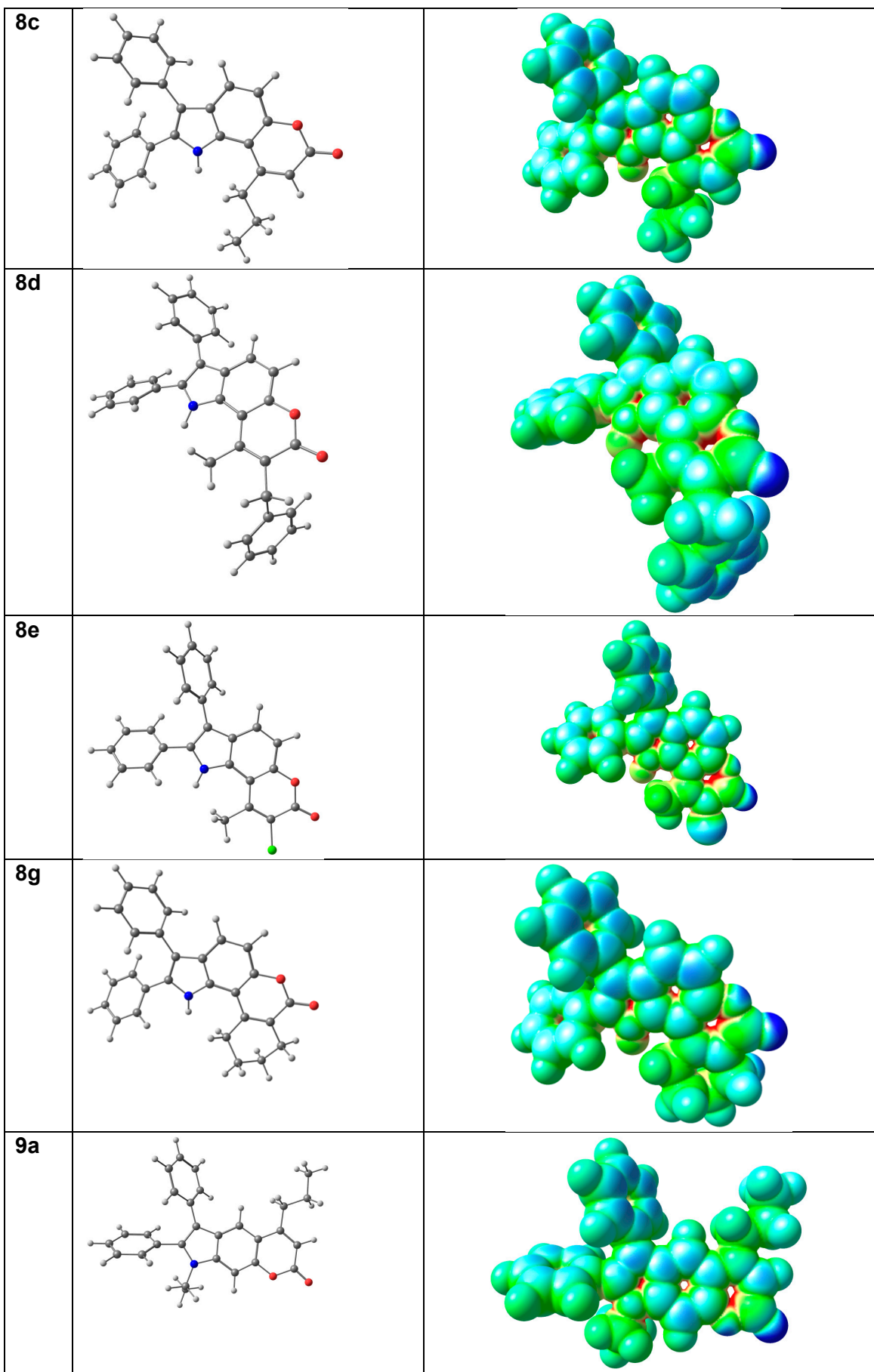


Table S22. Calculated indexes related to hole-electron distribution in model structures.

| Model structures | D _{CT} (Å) | S _r (a.u.) |
|------------------|---------------------|-----------------------|
| 7a | 1.388 | 0.75613 |
| 8a | 1.446 | 0.77065 |
| 7b | 1.269 | 0.76332 |
| 8b | 1.298 | 0.78534 |
| 7c | 1.344 | 0.75773 |
| 8c | 1.363 | 0.77740 |